Microtubules in Legume Root Hairs:
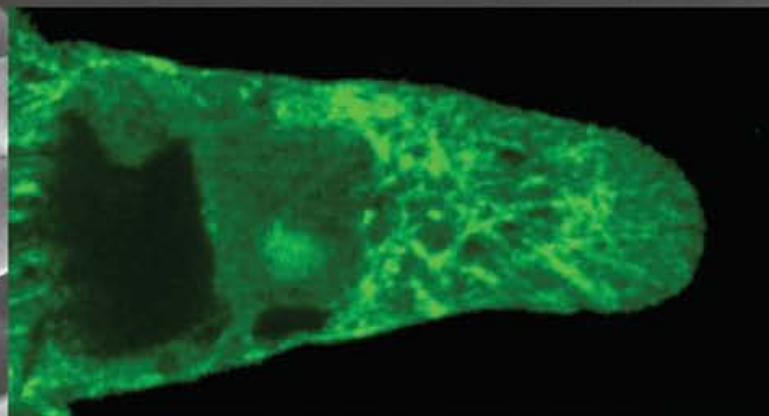
Cell Polarity and Response to Rhizobial Signal Molecules

Björn Sieberer

Microtubules in Legume Root Hairs:
Cell Polarity and Response to Rhizobial Signal Molecules

Björn Sieberer

Björn Sieberer

Microtubules in Legume Root Hairs:
Cell Polarity and Response to Rhizobial Signal
Molecules

Microtubules in Legume Root Hairs: Cell Polarity and Response to Rhizobial Signal Molecules

Sieberer, Björn

Contents

Outline

Root hairs of higher plants are lateral extensions of root epidermal cells and form together with the latter a unicellular system. They exclusively emerge in the differentiation zone of a primary root and elongate as cylindrical, uniaxilar structures with enormous final lengths compared to their widths. Root hairs enlarge the root-soil interface, thereby supporting the absorption of water and nutrients, enabling the plant to exploit new soil and probably serving in the anchoring of plants to the soil. Further, root hairs are important for the interaction of leguminous plants (legumes) with soil living rhizobacteria. Legumes, such as soybean, clover, alfalfa, beans and peas, can form a symbiosis with rhizobacteria. A specific developmental program involving both, plant and bacteria, leads to the formation of new plant organs, the root nodules. Within these nodules the bacteria chemically fix atmospheric nitrogen, which the plant uses to produce its proteins and serves as fertilizer for the soil when the plants decompose. The plant in turn provides the bacteria with sugar and other organic compounds. Nitrogen is essential for building proteins and nucleic acids. Nitrogen fixation by the legume-Rhizobia symbiosis is of considerable agricultural importance, firstly because it provides mankind with crops that are rich in proteins, secondly because it leads to a very significant increase of nitrogen compounds in the soil.

The symbiosis starts with the interaction between the legume root hairs and rhizobia. A highly specific molecular cross-talk between the plant and the bacteria allows (1) the recognition of the appropriate symbiotic partners, (2) root hair curling around rhizobia, (3) the infection of the root hair, and (4) the passage of the bacteria down the hair into the root cortex, where (5) finally a mature nodule forms. Lipochito-oligosaccharide signal molecules secreted by the rhizobacteria, the nodulation factors or Nod factors, play a key role in the early infection process. They induce root hair curling and trigger plant cell division in the root cortex, eventually leading to the formation of the nodule. Root hair curling is the consequence of an astonishing developmental switch: Upon perception of the Nod factor signal, a root hair alters its straight growth pattern (see below) and curls back on itself, trapping the bacteria within a pocket. Hair curling has been described as iterative tip growth reorientation. Our choice of legume root hairs as experimental system reflects an interest in the cellular and morphogenetic changes in these hairs by the nitrogen-fixing bacteria.

Chapter 1 is a review on cellular events in root hairs after Nod factor application and presents the state of the art at the beginning of my project concerning Nod factor induced

signaling events in legume root hairs with the actin cytoskeleton as target.

Root hairs elongate by a very special form of polarized growth, called tip growth. In general, plant cell growth implies the transport of exocytotic vesicles to confined areas in the cell cortex where they fuse with the plasma membrane, adding new membrane material. At the same time, the content of the vesicles, new cell wall material, is getting deposited into the existing cell wall. This leads to an irreversible increase in cell surface. In tip-growing plant cells such as root hairs and pollen tubes, the actual growth process is restricted to the very tip of the cell. Tip growth is a precisely orchestrated process characterized by the maintenance of a cylindrical shape with a constant diameter, a uniaxial extension pattern, and more or less straight growth directionality. Tip-growing root hairs have a highly polarized cytoarchitecture: cytoplasm, including the nucleus, is concentrated in the subapical tip region, whereas the basal part is filled with the central vacuole, except for a thin layer of cortical cytoplasm. Root hairs are an ideal system to study plant cell growth and related cellular events, as the growth machinery and the actual growth process are tightly localized to one region of the cell. Further, tip-growth occurs at a high speed, is very reproducible and predictable, easy to manipulate and to observe with microscopes. Plants with genetically manipulated root hair growth have the advantage over pollen tube mutants that they are usually fertile, so genetic research is easier to perform.

Chapter 2 is a cell biological characterization of root hairs of the model legume *Medicago truncatula*. In this chapter I describe cytoarchitecture and cell morphology during root hair development, and after Nod factor application. Secondly, I present the Nod factor-induced changes in the pattern of cytoplasmic streaming in these cells.

The cytoskeleton has been identified as the key player in the tip-growth process. The cytoskeleton is a system of protein filaments in the cytoplasm of eukaryotic cells that is organized in two complex and dynamic networks crucial to cell division, cell elongation, cell shaping, cell wall formation and for intracellular transport and movement. The two major compounds of the plant cytoskeleton are the actin filaments, also called F-actin, and the microtubules.
Actin filaments are tight helices of 6 nm in width that are composed of two subfilaments formed by the polymerization of actin monomers. The actin cytoskeleton in tip-growing hairs has a unique configuration: In the basal (vacuolated) part of the root hair tube thick bundles of F-actin lie net-axially oriented in cytoplasmic strands; these thick bundles flare

out into fine bundles of F-actin in the sub-apex. The very tip of a growing hair is devoid of F-actin. The actin cytoskeleton in root hairs is essential for the cytoplasmic organization and hence for cell polarity, for cell morphology, for organelle movement including movement of the nucleus, and for the transport and targeting of exocytotic vesicles to the very tip. It has been shown that the actin cytoskeleton is a target of early Nod factor signaling. Nod factors induce changes in F-actin configuration that are thought to affect tip-growth (see chapter 1).

Microtubules, the second major compound of the plant cytoskeleton, are hollow nano-tubes with a diameter of 25 nm, consisting of 13 protofilaments, which polymerize from alpha- and beta-tubulin heterodimers with the alpha-tubulin of one heterodimer binding to the beta-tubulin of the other heterodimer. Microtubules grow and shrink in a process called dynamic instability. This property of individual microtubules allows the plant cell to reconfigure its microtubule cytoskeleton according to external or internal stimuli. The microtubule cytoskeleton is highly regulated: Microtubule associated proteins serve to stabilize microtubules against disassembly and to mediate interactions with other microtubules and cell compounds, while other proteins are known to destabilize or sever microtubules. Post-translational modifications of tubulin (e.g., detyrosination) are also involved in the regulation of microtubule stabilization and interactions. During plant cell development, each developmental stage has a characteristic microtubule cytoskeleton organization. Even though the overall appearance of microtubules reminds of a static structure, individual microtubules are still highly dynamic. In intercalary interphase plant cells, microtubules are evenly distributed and localized in the cell cortex. They are somehow involved in determining the direction of cell elongation; they mostly appear to be transversely oriented to the axis of cell elongation. Microtubules are crucial to cell division. They determine the division plane of the cell, they separate the sister chromatides during nuclear division (mitosis), and during cytoplasmic division (cytokinesis) they are involved in the formation of the cell plate that finally separates the two new cells.

Whereas the role of the actin cytoskeleton during root hair development is fairly well understood (see chapters 1 and 5, and references given therein), only little was known about the role of microtubules in this process. Consequently, my work focused on configuration and function of the microtubule cytoskeleton during root hair development.

In chapter 3, I describe the microtubule cytoskeleton in developing *M. truncatula* root

hairs. Cortical microtubules are present in all developmental stages, but in the sub-apex of tip-growing root hairs I found a specific microtubule configuration that was not described in detail before. When tip growth begins, the hairs acquire an extensive endoplasmic microtubule array in their sub-apex, which they retain until growth stops. This endoplasmic microtubule array may be specific for tip-growing legume root hairs. Drugs studies showed that these endoplasmic microtubules are essential in maintaining the specific cytoarchitecture of growing legume root hairs, including keeping a fixed nucleus-tip distance, and in keeping the growth of these hairs at a high rate.

Since microtubules are important for tip-growth in legume root hairs, one can imagine that they somehow may be involved in the response of root hairs to Nod factors. In chapter 4, I present data on the microtubule cytoskeleton in *M. truncatula* root hairs after application of Nod factors. Indeed, results show that in addition to the actin cytoskeleton also the microtubule cytoskeleton is a target of early Nod factor signaling. Nod factors cause a subtle and short termed response of endoplasmic microtubules, whereas cortical microtubules were not obviously affected. Furthermore, the presented results demonstrate that the microtubule cytoskeleton contributes to sustaining tip-growth and to determining the growth direction of hairs after Nod factor application. The latter two features are crucial for root hair curling around rhizobia.

Chapter 5 is a review that focusses on the involvement of microtubules in root hair development and cell polarity of the model plants *M. truncatula* and *Arabidopsis thaliana*. It highlights similarities and differences in the microtubule organisation and function between these two species and proposes a microtubule based mechanism by which cell polarity in root hairs may be regulated.

Chapter 1

Time Course of Cell Biological Events Evoked in Legume Root Hairs by *Rhizobium* Nod Factors: State of the Art

F.G.P. Lhuissier, N.C.A. de Ruijter, B.J. Sieberer, J.J. Esseling and A.M.C. Emons

Department of Plant Sciences, Laboratory of Plant Cell Biology, Wageningen University, Arboretumlaan 4, 6703 BD, Wageningen, The Netherlands

Abstract

In many common legumes, when host-specific nodule bacteria meet their legume root they attach to it and enter through root hairs. The bacteria can intrude these cells because they instigate in the hairs the formation of an inward growing tube, the infection thread, which consists of wall material. Prior to infection thread formation, the bacteria exploit the cell machinery for wall deposition by inducing the hairs to form a curl, in which the dividing bacteria become entrapped. In most species, Nod factor alone (a lipochito-oligosaccharide excreted by bacteria) induces root hair deformation, though without curling, thus most aspects of the initial effects of Nod factor can be elucidated by studying root hair deformation. In this review we discuss the cellular events that host-specific Nod factors induce in their host legume root hairs. The first event, detectable only a few seconds after Nod factor application, is a Ca^{2+} influx at the root hair tip, followed by a transient depolarization of the plasma membrane potential, causing an increase in cytosolic $[Ca^{2+}]$ at the root hair tip. Also within minutes, Nod factors change the cell organization by acting on the actin cytoskeleton, enhancing tip cell wall deposition so that root hairs become longer than normal for their species. Since the remodelling of the actin cytoskeleton precedes the second calcium event, Ca^{2+} spiking, which is observed in the perinuclear area, we propose that the initial cytoskeleton events taking place at the hair tip are related to Ca^{2+} influx in the hair tip and that Ca^{2+} spiking serves later events involving gene expression.

Key words: Review, Nod factor, tip growth, root hair, *Rhizobium*, legume, cytoskeleton, calcium, symbiosis.

Introduction

The symbiotic relationship between legumes and rhizobia (legume root nodule bacteria, now classified in five genera *Azorhizobium*, *Bradyrhizobium*, *Mesorhizobium*, *Rhizobium* and *Sinorhizobium*) is a complex process that results in the formation of nitrogen-fixing nodules within the host plant roots. In many common legumes, infection by rhizobia occurs through root hairs [for a description of other routes of infection see for example Sprent (1992)]. Successful infection of the roots by rhizobia is dependent upon a reciprocal molecular dialogue between the host plant and the rhizobia (Fisher and Long, 1992; Bladergroen and Spaink, 1998; Schultze and Kondorosi, 1998). Central molecules involved in the mechanisms leading to nodule formation are the so-called Nod factors, which are lipochito-oligosaccharides. Nod factor production is induced in the rhizobia by molecules that are produced by the host plant. These molecules are phenolic compounds, mainly flavonoids (Djordjevic et al., 1985; for review, see Fisher and Long, 1992; Schultze and Kondorosi, 1998). Nod factors are excreted by the rhizobia and, even in the absence of the bacteria, trigger root hair deformation, cortical cell division and pre infection thread formation (Fisher and Long, 1992; Heidstra and Bisseling, 1996; Schultze and Kondorosi, 1998). Preinfection threads are cytoplasmic bridges in the root cortical cells (Timmers et al., 1998, 1999) which are reminiscent of phragmosomes, the first structures formed when cells initiate cell division (Venverloo and Libbenga, 1987). Infection threads, walled tubes formed by the plant cells in the root hairs and root cortical cells, and nodules, are formed in the root cortex only in the presence of bacteria. The appearance of all these cellular changes in the presence of bacteria is highly dependent upon the chemical structure of the Nod factor (Ardourel et al., 1994; Demont-Caulet et al., 1999). The first events triggered by Nod factors take place only a few seconds after their application (Ehrhardt et al., 1992; Felle et al., 1995), whereas some other events occur only after a few hours (Heidstra et al., 1994; Heidstra and Bisseling, 1996; De Ruijter et al., 1998; Schultze and Kondorosi, 1998; Downie and Walker, 1999; Jahraus and Bisseling, 2000; Sieberer and Emons, 2000). While studying Nod factor signalling, one has to bear in mind the spatio-temporal distribution of the induced responses. In this review, we describe the time course of the currently known events evoked by isolated Nod factors in root hairs, the first root cells to respond to Nod factors. Calcium (Ca^{2+}) appears to be crucial in the Nod factor-induced changes. Therefore, the other Nod factor-induced changes, i.e. root hair deformation, actin cytoskeleton remodelling, endoplasmic reticulum re-orientation, vacuolation, changes in the pattern of cytoplasmic streaming, nuclear

movement, cell wall deposition and cell wall loosening, will, if relevant, be related to Ca^{2+} dynamics.

Nod factor perception in root hairs

The fact that specific Nod factors trigger downstream events in their host plants at doses as low as 10^{-12}M (Lerouge et al., 1990; Heidstra et al., 1994), and that chito-oligosaccharides (the common inactive backbone of all Nod factors) are unable to trigger any, when externally applied, suggests the requirement of a receptor for the perception of Nod factors and the transduction of the signal. Though Nod factor receptors have not yet been cloned, two mechanisms have been proposed for the mediation of the Nod factor signal (Heidstra and Bisseling, 1996; Long, 1996; Bladergroen and Spaink, 1998). The first hypothesis involves the presence of a single receptor, the activity of which is dependent on the structure of the Nod factor (Hirsch, 1992). The Nod factor acyl chain could serve to anchor Nod factors into the plasma membrane close to a receptor (Bladergroen and Spaink, 1998). The fact that Nod factors integrate spontaneously in membranes but that transbilayer 'flip-flop' does not occur (Goedhart et al., 1999) is in good agreement with this hypothesis, but does not exclude the possibility of a multiple-receptor hypothesis. The second hypothesis suggests that two receptors are required to trigger all the downstream events (Ardourel et al., 1994; Heidstra and Bisseling, 1996; Long, 1996). The first receptor (signaling receptor) exhibits a low specificity for Nod factors (i.e. Nod factors lacking some substituted groups can bind to the signalling receptor) and induces root hair deformation, pre-infection thread formation, and cortical cell division in the presence or absence of the bacteria. The second receptor (uptake receptor) exhibits a high specificity for Nod factors (i.e. only host specific Nod factors can bind to the uptake receptor) and induces infection thread formation and nodule formation, but only in the presence of bacteria. To date, two Nod factor-binding sites (NFBS1 and NFBS2) have been identified in microsomal preparations of *Medicago sativa* spp. varia (Niebel et al., 1997; Gressent et al., 1999). NFBS1 exhibits a low affinity for Nod factors, whereas NFBS2 exhibits a high affinity for Nod factors. Both binding sites can discriminate between host specific and other forms of Nod factors. As such, they are potentially good candidates for Nod factor receptors. However, neither site is able to discriminate between sulfated (active) and non-sulfated (inactive) forms of Nod factors. The two-receptor model is attractive, since it can explain why structurally different Nod factors can elicit different sets of responses; nevertheless, no clear evidence has proven

that downstream events triggered by Nod factors are mediated through one or more receptors. The acyl tail of Nod factors has been proposed to be involved in uptake and transport of Nod factors, whereas the substituted oligo-saccharide moiety could activate an intracellular receptor (Philip-Hollingsworth et al., 1997; Schlaman et al., 1997). This hypothesis is very attractive as it could explain the fact that no Nod factor receptors have been clearly identified so far, but does not fit with the very early events that take place within a few seconds of Nod factor application (Ehrhardt et al., 1992; Felle et al., 1995).

Beside the possible involvement of receptors, several studies have shown that lectins might play a role in the recognition of Nod factors and/or bacteria (Diaz et al., 1986, 1995; Etzler et al., 1999; Hirsch, 1999). Indeed, Etzler et al. (1999) have shown that Nod factors from *Bradyrhizobium japonicum* bind to a *Dolichos biflorus* lectin and that this lectin possesses an apyrase (nucleotide phosphatase) activity that is stimulated by the addition of Nod factor. An enzymatic activity is quite unusual for a lectin but, if correct, might be a link between Nod factor recognition and signal transduction. However, no other lectins have been found so far with such an enzymatic activity. Thus, lectins are more likely to be involved in the interaction with the bacterial lipopolysaccharide in a host-specific manner, as proposed by Hirsch (1999).

Calcium changes at the plasma membrane of the root hair tip: the first root hair response to Nod factors

The first event occurring a few seconds after Nod factor application, namely a transient influx of Ca^{2+} into the root hairs, was reported for *Medicago sativa* by Felle et al. (1998), who used non-invasive ion-selective microelectrodes. An inwardly directed Ca^{2+} influx was observed for at least 1 h in root hairs of *Phaseolus vulgaris* (Cárdenas et al., 1999). The increase in cytosolic $[Ca^{2+}]$ ($[Ca^{2+}]_c$) within 3 min in root hair tips of *Medicago sativa* (Felle et al., 1999a) and the four-fold increase within 5 min in *Phaseolus vulgaris* root hair tips (Cárdenas et al., 1999), could activate anion channels in the plasma membrane. This could lead to an efflux of chloride ions (Cl^-) which is responsible for plasma membrane depolarization, as reported upon application of Nod factors by Ehrhardt et al. (1992) in *Medicago sativa*, Felle et al., (1995) and reviewed by White (1998) and Downie and Walker (1999). The mechanism(s) involved in Nod factor-induced Ca^{2+} influx remain unclear, but it has been proposed that Ca^{2+} fluxes across the plasma membrane could be mediated directly via G-protein regulation of the plasma membrane Ca^{2+} channels

(reviewed by Jan and Jan, 1997). Thuleau et al. (1998) reported the existence of two types of voltage- activated Ca^{2+} channels, hyperpolarization-activated Ca^{2+} channels and depolarization-activated Ca^{2+} channels, the latter are good candidates for the generation of the high $[Ca^{2+}]_c$ induced by Nod factors at the tips of root hairs. Nod factor-induced transient depolarization might thus activate depolarization-activated calcium channels leading to an increase in the $[Ca^{2+}]_c$ at the root hair tip. Nod factor-induced depolarization of the plasma membrane is a transient process that lasts between 15 and 30 min (Ehrhardt et al., 1992; Felle et al., 1995; Kurkdjian, 1995). Therefore, other mechanisms are likely to be involved to sustain the high $[Ca^{2+}]_c$ over the entire growth period - they are likely to be the same mechanisms as occur in normally-growing hairs prior to Nod factor application.

Microtubules have been proposed as potential regulatory elements of Ca^{2+} channel recruitment from experiments using the *Arabidopsis thaliana* ton mutant in which cortical microtubules are constitutively disorganized (Thion et al., 1998). In this mutant, Ca^{2+} channel activities were ten times higher, and their half-life three times longer than recorded in the *Arabidopsis thaliana* wild type (Thion et al., 1998). So far, the molecular basis of this recruitment process remains largely obscure, but would imply that Nod factors may influence the organization of the root hair microtubule cytoskeleton.

In an assay in which root hair bearing roots were grown between glass slides, De Ruijter et al. (1998) showed that Nod factor-induced deformation of root hair tips was a re-initiation of tip growth in *Vicia sativa* growth-terminating hairs. Indeed, several studies have shown that, in tip-growing cells, there is a close correlation between growth and the presence of an elevated $[Ca^{2+}]_c$ at the tip (Schiefelbein et al., 1992; Bibikova et al., 1997; Wymer et al., 1997; De Ruijter et al., 1998; Cárdenas et al., 1999; Felle et al., 1999a, b, for review see Miller et al., 1997). Wymer et al. (1997) showed that tip growth in Arabidopsis thaliana root hairs is correlated with a high $[Ca2.]c$ at the tip and that growth stops when the Ca^{2+} channel-blocker verapamil is added to the external medium. This cessation of growth is accompanied by a decrease in the $[Ca^{2+}]_c$ at the root hair tip. Using $MnCl_2$ to quench the fluorescence signal from the fluorescent calcium reporter dye indo-1 in the cytoplasm, these authors determined that there was a higher density of open manganese ion (Mn^{2+})-permeable channels at the root hair tip than at its base. Moreover, the controlled asymmetric photo-release of the caged Ca^{2+}-ionophore, Br-A23187, generated asymmetric $[Ca^{2+}]_c$ gradients in the tip of *Arabidopsis* root hairs and also in *Tradescantia* pollen tubes (Bibikova et al., 1997). In both cases, this led to a re-orientation

of growth towards the site of elevated $[Ca^{2+}]_c$. Together these results suggest that the presence of a high $[Ca^{2+}]_c$ in the tip of tip-growing cells is a requirement for tip growth. The Nod factor-induced increase of $[Ca^{2+}]_c$ in the root hair tips of legumes is consistent with this idea.

Nod factor-induced calcium mediated signaling in the root hair tip

Using the generic activator of animal G-proteins, mastoparan, Pingret et al. (1998) showed that mastoparan could mimic Nod factor-induced transcription of MtENOD12-GUS. In addition, pertussis toxin, which interferes with the interaction between G-proteins and receptors, inhibited the Nod factor-induced MtENOD12-GUS expression. Furthermore, the widely used eukaryotic phospholipase C (PLC) antagonist, neomycin, and the aminosteroid PLC inhibitor, U73122, inhibited Nod factor-elicited MtE-NOD12 expression. From these results, the authors concluded that part of the cascade involved in Nod factor signalling is mediated by a G-protein and PLC. However, one has to keep in mind that G-proteins may also activate phospholipase D (PLD) (De Vrije and Munnik, 1997; Van Himbergen et al., 1999) and phospholipase A2 (PLA2) (Munnik et al., 1998). Thus, the inhibition of MtENOD12 expression by G-protein inhibitors does not exclude the possibility that PLD and/or PLA2 are involved in Nod factor-induced processes. However, the experiments indicate that the inositol 1,4,5 trisphosphate (IP3) signal transduction cascade may well be employed by Nod factors, at least for gene expression.

Type II PLCs are predominantly bound to the plasma membrane, use polyphosphoinositides as preferred substrate, and are fully activated in the presence of micromolar $[Ca^{2+}]_c$ concentrations. Hydrolysis of phosphatidylinositol bisphosphate (PIP2) by PLC leads to the production of the water-soluble IP3 and the lipid product diacylglycerol (DAG), which remains in the plasma membrane (Fig. 1). In mammalian cells, the increase in DAG is rapidly counteracted by its reversible conversion to phosphatidic acid (PA) by the enzyme diacylglycerol kinase (DGK). DGK has been identified in various plant systems (for review see Munnik et al., 1998). In addition, PA can be produced by stimulation of PLD. Several plant PLD genes have been cloned (Pappan et al., 1997; Qin et al., 1997; Munnik et al., 1998) and the enzyme can be found either in soluble form or associated with the plasma membrane (see Table 3 in Munnik et al., 1998). *In vitro*, both forms have a strict requirement for millimolar $[Ca^{2+}]$, too high for an activity in vivo. However, Dyer et al. (1995) and Qin et al. (1997) reported the presence of three novel PLDs, namely PLDa, b and g. Whereas the a form is active at

millimolar [Ca^{2+}], the b and g forms are active at submicromolar [Ca^{2+}] (Pappan et al., 1997; Qin et al., 1997). Interestingly, the activity of the b and g forms is dependent on PIP2, whereas the activity of the a form is independent of PIP2 (Pappan et al., 1997; Qin et al., 1997).
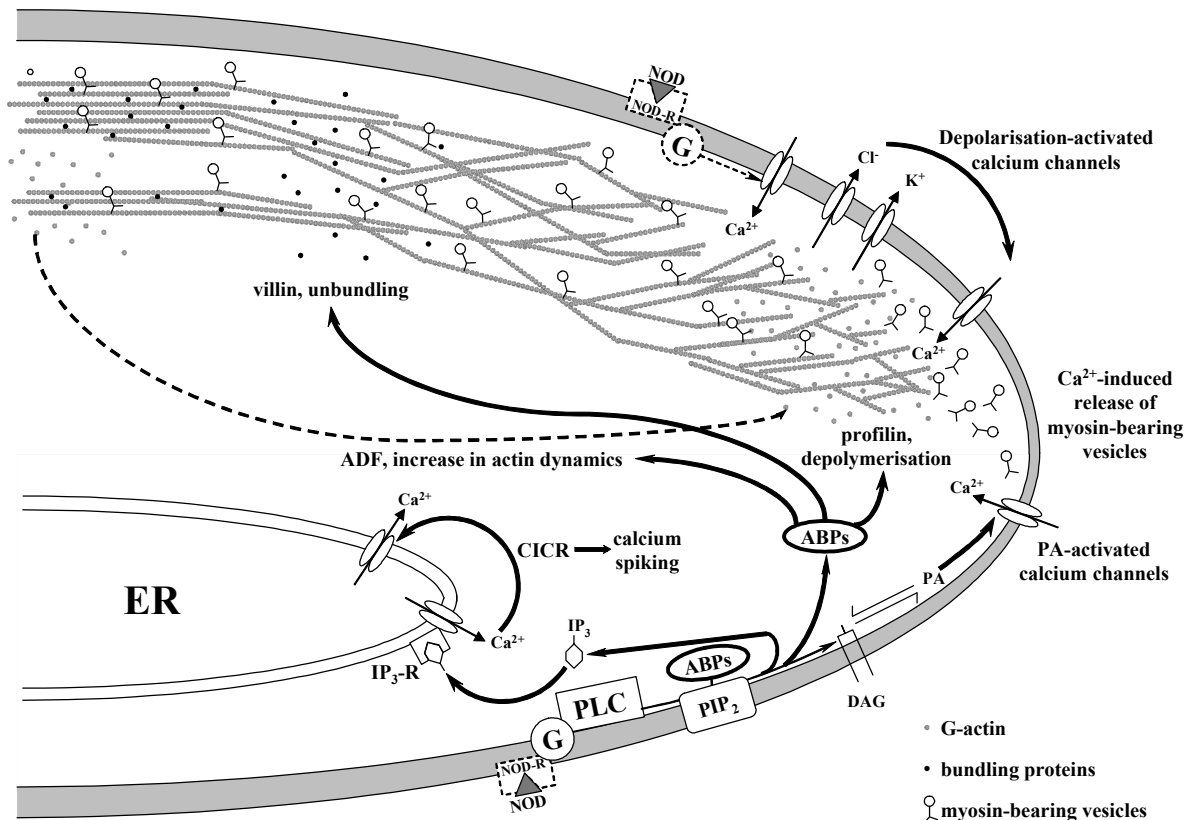
Figure 1. Scheme showing the putative mechanisms involved in the generation and the maintenance of the high [Ca^{2+}]$_c$ at the tip of root hairs after Nod factor application and the consequences of a high [Ca^{2+}]$_c$ on the actin cytoskeleton. See text for details. NOD: Nod factor; NOD-R: putative Nod factor receptor; G: G-protein; PLC: phospholipase C; PIP$_2$: phosphatidylinositol bisphosphate; ABPs: actin binding proteins; IP$_3$: inositol 1,4,5-trisphosphate; IP$_3$-R: inositol 1,4,5-trisphopshate receptor; DAG: diacylglycerol; PA: phosphatidic acid.

In animal cells, a group of PLDs is activated by Rho GTPases and PKC (Munnik et al., 1998). Interestingly, a Rho-like GTPase has been identified in pollen tubes, which is

involved in tip growth (Lin et al., 1996; Lin and Yang, 1997; Yang, 1998). On the other hand, PA, the product of PLD activity, can be dephosphorylated to give DAG (Fig. 1) (McCormac et al., 1993; Voisine et al., 1993; Griebau and Frentzen, 1994; Malherbe et al., 1995) which can, in turn, activate PKC. Several roles have been described for PA in plant cells, but one of them is of great interest in the context of Nod factor-related signalling. PA is an endogenous Ca^{2+} ionophore (Munnik et al., 1998; Wang, 1999). Thus, PA could autoamplify PLD signaling by increasing Ca^{2+} influx. Furthermore, PA can amplify the PLC signalling cascade by activating the enzyme phospha-tidylinositol 4-phosphate 5-kinase (PIP-kinase), leading to the production of PIP2, and/or PLC, leading to an increased production of DAG and IP3. This enhanced production of PA by either PLC alone or both PLC and PLD together might be part of the mechanism involved in sustaining the high $[Ca^{2+}]_c$ at the root hair tips during normal and Nod factor-induced tip growth.

Another mechanism that might be involved in sustaining the tip elevated $[Ca^{2+}]_c$ is the calcium-induced calcium release (CICR) from internal stores. This process has been extensively studied in animal cells and is potentially important for amplifying changes in $[Ca^{2+}]_c$ in plants (Bush, 1995). IP3 is known, mostly from animal studies [reviewed by Bush (1995) and Munnik et al. (1998)], to induce Ca^{2+} release from internal stores. Furthermore, it has been shown to exhibit a similar activity in plants (Alexandre et al., 1990; Alexandre and Lassalles, 1990; Bush, 1995; Munnik et al., 1998). Malhó (1998) reported that asymmetric photo-release of caged-IP3 in pollen tube tips resulted in a transient $[Ca^{2+}]_c$ elevation and also induced slight or transient growth re-orientation. However, the photo-release of caged IP3, either in the sub-apical area or in the nuclear area, induced transient $[Ca^{2+}]_c$ elevation in the nuclear region followed by slow waves, and random sustained growth re-orientation as observed by both Malhó and Trewavas (1996) and Franklin-Tong et al. (1996). From these results the authors suggest that, in pollen tubes, IP3 does not seem to be required for activation of Ca^{2+} entry at the tip, one of the primary events leading to re orientation. Instead, IP3-induced Ca^{2+} release seems to play a vital role in the transduction of the signal to the body of the tube.

Signalling towards the actin cytoskeleton

The actin cytoskeleton reacts to Nod factors within 3 min of their application (*Phaseolus vulgaris*: Cárdenas et al., 1998; *Vicia sativa*: De Ruijter et al., 1999). In *Vicia sativa*, this

reaction is manifested as an increase in the density of subapical fine bundles of actin filaments (De Ruijter et al., 1999) called FB-actin (Miller et al., 1999). Subapical FB-actin is always observed in growing root hairs. Also, there is an area, distal from it, at the extreme tip, which is devoid of bundles of actin filaments (Miller et al., 1999). Neither of these features is ever seen in full-grown hairs (Miller et al., 1999). Root hairs of all developmental stages (growing, growth-terminating and full-grown hairs), respond to Nod factors with an increase in length and density of FB-actin (Compare Fig. 2B, D, F and H with A, C, E and G, respectively). Interestingly, after Nod factor application, the FB-actin density in full-grown hairs never reaches the FB-actin density observed in control growing hairs (Compare Fig. 2B and A). This could be one reason why full-grown hairs do not usually exhibit deformation after Nod factor application. Alternatively, the presence of a secondary cell wall at the tip of full-grown root hairs - which has not yet been shown for legumes but is present in other species - may be another reason for the inability of these hairs to deform (Emons and Wolters-Arts, 1983). How does the process of re-organization of the actin cytoskeleton, following Nod factor application, take place? Actin exists in plant cells as either filaments or monomers.

The filaments (F-actin) consist of monomers (G-actin) and possess a determined polarity, a fast growing `plus end' (barbed end) and a slow growing `minus end' (pointed end). Actin filaments are dynamic structures controlled by an unstable equilibrium between polymerization and depolymerization. Actin monomers are present in the cytoplasm either bound to ADP or ATP; ATP-actin polymerizes more easily than ADP-actin. The function and organization of actin filaments is largely determined by their regulatory proteins, the so-called actin binding proteins (ABPs). Actin-binding proteins that also have phospho-inositide binding sites are good candidates for regulators of changes in the actin cytoskeleton after Nod factor application. Profilin, actin-depolymerizing factor (ADF), spectrin, gelsolin, the arp2/3 complex and myosin will be discussed with regard to their possible role(s) in actin cytoskeleton remodelling.

Profilin

Profilin is a 12±15 kDa protein that binds to monomeric actin to form profilactin. Two distinct activities have been reported for profilin: firstly, by binding actin monomers, profilin may promote actin filament depolymerization in plant cells, as shown by Staiger et al. (1994) and Valster et al. (1997). On the other hand, by modifying the ratio between ATP-actin and ADP-actin in favour of ATP-actin, profilin promotes actin polymerization in vitro (Goldschmidt-Clermont et al., 1992). Profilin can bind to poly- L-proline and to

PIP 2 (Machesky and Pollard, 1993; Staiger et al., 1997). Binding to PIP 2 results in a dissociation of the profilactin complexes (Machesky and Pollard, 1993). Since Nod factors induce Ca^{2+} influxes (Cárdenas et al., 1999; Felle et al., 1999a, b), possibly activated by PLC (Pingret et al., 1998), Nod factors may induce the hydrolysis of PIP 2 by PLC. The hydrolysis of PIP 2 releases bound profilin which can form profilactin complexes, thus displacing the equilibrium between F- and G-actin in favour of G-actin formation. This leads to the depolymerization of F-actin. The depolymerization of F-actin could then (1) induce disintegration of bundles of actin filaments at the tip of root hairs to increase the length of the actin filament-free area and (2) provide actin monomers for actin cytoskeleton re-arrangement. The time course of the appearance of FB-actin at the tips of *Vicia sativa* root hairs (Fig. 2; De Ruijter et al., 1999) and of the formation of the elevated tip focused $[Ca^{2+}]_c$ after Nod factor application (*Phaseolus vulgaris*: Cárdenas et al., 1999; *Medicago sativa*: Felle et al., 1999b) are consistent with the idea that the elevated $[Ca^{2+}]_c$ causes re-arrangement of the actin cytoskeleton. However, to date, there is no hard proof that functional profilin is indeed localized in the growing root hair tip. The report by Braun et al. (1999), showing the localization of profilin in maize root hairs, may indicate such a presence. However, accessible cell volume was not taken into account in this research, which may be relevant for the determination of the localization of a small, difficult-to-fix cytoplasmic protein like profilin (see discussion in Emons and De Ruijter, 2000). The presence of a weak tip-to-base gradient of PIP 2 in these hairs, which is lacking in full-grown hairs (Braun et al., 1999), is interesting, but should be interpreted with care.

Gelsolin

A second Ca^{2+}-regulated ABP that requires attention is gelsolin and its superfamily, including villin and supervillin (Robinson et al., 1999; Cooper and Schafer, 2000). These proteins possess severing and capping properties which model actin filaments. Activation of heterotrimeric and small GTP binding proteins dissociates gelsolin from the barbed ends of actin filaments (Cooper and Schafer, 2000). In addition to the severing and capping activities of the gelsolin-related portion of the protein, villin has a small headpiece that bundles actin filaments *in vitro* (Cooper and Schafer, 2000). In the presence of Ca^{2+}, villin can sever actin filaments into shorter filaments, whereas in the absence of Ca^{2+}, it bundles actin filaments (Yao and Forte, 1996). Recently, the presence of proteins from the villin-gelsolin family has been shown in *Lilium longiflorum* pollen tubes (Vidali et al., 1999), maize pollen (Wu and Yan, 2000) and *Hydrocharis* root hairs (Tominaga et al., 2000). For *Hydrocharis* root hairs, it was shown that a villin homologue

is involved in the bundling of actin filaments which are present in transvacuolar strands (Tominaga et al., 2000). This is an interesting observation for us, since the rearrangement of the actin cytoskeleton after Nod factor application may be described as bundling/unbundling of actin filaments at the base of the FB-actin area (arrow Fig. 2, see
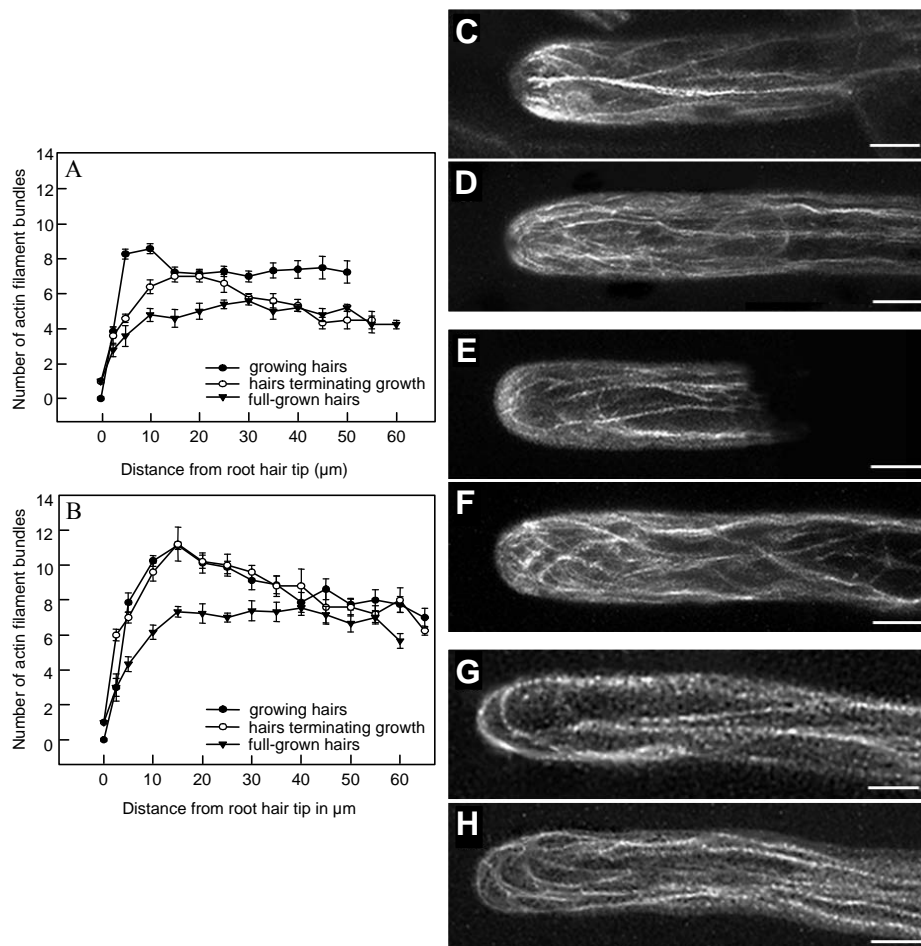
Figure 2. Changes in the density of fine bundles of actin filaments in the subapical area of *Vicia sativa* root hairs after Nod factor application. Graphs showing the increase in the number of actin filament bundles before (**A**) and between three to 15 minutes after (**B**) Nod factor application. **C**, **D**, **E**, **F**, **G** and **H**, Visualization of actin filaments after staining with rhodamine-phalloidin before (**C**, **E** and **G**) and after (**D**, **F** and **H**) Nod factor application to growing (**C** and **D**), growth-terminating (**E** and **F**) and full grown (**G** and **H**) *Vicia sativa* root hairs. Bar: 10 µm. (Adapted from De Ruijter *et al.*, 1999, MPMI).

also De Ruijter et al. 1999), i.e. the interface between the subapical FB-actin and the thicker bundles of actin filaments in the cytoplasmic strands.

Actin-depolymerizing factor (ADF)

A third group of ABPs that may be relevant in Nod factor-induced actin cytoskeleton remodelling is the actin depolymerizing factor (ADF) family, which includes destrin, cofilin and actophorin (Staiger et al., 1997). ADF/cofilin is a 15±22 kDa protein that possesses an actin- and a PIP 2 -binding domain (Sun et al., 1995; Staiger et al., 1997; Welch et al., 1997; for review on actin and ABPs in plant cells see De Ruijter and Emons, 1999; for review of ABPs see Cooper and Schafer, 2000). ADF binds to phosphoinositides and promotes actin dynamics in vitro. The ability of ADF to sever and depolymerize FB-actin is not directly dependent on the $[Ca^{2+}]_c$, but on pH (Staiger et al., 1997; Maciver et al., 1998). In maize growing root hairs, ADF can be localized in the apex and sub-apex (Jiang et al., 1997), where FB-actin is also present (Miller et al., 1999), whereas it is uniformly distributed in bulging trichoblasts in which no FB-actin has been detected (Miller et al., 1999). It has been shown that upon application of Nod factors a sustained alkalinization of the root hair cytoplasm occurred (Ehrhardt et al., 1992; Felle et al., 1995, 1996). This increase in pH might activate ADF, thus leading to F-actin depolymerization and subsequent remodelling of the actin cytoskeleton.

Spectrin

Animal spectrins possess at least two actin filament-binding sites, as well as binding sites for calcium and calmodulin (Tanaka et al., 1991; Puius et al., 1998). Spectrins are proteins involved in cross-linking actin filaments through Ca^{2+}/CaM-regulated coupling of plasma membrane proteins to actin (Tanaka et al., 1991) and also in mediating signal transduction through interactions with extracellular proteins via integrins (Burridge et al., 1988). Spectrin-like antigens are present in growing, but not in full-grown *Vicia sativa* root hair tips and reappear in hairs that are terminating growth when Nod factor is applied (De Ruijter et al., 1998). Unfortunately, a plant spectrin gene has not yet been cloned and its function is not known.

Arp2/3 complex

A protein complex that should be studied in root hairs before and after Nod factor application is the Arp2/3 complex. In vitro, purified Arp2/3 complex binds to the side of actin filaments and nucleates the formation of actin filaments with barbed ends (Mullins et al., 1998; Mullins, 2000). Mullins (2000) proposes that, in animal cells, prenylated GTP-bound CDC42 (a member of the Rho-GTPases family) localizes to the plasma membrane

where it recruits and activates WASP (Wiskott-Aldrich Syndrome Protein). WASP then recruits the Arp2/3 complex and stimulates its nucleation activity. The Arp2/3 complex then nucleates formation of actin filaments and cross-links them into a branching network. Finally, the elongation of free barbed-ends causes protrusion of the plasma membrane. A similar process of actin filament nucleation from existing filaments may be involved in FB-actin density increase after Nod factor application. The hypothesis cannot be extrapolated as such to root hairs, however, since in the hairs with FB-actin protrusion, i.e. in the growing and Nod factor stimulated hairs, the actin filaments do not appear to be close enough to the plasma membrane (Miller et al., 1999). The presence of a putative Arp2 homologue has been demonstrated in *Arabidopsis* (Klahre and Chua, 1999; Lin et al., 1999) and the study of its involvement in relation to tip growth and the re-arrangement of the actin cytoskeleton after Nod factor treatment would be an exciting challenge.

Myosin

Remodelling of the actin cytoskeleton is necessary for the Nod factor-induced root hair deformation to take place, but might not be suffcient in itself to explain the entire process. Yokota et al. (1999) reported that the absence of cyto-plasmic streaming at the tip of lily pollen tubes is due to the inhibition of a 170 kDa-myosin. This 170 kDa-myosin from lily pollen tubes possesses calmodulin (CaM) as a light chain. Binding of Ca^{2+} to this CaM induced a partial dissociation of the light chain from the heavy chain (Yokota et al., 1999) - this was sufficient to inhibit myosin activity. These authors also reported that in *Characean* cells the inhibition of myosin is triggered by phosphorylation through a Ca^{2+}-dependent protein kinase (CDPK). Moutinho et al. (1998) studied the distribution of CDPK activity in growing pollen tubes of *Agapanthus umbellatus* and found a higher CDPK activity at their tip. In non-growing pollen tubes, CDPK activity was uniformly distributed throughout the cell. The photo-release of caged Ca^{2+} on one side of the apical dome resulted in a local increase of CDPK activity at the site of release. From these results, it can be hypothesized that Ca^{2+} is responsible for the release of vesicles from actin filaments through inhibition of a 170 kDa-myosin homologue; myosin iso-forms responsible for the movement of bigger organelles might exhibit a lower or no sensitivity to Ca^{2+}. This hypothesis is in good agreement with the presence of a vesicle-rich region (clear zone), devoid of large organelles, at the tip of tip-growing cells.

Cytoplasmic streaming, endoplasmic reticulum re-orientation, vacuolation and nuclear movement

During root hair growth, large organelles are absent from the tip proper which contains only vesicles (Fig. 3A, see also Miller et al., 2000). Organelles in the rest of the root hair move upward towards the tip in the tube flanks. The organelles reverse the direction of movement in the cytoplasmic dense subapex, inside a cytoplasmic strand; this can occur either in the cell centre or near the flank of the tube. This pattern of organelle movement is called reverse fountain streaming (*Medicago truncatula*: Sieberer and Emons, 2000). The endoplasmic reticulum (ER) in the central part of the cytoplasmic dense region, the subapex of the cell, is aligned longitudinally (Fig. 3B; Miller et al., 2000). The large central vacuole is located below the nucleus at the base of the cytoplasmic dense region and has thin protrusions into this region. When root hairs terminate growth, the vacuole gradually overtakes the nucleus and moves towards the tip while the cytoplasmic dense region decreases in size (Sieberer and Emons, 2000). This process continues until the central vacuole fills the hair tip at hair maturity, except for a thin surrounding layer of cytoplasm. During growth termination, the ER becomes aligned transversely to the cell axis (Fig. 3C, see also Miller et al., 2000). When comparing actin data (Fig. 2, see also Miller et al., 1999) with TEM observations of ER (Fig. 3B and C, see also Miller et al., 2000), one can deduce that ER co-aligns with the actin filaments; however, this still needs to be proven in double-labelling experiments.

When Nod factors are applied to roots growing between glass slides, the central vacuole in hairs that are terminating growth expands towards the hair tip more rapidly than in normal growth-terminating hairs (Sieberer and Emons, 2000). At the same time, the vesicles that were present at the tip seem to be spread out over a larger plasma membrane area, as seen in TEM images (Miller et al., 2000). This could cause the swelling of the tip of these hairs, always seen in this assay. In the swelling the ER is aligned with the plasma membrane, meaning that at the cell tip the ER is transverse to the hair's long axis (Fig. 3C), as it was in these growth-terminating hairs before Nod factor application. Bundles of actin filaments in the swelling also have the same orientation. When the outgrowth emerges from the swelling, a new cytoplasmic dense region is rebuilt with reverse fountain cytoplasmic streaming, longitudinal ER and longitudinal FB-actin.

These results suggest that ER re-orientation upon application of Nod factors is likely to be related to the re arrangement of the actin cytoskeleton. The new outgrowth can become as long as a normal root hair, meaning that the final length is twice that of normal. Studying
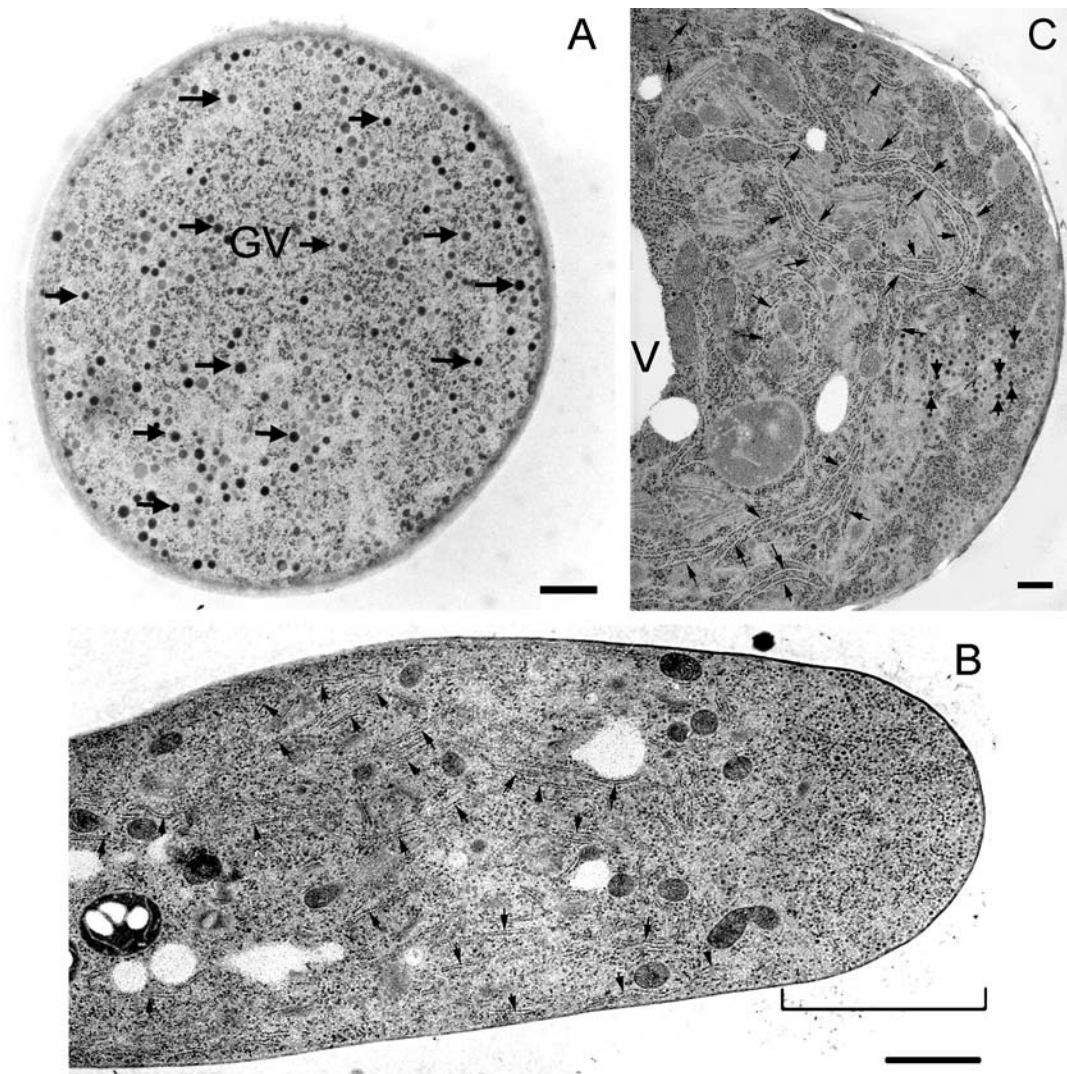
Figure 3

the dynamics of the actin cytoskeleton in living root hairs upon Nod factor application would lead to a better understanding of these processes. In this context, the use of transformed plants, able to produce green fluorescent protein-tagged actin, is very promising.

In a growing root hair, the nucleus exhibits an almost fixed position at the base of the cytoplasmic dense region, approx. 30 mm below the tip in *Medicago truncatula* (Fig. 4A; Sieberer and Emons, 2000). The nucleus, therefore, moves with the pace of tip growth (Ketelaar and Emons, 2000). When root hairs terminate growth, the nucleus loses this po-

Figure 3 (opposite page). Electron micrographs showing the ultrastructure of *Vicia sativa* root hairs. **A,** transverse section through the apical dome of a growing root hair, showing numerous vesicles (arrows) and the absence of any large organelles. GV: Golgi vesicles. Bar: 100 nm. **B,** longitudinal median section through the apex and sub-apex of a growing root hair, showing the presence of numerous longitudinally aligned ER cisternae in the sub-apex (arrows) and their absence in the apex (bracket). Bar: 2 μm. **C,** longitudinal section through the tip of a growth-terminating root hair (Bar: 1 μm). The vacuole is close to the tip and the cytoplasm is reduced to a thin layer along the plasma membrane. The ER (small arrows) at the tip is transversely aligned to the root hair axis. The vesicle-rich region is considerably reduced compared to that in a growing hair (**B**). Big arrows: Golgi vesicles. For material and methods, see Miller *et al.*, 2000).

sition and moves backwards in the shank (Fig. 4B; Sieberer and Emons, 2000) of the root hair where it assumes a random position. During Nod factor induced tip swelling, the nucleus is positioned at the base of the swelling (Fig. 4C; Sieberer and Emons, 2000). When the length of the new outgrowth has reached approx. 20 mm, the nucleus enters it.

The new outgrowth continues to grow and the nucleus again assumes a fixed position approx. 30 μm below the tip (Fig. 4D; Sieberer and Emons, 2000). When the outgrowth stops growing, the nucleus again moves backward in the shank of the root hair where it again assumes a random position. Although these results are not yet fully understood, they indicate that the position of the nucleus in the root hairs is important in the process of tip growth (Derksen and Emons, 1990; Ketelaar and Emons, 2000).

Calcium spiking

The above-mentioned cellular changes in actin, ER orientation, cytoplasmic streaming and vacuolation are rapid; they occur within minutes. They are related to Ca^{2+} by means of the $[Ca^{2+}]_c$ gradient at the cell tip. However, a different Ca^{2+} phenomenon has been observed approx. 9 min after Nod factor application. Ehrhardt et al. (1996) reported the presence of Ca^{2+} spikes originating from the perinuclear region of *Medicago sativa* root hairs to which host specific Nod factors were applied. The spikes propagated bi-directionally from the perinuclear area. Measurements taken along the root hairs showed that the amplitude of

the spikes decreased with distance from the perinuclear area and that no spikes were detected at the tip. A non-nodulating *Medicago sativa* mutant failed to show such Ca^{2+}
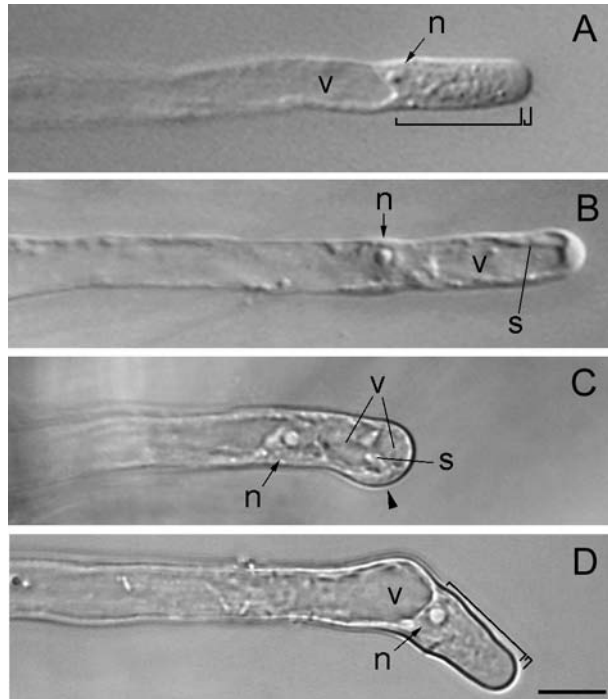

Figure 4. DIC microscopy images of control and Nod factor-induced root hair deformation in *Medicago truncatula* root hairs. **A,** Untreated growing hair. **B,** untreated growth-terminating root hair. **C,** Growth-terminating root hair approximately 105 minutes after Nod factor application with swollen tip. **D,** Nod factor-induced outgrowth from swelling approximately 210 minutes after Nod factor application. Note the similar cytoarchitecture of the growing hair (**A**) and of the outgrowth after Nod factor application (**D**). *n*, Nucleus, *v*, vacuole, *s*, strands of cytoplasm. Large bracket: cytoplasmic dense region. Small bracket: vesicle-rich region. Black arrowhead: site of new outgrowth emergence from the swollen tip. Bar: 20 μm. (Reproduced with the permission of Protoplasma from Sieberer and Emons, 2000).

spiking, whereas seedlings from the parental line from which the mutant was isolated showed a normal pattern of spiking. From these results, the authors suggested that the initiation of Ca^{2+} elevation in the region of the cell nucleus implies that either Ca^{2+} stores or channels, which mediate Ca^{2+} release, are localized in this region and are probably internal. Similar spiking has been observed in the root hairs of other species, e.g. *Vicia*, *Lotus*, *Medicago* and *Pisum* (Downie and Walker, 1999). IP 3 is known to induce Ca^{2+} release from internal stores such as vacuoles (Alexandre and Lassalles, 1990; Alexandre et al., 1990) and ER (in animal cells: De Young and Keizer, 1992; in plant cells: Bush, 1995; Muir and Sanders, 1997; Gong et al., 1998).

Because ER is especially located in the perinuclear area of root hairs (not shown), the spikes observed by Ehrhardt et al. (1996) and Cárdenas et al. (1998) are possibly initiated by Ca^{2+} release from IP 3 -sensitive ER stores. The lag phase between Nod factor

application and the appearance of the spikes, and the fact that they are only clearly detectable in the vicinity of the nucleus, indicate they are unlikely to be related to the early Nod factor-induced cellular changes discussed above. The role of the spikes is currently unclear; however, they may carry information to other parts of the cell or be involved in gene expression (Schultze and Kondorosi, 1998; Felle et al., 1999a, b) and subsequent protein synthesis. The spikes originate from the perinuclear region and a high $[Ca^{2+}]$ can be observed in the nucleus 5 s after the initiation of spiking (Ehrhardt et al., 1996), which is consistent with mechanisms involving the nucleus. Whether the experiments of Pingret et al. (1998) showing the involvement of G-proteins and PLC are related to the high $[Ca^{2+}]_c$ at the cell tip or calcium spiking around the nucleus should be studied further by application of drugs and the scoring of cellular events over time.

Spikes were observed for at least 60 min and up to 3 h (Ehrhardt et al., 1996). It seems unlikely that the internal stores contain such high amounts of Ca^{2+} as to sustain spiking for hours. Thus a process for store refilling is required. Felle et al. (1999a) suggested that at least a part of the Nod factor response is triggered by Ca^{2+} from internal stores. This response was blocked using the endomembrane Ca^{2+}-ATPase inhibitor, 2,5-di(t-butyl)-1,4 benzohydroqui-none, which presumably mobilizes Ca^{2+} from IP 3–sensitive stores. Their results suggest that Ca^{2+}-ATPase might be involved in refilling of internal stores as described for animal cells (Alberts et al., 1994). In addition, the mathematical model of De Young and Keizer (1992) shows that a single pulse of IP 3 is enough to generate spikes through a self-sustained mechanism involving Ca^{2+}-activation of PLC and Ca^{2+}-ATPase. In this model, a single pulse of IP 3 is su†cient to induce Ca^{2+} spiking according to the following process: binding of IP 3 to its receptor on the endoplasmic reticulum membrane induces the opening of Ca^{2+} channels and a subsequent rapid release of Ca^{2+} into the cytosol. The increasing $[Ca^{2+}]_c$ slowly inactivates the IP 3 receptor and activates Ca^{2+}-ATPase pumps on the ER membrane, thus initiating the refilling of the ER. When the $[Ca^{2+}]_c$ has been reduced sufficiently, the inactivation disappears and the channel again quickly activates. In addition, elevated $[Ca^{2+}]_c$ can directly activate PLC leading an increased production of IP 3 .Ca^{2+} spikes can thus be generated and maintained by a single pulse of IP 3 and a single Ca^{2+} store (ER) using a mechanism involving positive and negative feedback of Ca^{2+} on PLC and the IP 3 -receptor. This model is highly consistent with the spikes observed by Ehrhardt et al. (1992) and Cárdenas et al. (1999), which were initiated approx. 9 min after Nod factor application and lasted for several hours. According to this model, IP 3 in root hairs might be responsible for Ca^{2+} spikes, but not for the elevated tip-focused $[Ca^{2+}]$.

Exocytosis and cell wall formation

In tip growing cells, growth takes place by the fusion of exocytotic Golgi vesicles at the tip. The membrane of the vesicles is inserted into the plasma membrane and the vesicle content is delivered into the extracellular matrix and assembles within the cell wall. Using differential interference contrast (DIC) microscopy, we have shown that just below the tip of a growing root hair, a thin area devoid of large organelles is present, the so called clear zone (Miller et al., 1997; *Vicia sativa*: De Ruijter et al., 1998; *Medicago truncatula*: Sieberer and Emons, 2000). The area is in fact filled completely with vesicles (Fig. 3A; Miller et al., 2000; for more references see reviews by Miller et al., 1997; Emons and De Ruijter, 2000), and, thus, is also called the vesicle-rich region. We do not know how the vesicles move within the vesicle-rich region. If they are continually delivered at the base of this region by the FB-actin and consumed at the plasma membrane by exocytosis, they may not need a transport system.

As far as is known now, the docking and fusion of vesicles with the plasma membrane involves Ca^{2+} (Blackbourn et al., 1991, 1992; Blackbourn and Battey, 1993; Clark and Roux, 1995; Lin and Yang, 1997; Carroll et al., 1998; Yang, 1998; Battey et al., 1999), annexins (Blackbourn et al., 1991, 1992; Blackbourn and Battey, 1993; Clark and Roux, 1995; Carroll et al., 1998; Yang, 1998; Battey et al., 1999), Rho-GTPases (Lin et al., 1996; Lin and Yang, 1997; Yang, 1998; Battey et al., 1999; Sanderfoot and Raikhel, 1999) and proteins from the Soluble N-ethylmaleimide-sensitive factor Attachment Protein Receptor (SNARE) family (Battey and Blackbourn, 1993; Battey et al., 1999; Sanderfoot and Raikhel, 1999). A general hypothesis for the mechanism of exocytosis has been proposed for animal cells (for review see Sanderfoot and Raikhel, 1999), which is in good agreement with what is known about the control of exocytosis in plant cells (for review see Battey and Blackbourn, 1993), and with other work that has shown the presence of Rho-GTPases in pollen tubes (Lin et al., 1996; Lin and Yang, 1997; Yang, 1998) and t-SNARE-like proteins in plant cells (Battey et al., 1999). The mechanism behind Rho-GTPases–Ca^{2+} interaction is still unknown; an explanation could be that Rho-GTPases regulate the accumulation of intracellular Ca^{2+} which itself is thought to be involved in the regulation of exocytosis through annexins (Blackbourn and Battey, 1993). The fact that in tip growing cells a high tip focused $[Ca^{2+}]_c$, Rho-GTPases (in *Pisum sativum* pollen tube: Lin et al., 1996; Lin and Yang, 1997) and annexin-like proteins (in *Pisum sativum* pollen tube: Blackbourn et al., 1991) can be detected at the tip only during growth supports the suggested mechanism.

Cell wall deposition and exocytosis are inter-related phenomena. Golgi vesicles carry newly synthesized cell wall materials which are delivered to the extra-cellular matrix by exocytosis. Meanwhile, the Golgi vesicle membranes carry the rosettes (Haigler and Brown Jr, 1986) which are the cellulose synthases (Kimura et al., 1999). Assembly of the cell wall material within the existing wall contributes to its rigidification. In tip growing cells, there is a delicate balance between cell wall rigidification and cell expansion (pollen tube: Derksen, 1996): a rapid cell wall rigidification will prevent cell expansion, whereas a high degree of membrane insertion coupled to slow cell wall rigidification will lead to a swollen tip and even bursting (Schnepf, 1986; Battey and Blackbourn, 1993). To date, little research has been done on the molecular composition and subsequent alterations in the cell wall during root hair development.

After application of Nod factors to *Vicia sativa* or *Medicago truncatula* roots growing between glass slides, growth-terminating root hair tips swell (Fig. 4C) and the cell wall of the swelling exhibits a mottled aspect (Fig. 5A, see also Miller et al., 2000). This is comparable to the appearance of the cell wall during bulge formation (Fig. 5B), but different from the wall before bulging or swelling (Fig. 5C, see also Miller et al., 2000). Cell wall acidification has also been demonstrated during bulge formation (Bibikova et al., 1998); the initiation of root hair formation was arrested when acidification was prevented. A role for acidification in cell wall relaxation has been proposed (Pritchard, 1994) and expansins – proteins that trigger cell wall relaxation under acidic pH – are likely to be involved in this process (Cosgrove, 2000). Thus, it can be suggested that Nod factors induce cell wall relaxation during swelling of root hair tips and that this mechanism may be comparable to that of bulge formation. Immunogold electron microscopy studies are required to further identify the molecules, both structurally and enzymatically, involved in the synthesis and Nod factor-induced modification of the root hair cell wall.

Early nodulin genes (ENODs) are induced shortly (a few hours) after Nod factor application (Nap and Bisseling, 1990; Hadri and Bisseling, 1998). Most of the ENOD genes are hydroxyproline-rich glycoproteins (HPRG-proteins) and are thought to be cell wall proteins, which are extensively post-translationally modified (Hadri and Bisseling, 1998; Schultze and Kondorosi, 1998; Jahraus and Bisseling, 2000). Due to their sequence, these genes are thought to be involved in the formation of the infection thread (extensins, glycine-rich proteins and a peroxidase) (for a review of Nod factors-induced gene expression see Hadri and Bisseling, 1998; Schultze and Kondorosi, 1998; Jahraus and
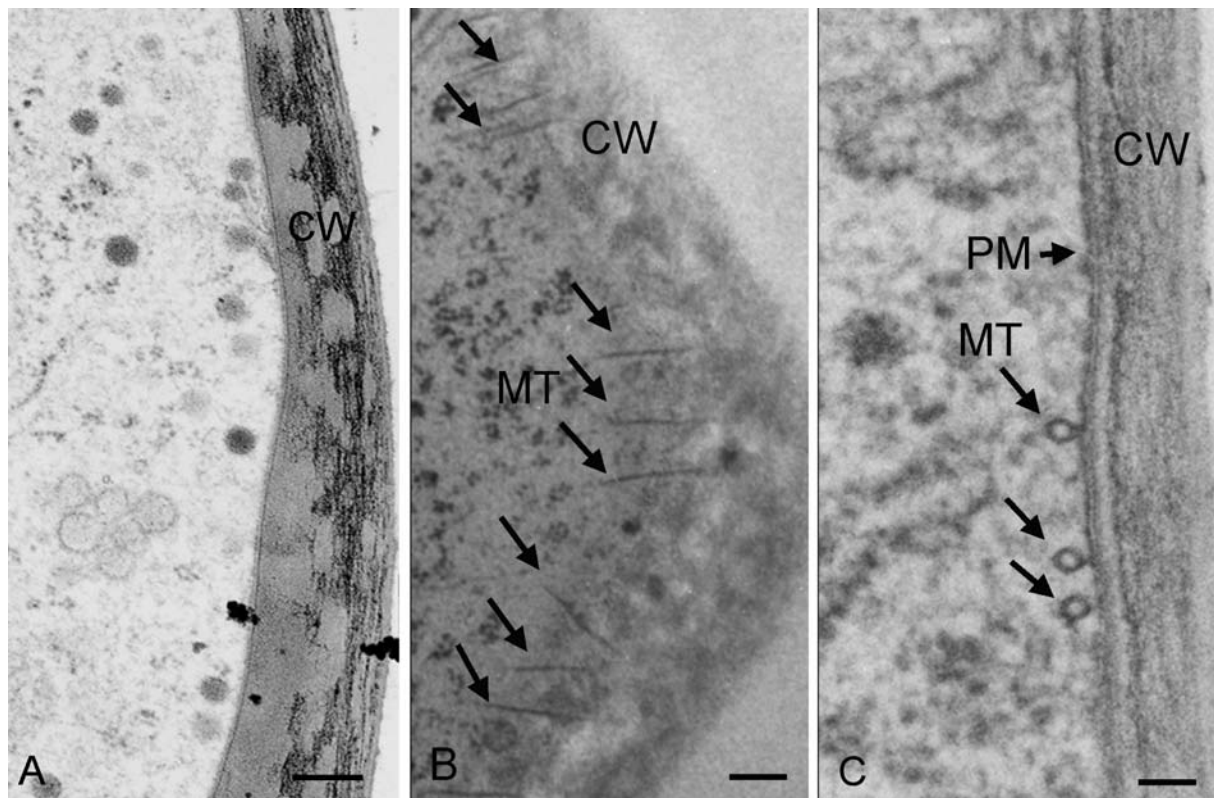
Figure 5. Electron micrographs of longitudinal sections of *Vicia sativa* root hairs. **A**, swollen tip of *Vicia sativa* root hair 52 minutes after Nod factor application. Bar: 200 nm. Note the mottled aspect of the cell wall at the tip that is similar to the aspect of cell wall during bulge formation (**B**, bar: 100 nm) and completely different from the cell wall of an epidermal cell before bulge formation (**C**, bar: 100 nm). CW: cell wall, MT: microtubules, PM: plasma membrane, arrows: microtubules. For material and methods, see Miller *et al*., 2000).

Bisseling, 2000). Interestingly, the first gene expressed (Vb1) encodes for a leghaemoglobin; its expression is even faster than ENOD12. Vb1 is expressed in root hairs, but its expression is markedly higher in nodules (Hadri and Bisseling, 1998; Schultze and Kondorosi, 1998).

Future prospects

When rhizobia colonize roots, only growing root hairs become infected and curl around the colony of dividing bacteria (Kijne, 1992). However, in assays in which the purified

Figure 6. DIC microscopy image of a *Medicago truncatula* root hair 2 days after spot inoculation with *Rhizobium meliloti*. The root hair has curled forming a pocket in which the bacteria are entrapped, the so-called 'shepherd's crook'.

Nod factor is added to roots growing between glass slides, root hair deformation is induced in growth-terminating root hairs, as discussed above. From these experiments it is clear that Nod factor reinforces tip growth. This can be observed in hairs that are terminating growth, but we know that Nod factor gives the same membrane depolarization, calcium ion influx, increase in FB-actin density and gene expression in growing hairs. It seems that tip growth is also reinforced in the growing hairs. Therefore, we propose that curling is due to reinforcement of tip growth, though only at one side of the hair. This curling can be understood as follows. When a host-specific bacterium attaches close to the root hair tip hemisphere and excretes Nod factors, which are immobile inside the cell wall (Goedhart et al., 1999), tip growth is stimulated but only at the attachment side (Emons and Mulder, 2000). The bacteria create a new centre of influence, thus redirecting tip growth towards them. Because the bacteria multiply, the surface contact area between the two organisms enlarges. Therefore, the new cell tip will touch the new bacteria, which excrete Nod factors too, and again redirect root hair tip growth towards the colony of bacteria. Since this happens continuously in time, the orientation of tip growth rotates in one direction and this gives rise to a tight curl in which the bacteria are entrapped (Fig. 6), a so-called shepherd's crook. It is essential that experiments to verify the redirection of the FB-actin and the tip-localized $[Ca^{2+}]_c$ in the direction of a colony of bacteria are now performed. Other fields for future research are the occurrence and mode of action of actin binding proteins, Rho-GTPases, and, directly

related to this point, the role of second messengers, especially IP 3 and PA. In our laboratory, work is currently in progress to elucidate the involvement and role of these molecules in studies that combine the use of drugs and mutant plants.

Acknowledgments

Literature cited

Alberts B, Bray D, Lewis J, Raff M, Roberts K, Watson JD. 1994. Cell signaling. In: Robertson M, Adams R, Cobert SM, Goertzen D, eds. Molecular biology of the cell. New York: Garland Publishing, 721-786.

Alexandre J, Lassalles JP. 1990. Effect of D-myo-inositol 1,4,5-trisphosphate on the electrical properties of the red beet vacuole membrane. Plant Physiology 93: 837-840.

Alexandre J, Lassalles JP, Kado RT. 1990. Opening of Ca^{2+} channels in isolated red beet root vacuole membrane by inositol 1,4,5- trisphosphate. Nature 343: 567-570.

Ardourel M, Demont N, Debellé F, Maillet F, De Billy F, Promé J-C, Dénarié J, Truchet G. 1994. *Rhizobium meliloti* lipooligosacchar-ide nodulation factors: different structural requirements for bacterial entry into target root hair cells and induction of plant symbiotic developmental responses. Plant Cell 6: 1357-1374.

Battey NH, Blackbourn HD. 1993. Tansley review No. 57. The control of exocytosis in plant cells. New Phytologist 125: 307-338.

Battey NH, James NC, Greenland AJ, Brownlee C. 1999. Exocytosis and endocytosis. Plant Cell 11: 643-659.

Bibikova T, Zhigilei A, Gilroy S. 1997. Root hair growth in *Arabidopsis thaliana* is directed by calcium and an endogenous polarity. Planta 203: 495-505.

Bibikova TN, Jacob T, Dahse I, Gilroy S. 1998. Localized changes in apoplastic and cytoplasmic pH are associated with root hair development in *Arabidopsis thaliana*. Development 125: 2925-2934.

Blackbourn HD, Battey NH. 1993. Annexin-mediated secretory vesicle aggregation in plants. Physiologia Plantarum 89: 27-32.

Blackbourn HD, Walker JH, Battey NH. 1991. Calcium-dependent phospholipid-binding proteins in plants – Their characterization and potential for regulating cell growth. Planta 184: 67-73.

Blackbourn HD, Barker PJ, Huskisson NS, Battey NH. 1992. Properties and partial protein sequence of plant annexins. Plant Physiology 99: 864-871.

Bladergroen MR, Spaink HP. 1998. Genes and signal molecules involved in the rhizobia-leguminoseae symbiosis. Current Opinion in Cell Biology 1: 353-359.

Braun M, Balusĭka F, Von Witsch M, Menzel D. 1999. Redistribution of actin, profilin and phosphatidylinositol-4,5-bisphosphate in growing and maturing root hairs. Planta 209: 435-443.

Burridge K, Fath K, Kelly T, Nuckolls G, Turner C. 1988. Focal adhesions: Transmembrane junctions between the extracellular matrix and the cytoskeleton. Annual Review of Cell Biology 4: 487-525.

Bush DS. 1995. Calcium regulation in plant cells and its role in signaling. Annual Review of Plant Physiology and Plant Molecular Biology 46: 95-122.

Cárdenas L, Vidali L, Dominguez J, Pérez D, Sánchez F, Hepler PK, Quinto C. 1998. Rearrangement of actin microfilaments in plant root hairs responding to *Rhizobium etli* nodulation signals. Plant Physiology 116: 871-877.

Cárdenas L, Feijó JA, Kunkel JG, Sánchez F, Holdaway-Clarke T, Hepler PK, Quinto C. 1999. *Rhizobium* Nod factors induce increases in intracellular free calcium influxes in bean root hairs. Plant Journal 19: 347-352.

Carroll AD, Moyen C, Van Kesteren P, Tooke F, Battey NH, Brownlee C. 1998. Ca^{2+}, annexins, and GTP modulate exocytosis from maize root cap protoplasts. Plant Cell 10: 1267-1276.

Clark GB, Roux SJ. 1995. Annexins of plant cells. Plant Physiology 109: 1133-1139.

Cooper JA, Schafer DA. 2000. Control of actin assembly and disassembly at filament ends. Current Opinion in Cell Biology 12: 97-103.

Cosgrove DJ. 2000. New genes and new biological roles for expansins. Current Opinion in Cell Biology 3: 73-78.

Demont-Caulet N, Maillet F, Tailler D, Jacquinet J-C, Promé J-C, Nicolaou KC, Truchet G, Beau J-M, Dénarié J. 1999. Nodule-inducing activity of synthetic *Sinorhizobium meliloti* nodulation factors and related lipo-chitooligosaccharides on alfalfa. Importance of the acyl chain structure. Plant Physiology 120: 83-92.

Derksen J. 1996. Pollen tubes: a model system for plant cell growth. Botanica Acta 109: 341-345.

Derksen J, Emons AMC. 1990. Microtubules in tip growth systems. In: Heath IB, ed. Tip growth in Plant and Fungal Cells. San Diego: Academic Press, 147-181.

De Ruijter NCA, Emons AMC. 1999. Actin-binding proteins in plant cells. Plant Biology 1: 26-35.

De Ruijter NCA, Bisseling T, Emons AMC. 1999. *Rhizobium* Nod factors induce an increase in sub-apical fine bundles of actin filaments in *Vicia sativa* root hairs within minutes. Molecular Plant-Microbe Interaction 12: 829-832.

De Ruijter NCA, Rook MB, Bisseling T, Emons AMC. 1998. Lipochito-oligosaccharides re-initiate root hair tip growth in *Vicia sativa* with high calcium and spectrin-like antigen at the tip. Plant Journal 13: 341-350.

De Vrije T, Munnik T. 1997. Activation of phospholipase D by calmodulin antagonists and mastoparan in carnation petals. Journal of Experimental Botany 314: 1631-1637.

De Young GW, Keizer J. 1992. A single-pool inositol 1,4,5-trispho-sphate-receptor based model for agonist-stimulated oscillation in Ca^{2+} concentration. Proceedings of the National Academy of Sciences, USA 89: 9895-9899.

Diaz CL, Logman TJJ, Stam HC, Kijne JW. 1995. Sugar-binding activity of pea lectin expressed in white clover hairy roots. Plant Physiology 109: 1167-1177.

Diaz CL, Spronsen PC, Bakhuizen R, Logman GJJ, Lugtenberg BJJ, Kijne JW. 1986. Correlation between infection by *Rhizobium leguminosarum* and lectin on the surface of *Pisum sativum* L. roots. Planta 168: 350-359.

Djordjevic MA, Schofield PR, Rolfe BG. 1985. Tn5 mutagenesis of *Rhizobium trifolii* host-specific nodulation genes results in mutants with altered host-range ability. Molecular and General Genetics 200: 463-471.

Downie AJ, Walker SA. 1999. Plant responses to nodulation factors. Current Opinion in Cell Biology 2: 483-489.

Dyer JH, Zheng L, Wang X. 1995. Cloning and nucleotide sequence of a cDNA encoding phospholipase D from Arabidopsis (accession No. U36381) (PGR 95-096). Plant Physiology 109: 1497.

Ehrhardt DW, Atkinson EM, Long SR. 1992. Depolarization of Alfalfa root hair membrane potential by *Rhizobium meliloti* Nod factors. Science 256: 998-1000.

Ehrhardt DW, Wais R, Long SR. 1996. Calcium spiking in plant root hairs responding to *Rhizobium* nodulation signals. Cell 85: 673-681.

Emons AMC, De Ruijter NCA. 2000. Actin: a target for signal transduction in root hairs. In: Staiger C, Baluska F, Volkmann D, Barlow P, eds. Actin: a dynamic framework for multiple plant cell functions. Dordrecht: Kluwer Academic Publishers, 373-390.

Emons AMC, Mulder B. 2000. Nodulation factors trigger an increase of fine bundles of subapical actin filaments in Vicia root hairs: Implications for root hair curling around bacteria. In: De Wit JGM, Bisseling T, Stiekema W, eds. Biology of plant-microbe interaction (vol. 2). St. Paul, USA: International Society for Molecular Plant-Microbe Interactions, 44-49.

Emons AMC, Wolters-Arts AMC. 1983. Cortical microtubules and microfibril deposition in the cell wall of root hairs of *Equisetum hyemale*. Protoplasma 117: 68-81.

Etzler ME, Kalsi G, Ewing NN, Roberts NJ, Days RB, Murphy JB. 1999. A nod factor binding lectin with apyrase activity from legume roots. Proceedings of the National Academy of Sciences, USA 96: 5856-5861.

Felle HH, Kondorosi E, Kondorosi A, Schultze M. 1995. Nod signal-induced plasma membrane potential changes in alfalfa root hairs are di•erentially sensitive to structural modifications of the lipochitooligosaccharide. Plant Journal 7: 939-947.

Felle HH, Kondorosi E, Kondorosi A, Schultze M. 1996. Rapid alkalinization in alfalfa root hairs in response to rhizobia lipochitooligosaccharide signals. Plant Journal 10: 295-301.

Felle HH, Kondorosi E, Kondorosi A, Schultze M. 1998. The role of ion fluxes in Nod factor signalling in *Medicago sativa*. Plant Journal 13: 455-463.

Felle HH, Kondorosi E, Kondorosi A, Schultze M. 1999a. Elevation of the cytosolic free $[Ca^{2+}]$ is indispensable for the transduction of the Nod factor signal in alfalfa. Plant Physiology 121: 273-279.

Felle HH, Kondorosi E, Kondorosi A, Schultze M. 1999b. Nod factors modulate the concentration of cytosolic free calcium differently in growing and non-growing root hairs of *Medicago sativa* L. Planta 209: 207-212.

Fisher RF, Long SR. 1992. *Rhizobium*-plant signal exchange. Nature 357: 655-660.

Franklin-Tong VE, Drøbak BK, Allan AC, Watkins PAC, Trewavas AJ. 1996. Growth of pollen tubes of *Papaver rhoeas* is regulated by a slow-moving calcium wave propagated by inositol 1,4,5-trisphosphate. Plant Cell 8: 1305-1321.

Goedhart J, RoÈhrig H, Hink MA, Van Hoek A, Visser AJWG, Bisseling T, Gadella TWJ Jr. 1999. Nod factors integrate spontaneously in biomembranes and transfer rapidly between membranes and to root hairs, but transbilayer flip-flop does not occur. Biochemistry 38: 10898-10907.

Goldschmidt-Clermont PJ, Furman MI, Wachsstock D, Safer D, Nachmias VT, Pollard TD. 1992. The control of actin nucleotide exchange by thymosin b4 and profilin. A potential regulatory mechanism for actin polymerisation in cells. Molecular Biology of the Cell 3: 1015-1024.

Gong M, Van der Luit AH, Knight MR, Trewavas AJ. 1998. Heat-shock-induced changes in intracellular Ca^{2+} level in tobacco seedlings in relation to thermotolerance. Plant Physiology 116: 429-437.

Gressent F, Drouillard S, Mantegazza N, Samain E, Geremia RA, Canut H, Niebel A, Driguez H, Ranjeva R, Cullimore J, Bono JJ. 1999. Ligand specificity of a high affinity binding site for lipo-chitooligosaccharidic Nod factors in *Medicago* cell suspension culture. Proceedings of the National Academy of Sciences, USA 96: 4704-4709.

Griebau R, Frentzen M. 1994. Biosynthesis of phosphatidylglycerol in isolated mitochondria of etiolated mung bean (*Vigna radiata* L.) seedlings. Plant Physiology 105: 1269-1274.

Hadri A-E, Bisseling T. 1998. Responses of the plant to Nod factors. In: Spaink HP, Kondorosi A, Hooykaas PJJ, eds. The Rhizobiaceae–molecular biology of model plant-associated bacteria. Dordrecht, Boston, London: Kluwer Academic Publishers, 403-416.

Haigler CH, Brown RM Jr. 1986. Transport of rosettes from the Golgi apparatus to the plasma membrane in isolated mesophyll cells of *Zinnia elegans* during differentiation to tracheary elements in suspension culture. Protoplasma 134: 111-120.

Heidstra R, Bisseling T. 1996. Nod factor-induced host responses and mechanisms of Nod factor perception. New Phytologist 133: 25-43.

Heidstra R, Geurts R, Franssen H, Spaink HP, Van Kammen A, Bisseling T. 1994. Root hair deformation activity of nodulation factors and their fate on Vicia sativa. Plant Physiology 105: 787-797.

Hirsch AM. 1992. Tansley review No 40. Developmental biology of legume nodulation. New Phytologist 122: 211-237.

Hirsch AM. 1999. Role of lectin (and rhizobial exopolysaccharides) in legume nodulation. Current Opinion in Plant Biology 2: 320-326.

Jahraus A, Bisseling T. 2000. *Rhizobium* induced plant gene expression in root hairs. In: Ridge RW, Emons AMC, eds. Cell and molecular biology of plant root hairs. Heidelberg, New York: Springer, 267-283.

Jan LY, Jan YN. 1997. Receptor-regulated ion channels. Current Opinion in Cell Biology 9: 155-160.

Jiang CJ, Weeds AG, Hussey PJ. 1997. The maize actin-depolymerizing factor, ZmADF3, redistributes to the growing tip of elongating root hairs and can be induced to translocate into the nucleus with actin. Plant Journal 12: 1035-1043.

Ketelaar T, Emons AMC. 2000. The role of microtubules in root hair growth and cellulose microfibril deposition. In: Ridge RW, Emons AMC, eds. Cell and molecular biology of plant root hairs. Heidelberg, New York: Springer, 17-28.

Kijne JW. 1992. The *Rhizobium* infection process. In: Stacey G, Burris R, Evans H, eds. Biological nitrogen fixation. New York, London: Chapman and Hall, 349-398.

Kimura S, Laosinchai W, Itoh T, Cui X, Linder CR, Brown RM Jr. 1999. Immunogold labeling of rosette terminal cellulose-synthesizing complexes in the vascular plant *Vigna angularis*. Plant Cell 11: 2075-2085.

Klahre U, Chua NH. 1999. The *Arabidopsis* actin-related protein 2 (AtARP2) promoter directs expression in xylem precursor cells and pollen. Plant Molecular Biology 41: 65-73.

Kurkdjian AC. 1995. Role of the differentiation of root epidermal cells in Nod factor (from *Rhizobium meliloti*)-induced root hair depolarization of *Medicago sativa*. Plant Physiology 107: 783-790.

Lerouge P, Roche P, Faucher C, Maillet F, Truchet G, Promé J-C, Dénarié J. 1990. Symbiotic host-specificity of *Rhizobium meliloti* is determined by a sulfated and acetylated glucosamine oligosac-charide signal. Nature 344: 781-784.

Lin Y, Yang Z. 1997. Inhibition of pollen tube elongation by microinjected anti-Rop1Ps antibodies suggests a crucial role for Rho-type GTPases in the control of tip growth. Plant Cell 9: 1647-1659.

Lin Y, Wang Y, Zhu J-K, Yang Z. 1996. Localization of a Rho GTPase implies a role in tip growth and movement of the generative cell in pollen tubes. Plant Cell 8: 293-303.

Lin X, Kaul S, Rounsley S and 34 others. 1999. Sequence and analysis of chromosome 2 of the plant *Arabidopsis thaliana*. Nature 402:761-768.

Long SR. 1996. *Rhizobium* symbiosis: Nod factors in perspective. Plant Cell 8: 1885-1898.

Mc Cormac DJ, Todd JF, Paliyath G, Thompson JE. 1993. Modulation of bilayer fluidity affects lipid catabolism in microsomal membranes of tomato fruit. Plant Physiology and Biochemistry 31: 1-8.

Machesky LM, Pollard TD. 1993. Profilin as a potential mediator of membrane-cytoskeleton communication. Trends in Cell Biology 3: 381-385.

Maciver SK, Pope BJ, Whytock S, Weeds AG. 1998. The effect of two actin depolymerizing factors (ADF/cofilins) on actin filament turnover: pH sensitivity of F-actin binding by human ADF, but not of *Acanthamoeba actophorin*. European Journal of Biochemistry 256: 388-397.

Malherbe A, Block MA, Douce R, Joyard J. 1995. Solubilization and biochemical properties of phosphatidate phosphatase from spinach chloroplast envelope membranes. Plant Physiology and Biochemistry 33: 149-161.

Malhó R. 1998. Role of 1,4,5-inositol triphosphate-induced Ca^{2+} release in pollen tube orientation. Sexual Plant Reproduction 11: 231-235.

Malhó R, Trewavas AJ. 1996. Localized apical increases of cytosolic free calcium control pollen tube orientation. Plant Cell 8: 1935-1949.

Miller DD, De Ruijter NCA, Emons AMC. 1997. From signal to form: aspects of the cytoskeleton-plasma membrane-cell wall continuum in root hair tip. Journal of Experimental Botany 316: 1881-1896.

Miller DD, De Ruijter NCA, Bisseling T, Emons AMC. 1999. The role of actin in root hair morphogenesis: studies with lipochito-oligosaccharide as a growth stimulator and cytochalasin as an actin perturbing drug. Plant Journal 17: 141-154.

Miller DD, Leferink-ten Klooster HB, Emons AMC. 2000. Lipochito-oligosaccharide nodulation factors stimulate cytoplasmic polarity with longitudinal endoplasmic reticulum and vesicles at the tip in Vetch root hairs. Molecular Plant-Microbe Interaction 13: 1385-1390.

Moutinho A, Trewavas AJ, Malhó R. 1998. Relocation of a Ca^{2+}-dependent protein kinase activity during pollen tube reorientation. Plant Cell 10: 1499-1509.

Muir SR, Sanders D. 1997. Inositol 1,4,5-trisphopshate-sensitive Ca^{2+} release across nonvacuolar membranes in cauliflower. Plant Physiology 114: 1511-1521.

Mullins RD. 2000. How WASP-family proteins and the Arp2/3 complex convert intracellular signals into cytoskeletal structures. Current Opinion in Cell Biology 12: 91-96.

Mullins RD, Heuser JA, Pollard TD. 1998. The interaction of Arp 2/3 complex with action: nucleation, high-affinity pointed end capping, and formation of branching networks of filaments. Proceedings of the National Academy of Sciences, USA 95: 6181-6186.

Munnik T, Irvine RF, Musgrave A. 1998. Phospholipid signalling in plants. Biochemica et Biophysica Acta 1389: 222-272.

Nap JP, Bisseling T. 1990. Nodulin function and nodulin gene regulation in root nodule development. In: Gresshoff PM, ed. Molecular biology of symbiotic nitrogen fixation. Boca Raton, Florida: CRC Press, Inc., 181-229.

Niebel A, Bono JJ, Ranjeva R, Cullimore JV. 1997. Identification of a high affinity binding site for lipo-oligosaccharidic NodRm factors in the microsomal fraction of *Medicago* cell suspension cultures. Molecular Plant-Microbe Interaction 10: 132-134.

Pappan K, Qin W, Dyer JH, Zheng L, Wang X. 1997. Molecular cloning and functional analysis of polyphosphoinositide-dependent phospholipase D, PLDb, from *Arabidopsis*. Journal of Biological Chemistry 11: 7055-7061.

Philip-Hollingsworth S, Dazzo FB, Hollingsworth RI. 1997. Structural requirements of *Rhizobium* chitolipooligosaccharides for uptake and bioactivity in legume roots as revealed by synthetic analogs and fluorescent probes. Journal of Lipid Research 38: 1229-1241.

Pingret J-L, Journet E-P, Barker DG. 1998. *Rhizobium* Nod factor signaling: evidence for a G protein-mediated transduction mechanism. Plant Cell 10: 659-671.

Pritchard J. 1994. The control of cell wall expansion in roots. New Phytologist 127: 3-26.

Puius YA, Mahoney NM, Almo SC. 1998. The modular structure of actin-regulatory proteins. Current Opinion in Cell Biology 10: 23-34.

Qin W, Pappan K, Wang X. 1997. Molecular heterogeneity of phospholipase D (PLD): cloning of PLDg and regulation of plant PLDa, b and g by polyphosphoinositides and calcium. Journal of Biological Chemistry 272: 28267-28273.

Robinson RC, Mejillano M, Le VP, Burtnick LD, Yin HL, Choe S. 1999. Domain movement in gelsolin: a calcium-activated switch. Science 286: 1939-1942.

Sanderfoot AA, Raikhel NV. 1999. The specificity of vesicle trafficking: coat proteins and SNAREs. Plant Cell 11: 629-641.

Schiefelbein JW, Shipley A, Rowse P. 1992. Calcium influx at the tip of growing root-hair cells of *Arabidopsis thaliana*. Planta 187: 455-459.

Schlaman HRM, Gisel AA, Quaedvlieg NEM, Bloemberg GV, Lugtenberg BJJ, Kijne JW, Potrykus I, Spaink HP, Sauter C. 1997. Chitin oligosaccharides can induce cortical cell division in roots of *Vicia sativa* when delivered by ballistic microtargeting. Development 124: 4887-4895.

Schnepf E. 1986. Cellular polarity. Annual Review of Plant Physiology 37: 23-47.

Schultze M, Kondorosi A. 1998. Regulation of symbiotic root nodule development. Annual Review of Genetics 32: 33-57.

Sieberer B, Emons AMC. 2000. Cytoarchitecture and pattern of cytoplasmic streaming in developing root hairs of *Medicago truncatula* and during deformation by Nod factors. Protoplasma 214: 118-127.

Sprent JI. 1992. Evolution of nitrogen fixing symbioses. In: Stacey G, Burris RH, Evans HJ, eds. Biological nitrogen fixation. New York, London: Chapman and Hall, 461-496.

Staiger CJ, Gibbon BC, Kovar DR, Zonia LE. 1997. Profilin and actin-depolymerizing factor: modulators of actin organization in plants. Trends in Plant Science 2: 275-281.

Staiger CJ, Yuan M, Valenta R, Shaw PJ, Warn RM, Lloyd CW. 1994. Microinjected profilin affects cytoplasmic streaming in plant cells by rapidly depolymerizing actin microfilaments. Current Biology 4: 215-219.

Sun HQ, Kwiatkowska K, Yin HL. 1995. Actin monomer binding proteins. Current Opinion in Cell Biology 7: 102-110.

Tanaka T, Kadowaki K, Lazarides E, Sobue K. 1991. Calcium ion-dependent regulation of the spectrin-actin interaction by calmodulin and protein 4.1. Journal of Biological Chemistry 266: 1134-1140.

Thion L, Mazars C, Nacry P, Bouchez D, Moreau M, Ranjeva R, Thuleau P. 1998. Plasma membrane depolarization-activated calcium channels, stimulated by microtubule-depolymerizing drugs in wild-type *Arabidopsis thaliana* protoplasts, display constitutively large and stable activities in ton 2 mutant cells affected in the organization of cortical microtubules. Plant Journal 16: 603-610.

Thuleau P, Schroeder JI, Ranjeva R. 1998. Recent advances in the regulation of plant calcium channels: evidence for regulation by G-proteins, the cytoskeleton and second messengers. Current Opinion in Cell Biology 1: 424-427.

Timmers ACJ, Auriac M-C, Truchet G. 1999. Refined analysis of early symbiotic steps of the *Rhizobium-Medicago* interaction in relationship with microtubular cytoskeleton rearrangements. Development 126: 3617-3628.

Timmers ACJ, Auriac M-C, De Billy F, Truchet G. 1998. Nod factor internalization and microtubular cytoskeleton change occur concomitantly during nodule differentiation in alfalfa. Development 125: 339-349.

Tominaga M, Yokota E, Vidali L, Sonobe S, Hepler PK, Shimmen T. 2000. The role of the plant villin in the organization of the actin cytoskeleton, cytoplasmic streaming and the architecture of the transvacuolar strand in root hair cells of *Hydrocharis*. Planta 210: 836-843.

Valster AH, Pierson ES, Valenta R, Hepler PK, Emons AMC. 1997. Probing the plant actin cytoskeleton during cytokinesis and interphase by profilin microinjection. Plant Cell 9: 1815-1824.

Van Himbergen JAJ, Ter Riet B, Meijer HJG, Van den Ende H, Musgrave A, Munnik T. 1999. Mastoparan analogues stimulate phospholipase C- and phospholipase D-activity in *Chlamydomonas*: a comparative study. Journal of Experimental Botany 341: 1735-1742.

Venverloo CJ, Libbenga KR. 1987. Regulation of the plane of cell division in vacuolated cells I. The function of nuclear positioning and phragmosome formation. Journal of Plant Physiology 131: 267-284.

Vidali L, Yokota E, Cheung AY, Shimmen T, Hepler PK. 1999. The 135 kDa actin-bundling protein from *Lilium longiflorum* pollen is the plant homologue of villin – Rapid communication. Protoplasma 209: 283-291.

Voisine R, Vezina LP, Willemot C. 1993. Modification of phospholipids catabolism in microsomal membrane of gamma-irradiated cauliflower (*Brassica oleracea* L.). Plant Physiology 102: 213-218.

Wang X. 1999. The role of phospholipase D in signaling cascades. Plant Physiology 120: 645-651.

Welch MD, Mallavarapu A, Rosenblatt J, Mitchison TJ. 1997. Actin dynamics *in vivo*. Current Opinion in Cell Biology 9: 54-61.

White PJ. 1998. Calcium channels in the plasma membrane of root cells. Annals of Botany 81: 173-183.

Wu W, Yan LF. 2000. Immunochemical identification of gelsolin in maize pollen. Chinese Science Bulletin 45: 256-259.

Wymer C, Bibikova TN, Gilroy S. 1997. Cytoplasmic free calcium distribution during the development of root hairs of *Arabidopsis thaliana*. Plant Journal 12: 427-439.

Yang Z. 1998. Signaling tip growth in plants. Current Opinion in Plant Biology 1: 525-530.

Yao X, Forte JG. 1996. Membrane-cytoskeleton interaction in regulated exocytosis and apical insertion of vesicles in epithelial cells. In: James NW, ed. Current Topics in Membranes, vol. 43. San Diego: Academic Press, 73-96.

Yokota E, Muto S, Shimmen T. 1999. Inhibitory regulation of higher-plant myosin by Ca^{2+} ions. Plant Physiology 119: 231-239.

Chapter 2

Cytoarchitecture and pattern of cytoplasmic streaming in developing root hairs of *Medicago truncatula* and during deformation by Nod factors

B. Sieberer and A. M. C. Emons

Laboratory of Experimental Plant Morphology and Cell Biology, Wageningen University, Wageningen

Summary

Cytoarchitecture and pattern of cytoplasmic streaming change during development of root hairs of *Medicago truncatula* and after challenge with Nodulation (Nod) factors. We measured the speed and orientation of movement of 1-2 μm long organelles. The speed of organelle movement in cytoplasmic strands in the basal part of growing root hairs is 8-14 μm/s and is of the circulation type like in trichoblasts, bulges before tip-growth initiation, and full-grown hairs. In the sub-apical area of growing hairs, reverse fountain streaming occurs discontinuously at a slower net-speed. The reason for the slower speed is the fact that organelles often stop and jump. Reverse fountain streaming is a pattern in which the main direction of organelle transport reverses 180 degrees before the cell tip is reached. Within minutes after their application to roots, *Rhizobium* derived Nod factors, cause an increase and divergence in the sub-apical cytoplasmic strands. This phenomenon can best be observed in the growth terminating hairs, since in hairs of this developmental stage, sub-apical cytoplasmic strands are transvacuolar. First, the tips of these hairs swell. The organelle movement in the swelling tip increases up to the level normal for circulation streaming, and the number of strands with moving organelles increases. When a new polar outgrowth emerges, reverse fountain streaming is set up again, with all its characteristics like those seen in growing hairs. This outgrowth may obtain a new full root hair length, by which these hairs may become twice as long as non-challenged hairs.

Key words: lipochito-oligosaccharides, *Medicago truncatula*, organelle movement, plant-*Rhizobium* interaction, tip growth, video microscopy

Abbreviations: DIC: differential interference contrast, LCO: lipochito-oligosaccharide, PGM: plant growth medium, FESEM: field emission scanning electron microscopy, VEC microscopy: video enhanced contrast microscopy

Introduction

During development of a root hair, from its initiation at the trichoblast to its full-grown state, the cytoarchitecture changes and with it the pattern of cytoplasmic streaming (for review see: Miller et al. 1997). These changes are intrinsically coupled to the occurrence of tip growth. Nod factors, lipochito-oligosaccarides excreted by *Rhizobium* bacteria, influence both cytoarchitecture and cytoplasmic streaming in root hairs of their host legume plants (for alfalfa see: Allen and Bennett 1996, for vetch see: De Ruijter et al. 1998, Miller et al. 1999). This leads to root hair deformation (Heidstra et al. 1994) in growth terminating hairs (De Ruijter et al. 1998). Root hair deformation is swelling of the root hair tip and subsequent tip growth from that swelling. In our assay in which roots are growing between glass slides, so-called Fåhraeus slides (Fåhraeus 1957), root hair deformation occurs only in hairs that are terminating growth. This does not mean that only those hairs are susceptible to Nod factors, nor, that those are the hairs that respond in the soil when in contact with rhizobacteria (Kijne 1992). In fact, all developmental stages of root hairs react with a change in the actin cytoskeleton (De Ruijter et al. 1999). We further want to make clear, like we have done before (Miller et al. 1997, De Ruijter et al.1998, Miller et al. 1999), that not the hairs that have just stopped growing deform in this assay, as was initially thought (Heidstra et al. 1994), but those hairs that can still grow for up to 10 %. In the present paper, we describe in *Medicago truncatula* the cytoarchitecture and pattern of cytoplasmic streaming in epidermal cells, bulges, tip polarity initiating bulges, tip growing hairs, growth terminating hairs, full-grown hairs, and hairs challenged with host-specific LCOs. The latter span the time interval from the disturbance of the cytoplasmic strands, swelling of the root hair tip, acquisition of new polarity and new sustained polar growth.

Material and Methods

Plant materials and growth conditions

Seeds from *Medicago truncatula* L. var. Jemalong (Fabaceae) were surface sterilized, imbibed in sterile water and placed on 1 % agarose plates. The plates were stored in the dark for 2-4 days at 4ºC to synchronize germination. During germination (6-8h, 24ºC) the seeds were protected from light.

Seedlings were grown in vertical orientation for 24-30h in micro-chambers in between a cover slip and a glass slide (Fåhraeus slides, Heidstra et al. 1994), stored at 24ºC and 16 h day length. The space in between the slide and the cover slip was 1.2 mm. The Fåhraeus slides contained 800 µl plant growth medium (PGM) consisting of an aqueous solution of 1.36 mM $CaCl_2$, 0.97 mM $MgSO_4$, 1.12 mM Na_2PO_4, 1.36 mM KH_2PO_4 and 20 µM Fe-citrate, pH 6.5 (Miller et al. 1999, modified from Fåhraeus 1957) and two seedlings.

Root hair deformation

Some seedlings were treated with 10^{-9} M or 10^{-10} M *Rhizobium leguminosarum* Nodulation (Nod) factors NodRm IV (Ac, S) diluted in PGM, while controls were treated with fresh PGM only.

Microscopy and image analysis

Root hairs during growth and Nod factor induced deformation were observed in the Fåhraeus slides in a Nikon Optiphot microscope (Nikon 20x, NA = 0.5 or 40x, NA = 0.7; Nomarski-DIC). Images were recorded on a Sony 3-CCD camera equipped with a framegrabbing unit (Sony DKR 700).

For higher magnification and resolution, root hairs were observed in a Univar microscope (Reichert-Leica) with Nomarski-DIC or brightfield (Reichert-Leica 40x oil immersion, Plan Apo 100x oil immersion, NA = 1.32, additional magnification changer 1.25x in the optical pathway of the microscope). Illumination was provided either by a low-voltage halogen lamp or a xenon lamp. For DIC the diaphragm of the oil immersion condenser (NA = 1.40) was fully open, for bright field it was closed to 1/3.

For VEC microscopy (DIC and bright field) (for further details about video enhancement see Lichtscheidl 1995, Lichtscheidl and Foissner 1996) images were collected either with a Sony-CCD camera or with a high resolution analog video camera (Chalnikon C2400, Hamamatsu) and then digitally processed with a Hamamatsu DVS 3000 image processing computer, displayed on a Sony high-resolution monitor, and recorded on a digital video recorder. Contrast enhancement was done with the analog control unit of the video camera and the image processor.

Measurements of the cell dimensions and organelle speed in cytoplasmic strands were done with a Hamamatsu Argus-20 real time digital contrast and low light enhancement image processor linked to a Hamamatsu C3077 CCD camera on a Nikon Diaphot 200

inverted microscope with Hoffman modulation contrast system. Measurements and tracking of organelle speed was measured with a micrometer-ocular at some of the samples.

Furthermore, the organelle dynamics in the cytoplasmic dense region at the tip of the root hairs were studied by slow motion or frame-by-frame playbacks of recorded video sequences.

For cryo-scanning electron microscopy, air grown roots were stuck on stubs with carbon glue, plunged into liquid nitrogen and coated with 2 nm platinum in an Oxford Instruments CT 1500 HF cryo-transfer unit mounted on a JEOL 6300F field emission cryo-scanning electron microscope.

Results

Medicago truncatula roots have a root hair on every root epidermal cell

Medicago truncatula roots have a root hair on every epidermal cell, as seen in Figures 1a and 1b which are FESEM images of an intact root (a) and a higher magnification of a root from which the root hairs had been shaved off (b). So in this species, every epidermal cell is a trichoblast. Since we suspected that this might be caused by ethylene levels caused by the growth conditions in the Fåhraeus slides, we took for Figures 1a,b roots grown in moist air on closed agar plates, the growth condition generally used for genetic screening of *Arabidopsis* root hair mutants. Figure 1c shows root hair length during development and deformation by Nod factors.

Cytoarchitecture and pattern of cytoplasmic streaming change during development of Medicago truncatula root hairs

The cytoarchitecture of living root hairs is shown in Fig. 2, the matching pattern of cytoplasmic streaming in Fig. 3.

Epidermal cell
Epidermal cells of *Medicago truncatula* roots consist of a peripheral cytoplasmic layer, containing all types of organelles, around a large vacuole, which may be traversed by cytoplasmic strands, also called transvacuolar strands. The nucleus can be anywhere in the

cell but always lies in the cytoplasm against a cell wall.

Cytoplasmic streaming is the overall transport of light microscopically visible organelles.
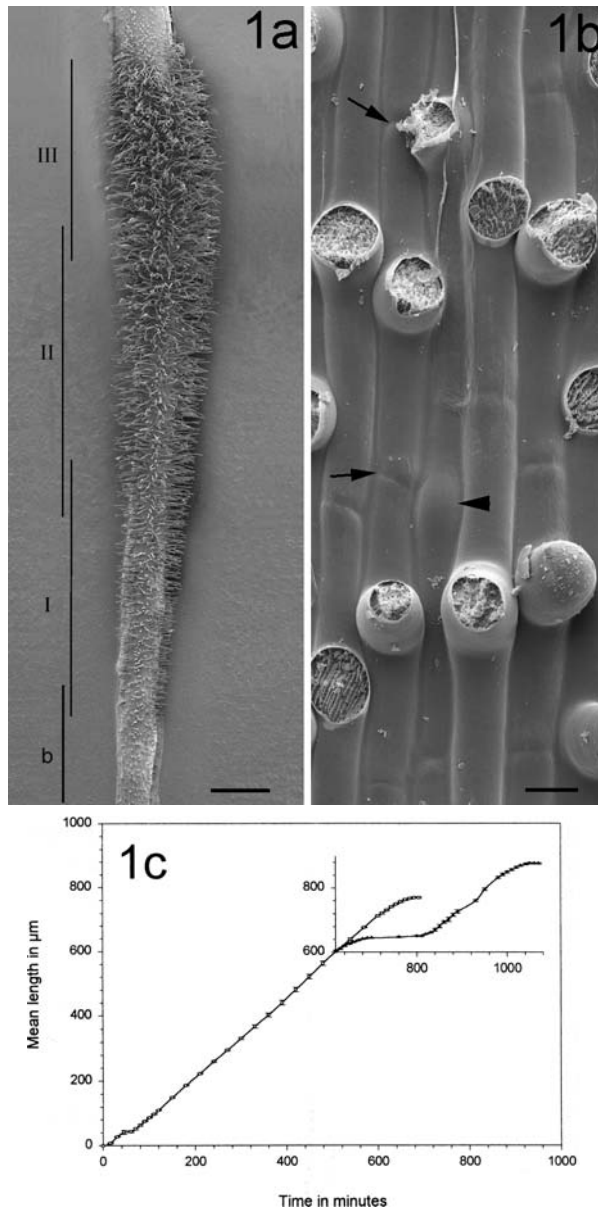

Figure 1. A and **B**, FESEM images of an air-grown *M. truncatula* primary root with root hairs.

A, On a growing root the root hairs form a cone which represents successive stages of root hair development: bulges (b), growing root hairs (I), hairs terminating growth (II) and full-grown hairs (III). Bar: 1 mm.

B, Root with root hairs shaved off. Arrows indicate the boundaries of the epidermal cells. Each root epidermal cell (trichoblast) has developed one root hair or a bulge (arrowhead). Bar: 20 μm.

C, Growth rate of root hairs. For each sample results are expressed as the mean length with standard error of 3 root hairs of similar developmental stages and lengths from the same root untreated or treated with 10^{-9} M LCOs (**inset**).

Since organelles move with different velocities, which is not the topic of this report, we have chosen to measure the speed and orientation of 1-2 μm long organelles to obtain a picture of the general streaming pattern of organelles such as spherosomes, plastids and mitochondria. The overall streaming pattern in trichoblasts is shown in Figure 3a. This pattern is clearly of the type that has been called circulation streaming, which is the common type for most plant cells.

Bulge

Like in all species studied, root hair development starts with the formation of a bulge (Figure 2a) on the outer periclinal cell wall at a species-specific site, which is in *M. truncatula* in the middle of the periclinal wall. The streaming pattern (Figure 3b) and velocity of movement of the 1-2 μm long organelles, is the same as in the preceding trichoblast stage (8-14 μm/s). Just before bulge formation, the nucleus moves to the middle of the inner periclinal wall. The bulge will be formed opposite to the nucleus at the outer periclinal wall. During bulge formation, the nucleus moves from the inner periclinal wall to the outer periclinal wall inside a cytoplasmic strand that traverses the large vacuole in the middle of the cell, and contacts the cortical cytoplasm at the base of the bulge. This relocation of the nucleus shows that polarity directed towards the forming root hair is already being set up at bulge stage, although we do not see yet an accumulation of vesicles at the tip of the bulge.

In the next stage of development the triangular shape of the bulge changes into a pointed shape typical for a growing root hair (Fig. 2b-d). Dense cytoplasm accumulates at the tip of the bulge and is connected to the nucleus by a transvacuolar cytoplasmic strand. At this initial stage of polar growth, tip growth is slow. We measure a growth speed here of 0.6 – 0.8 μm/min which is slower than during actual tip growth (Fig. 1c). The nucleus moves into the root hair (Fig. 2d).

Tip-growing hair

The next developmental stage is the actual stage of vigorous tip growth. During this stage, tip growth is occurring at a speed of 0.8 - 1.4 μm/min at room temperature and on the stage of the microscope (Fig. 1c). The characteristic cytoarchitecture of a growing root hair is built up of a smooth tip of approximately 2-3 μm, a cytoplasmic dense area behind this smooth region which contains the nucleus at its base at a distance of 30 μm (? 5 μm) from the tip, and the vacuolated part of the root hair (Figure 2e). This large vacuole basal of the sub-apical area increases in size while the root hair is growing, but except for thin extensions never moves into the cytoplasmic dense region. A peripheral layer of cytoplasm surrounds the vacuole. In these hairs different types of organelle movement occur.

In the shank of a growing root hair, below the sub-apical cytoplasmic dense region, there is only a thin peripheral cytoplasmic layer around the large vacuole (Fig. 2e). Within the cell periphery, the organelles are moving in strands with a speed of 8-14 μm/sec and are directed mainly parallel to the hair's long axis. The pattern of organelle movement is of the circulation type. The velocity of moving organelles in the shank of the hair is the same
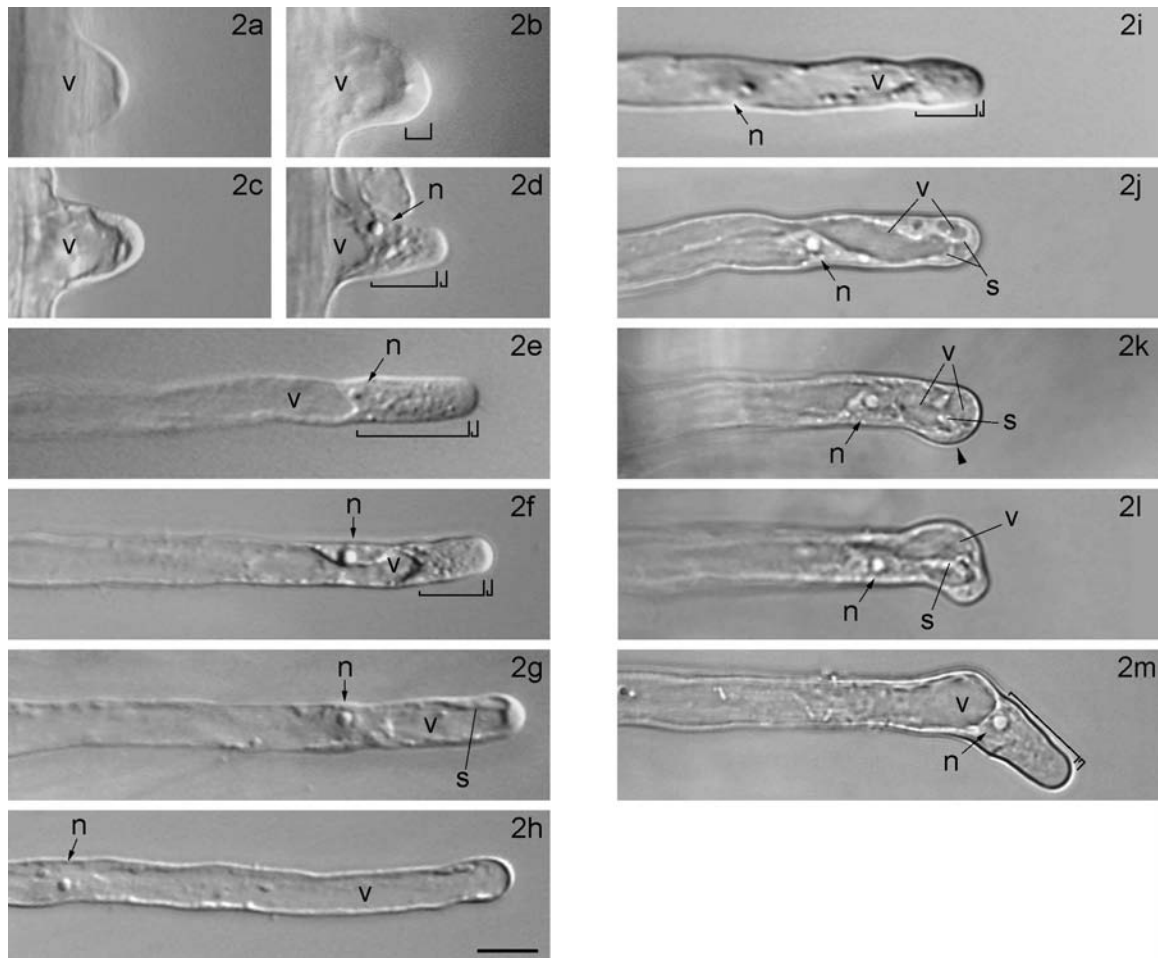
Figure 2

as in the epidermal part of the cell (8-14 μm/s). The streaming in the shank is not uncoupled from that one in the epidermal part; there is an exchange of organelles between these two regions of the cell.

In the sub-apical cytoplasmic dense region cytoplasmic streaming is of the reverse fountain type. The predominant direction of organelle movement is towards the tip. A reversal of direction takes place somewhere in the sub-apical cytoplasmic dense area (Fig. 3c). The downward movement has the same predominant axial/helical orientation as the upward movement. In the thin *M. truncatula* hairs, the mainly downward movement is often in the periphery and the area in which the reversal takes place is relatively long up to 30 μm (Figs. 2e, 3c). The net-speed of organelles in the cytoplasmic dense region of growing *M. truncatula* root hairs is very low. This means that the 1-2 μm long organelles often stop and the distance an organelle is "jumping" is very short

Figure 2 (opposite page). A-H Cytoarchitecture of *M. truncatula* root hairs during development. DIC images of subsequent stages of living root hairs. **I-M** Changes in the cytoarchitecture of a growth terminating root hair after 10^{-9} M Nod factor application. Root hair deformation is swelling of the tip and subsequent polar outgrowth from the swelling. Magnification is the same in all images. *n* Nucleus, *s* cytoplasmic strand, *v* vacuole. Bar = 20 μm. **A**, Early bulge: slightly swollen cytoplasm at the periphery. **B**, Cytoplasmic layer (bracket) at the tip of the bulge increases in thickness. **C**, Stage in between bulge and growing root hair with a building up of polar cytoarchitecture. **D**, Growing hair. Tip-oriented cytoplasmic polarity: smooth region at the very tip (small bracket), sub-apical region with dense cytoplasm (large bracket). **E**, Growing hair. The cytoplasmic dense region (large bracket) has increased in volume and contains the nucleus (n) at its base, other organelles, small vacuoles or thin extensions of the large vacuole (v). The smooth region is present at the very tip of the root hair (small bracket). **F**, Hair terminating growth (early stage). The large vacuole overtakes the nucleus and expands towards the tip, while the volume of the cytoplasmic dense region (large bracket) decreases. **G**, Hair terminating growth (late stage). The vacuole is almost in the tip but still traversed by one cytoplasmic strand (s). **H**, Fully grown hair with large vacuole, thin layer of peripheral cytoplasm, and the nucleus in a random position. **I**, Growth terminating hair shortly before application of Nod factors. The large bracket indicates the cytoplasmic dense region, the small bracket the smooth region. **J**, Root hair 5 min after application of Nod factors. Cytoplasmic strands traverse the vacuole. **K**, 105 min after LCO application; swelling of the tip with concentration of cytoplasm at the site of the new outgrowth (arrowhead). A cytoplasmic strand is connected with the cytoplasmic dense spot. **L**, 135 min. after LCO application; outgrowth at one side of the swelling. A new polarized tip is formed which continues to grow. A cytoplasmic strand is connected with the dense cytoplasm at the new outgrowth. **M**, 210 min after LCO application. The cytoarchitecture of the outgrowth resembles a growing root hair with smooth area at the very tip (small bracket), subapical cytoplasmic dense region (large bracket) and the nucleus at its base.

and the movement discontinuous; when the organelles are in a period of stopping they often show Brownian movement. Between the shank and the cytoplasmic dense region there is a zone, where the organization of the circulation streaming in the shank is lost (upward to the tip) or rebuilt (downward in the shank). In this zone the nucleus is positioned.
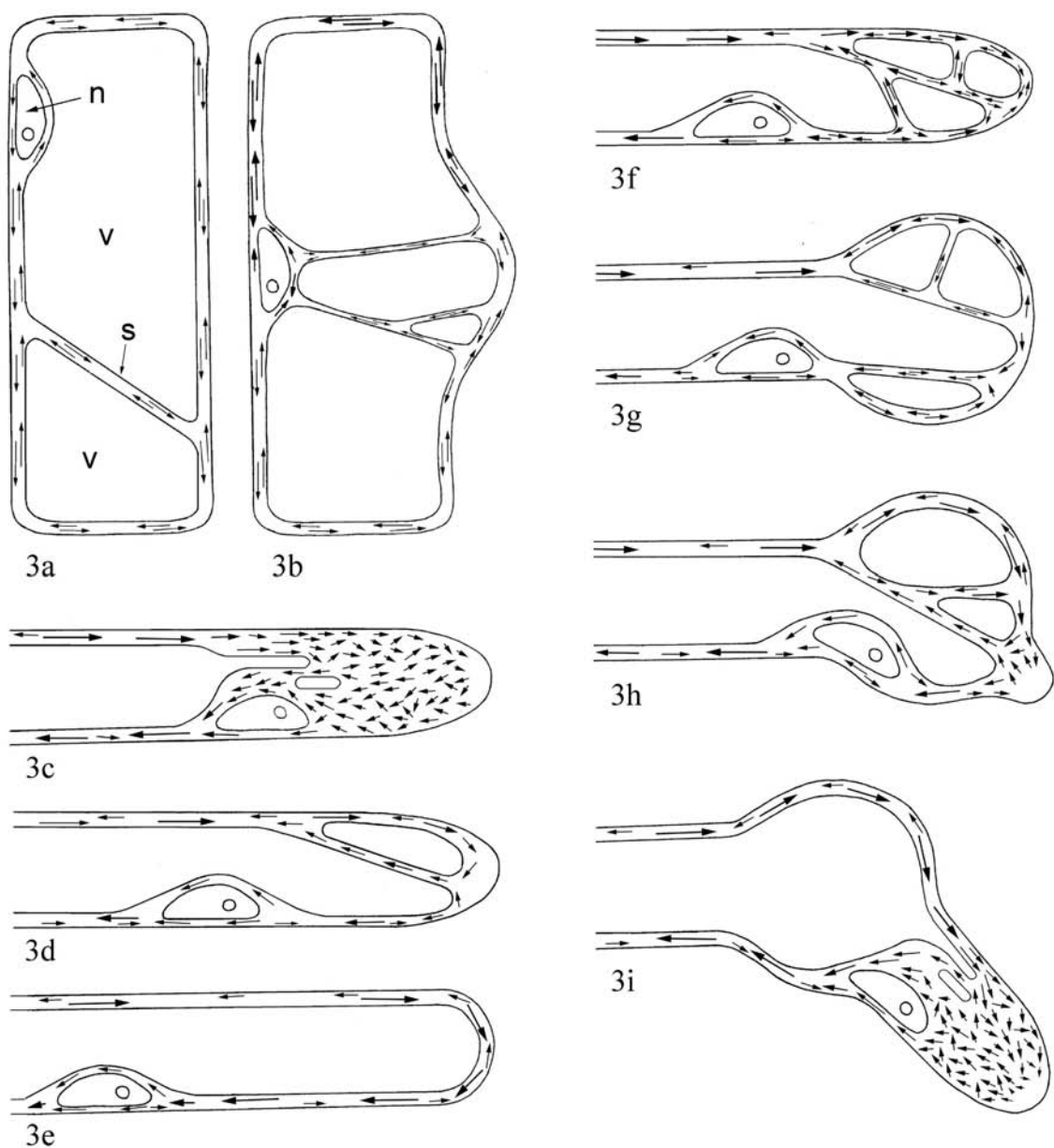
Figure 3

The smooth region at the very tip of a growing root hair does not contain the 1-2 μm long organelles. Only in VEC microscopy we could observe, but hardly image, vesicles in this area. Individually, these vesicles showed Brownian movement (data not shown), but as a population they moved slowly from the base of the vesicle rich region to its tip where they disappeared at the plasma membrane. A logical interpretation for the cause of this movement is the continuous supply of vesicles at the base of this region and their consumption by exocytosis at the plasma membrane of the very tip. Actual exocytosis could not be visualized, probably because of vesicle crowding.

Figure 3 (opposite page). **A-E** Drawings showing the patterns of cytoplasmic streaming during root hair development. **F-I** Patterns of cytoplasmic streaming after application of Nod factors. Arrows give the main direction of organelle movement. Drawings not to scale, *n* Nucleus, *v* vacuole, *s* transvacuolar cytoplasmic strand. **A**, Epidermal root cell; circulation streaming. **B**, Bulge on trichoblast; circulation streaming. **C**, Growing root hair; reverse fountain streaming. **D**, Hair terminating growth; reverse fountain streaming. **E,** Fully grown hair; circulation streaming. **F**, Hair terminating growth. Drawing resembles situation in a root hair 5min after application of Nod factors. **G**, Swollen tip (75 min after LCO application); circulation streaming. **H**, New outgrowth from one site of the swelling (135 min after LCO application); reverse fountain streaming becomes restored. **I**, The outgrowth has the same pattern of organelle movement as a growing root hair.

Growth terminating hair

Since in our assay, the growth-terminating hairs are the ones that deform by Nod factors, this was an important developmental stage to study. A root hair starts slowing down growth when the vacuole overtakes the nucleus. Then the nucleus does not follow the tip anymore which causes an increase in the distance between nucleus and tip, while the length of the cytoplasmic dense region is decreasing because the vacuole expands towards the tip (Fig. 2f). In parallel with this goes the decrease of the length of the smooth area, which is the vesicle rich area. Tiny vacuoles appear in the very tip. Growth-termination is a gradual process: the growth speed decreases continually till the hair has stopped growing. Some growth-terminating root hairs still can grow up to 10% of the length they had when they started terminating growth. The velocity and organization of cytoplasmic streaming in the shank does not change while root hairs are terminating growth. As long as the cytoplasmic dense region is present, the patterns of cytoplasmic streaming are the same as mentioned above for a growing hair. When the vacuole is almost in the tip but still traversed by one or more transvacuolar cytoplasmic strands, the reverse fountain streaming just below the very tip is still there. Organelle movement in the transvacuolar strand mainly has an opposite direction to that in the peripheral strands (Fig. 2g and 3d). This reverse fountain streaming switches to circulation streaming but a short term restoration of reverse fountain streaming may occur a number of times before circulation streaming becomes permanent, when growth has stopped (Fig.3e).

Fully grown hair

A full-grown hair consists of a thin layer of cytoplasm around a large vacuole, the nucleus can be anywhere in the cell and the pattern and speed of organelle movement has again become the circulation type (Figure 3e). In a full-grown hair, the smooth region as well as the cytoplasmic dense region seen in the sub-apex of growing hairs have disappeared completely (Figure 2h). A full-grown root hair of *M. truncatula* can reach a maximal length of 1 mm and has a diameter of 15-20 µm. The shape of the tip of a full-grown hair is different from that of a growing hair. While in the latter one the tip is slightly pointed (Fig. 2d, e), it is a hemisphere, which may be slightly swollen in a full-grown hair (Figure 2h).

Cytoarchitecture and cytoplasmic streaming in root hairs of M. truncatula after application of LCOs

Root hairs were treated with 10^{-9} M or 10^{-10} M host-specific LCOs. After application of LCOs, the tip of growth terminating hairs of *M. truncatula* started to swell and a new outgrowth subsequently developed from the swelling. Growing and full-grown root hairs did not deform but also hairs terminating growth reacted in different ways, depending on their developmental stage. Hairs in which the process of growth termination had started (Fig. 2f) reacted to LCO application with less swelling before new outgrowth than older root hairs. Fig. 4 is a time series, starting 70 min after LCO application of one growth terminating hair. Shortly after LCO application, extensions of the vacuole expand towards the tip much faster than the vacuole does in an untreated growth terminating hair. There is a difference between what happens after Nod factor application and what happens during normal growth termination. During normal growth termination the large central vacuole overtakes the nucleus and expands slowly towards the tip, while after Nod factor application thin extensions of the vacuole expand quickly towards the tip. These extensions fuse and after 5 minutes the vacuole fills the tip nearly completely and only a few, but more than in a untreated growth terminating hair, transvacuolar strands in orientations up to perpendicular to the long axis of the hair, are left (Fig. 2j, Fig. 4a). During swelling of the hair tip, the number and position of transvacuolar strands in the swelling change continually (Fig. 4a-d). In VEC microscopy we see vesicles in the apical hemisphere of the swelling along the plasma membrane (data not shown). The pattern of cytoplasmic streaming in a hair that is swelling resembles the pattern we find in a growth terminating root hair in a late stage (Fig. 3f-h). Cytoplasmic streaming switches from

reverse fountain to circulation streaming and back for several times. The speed of the 1-2 μm long organelles in the thin cytoplasmic layer near the tip is the same as in the shank (8-14 μm/sec). The overall speed of organelles does not change after LCO application. We do not know yet if there are short-term effects in the velocity of organelles in the thin cytoplasmic dense region of a growth terminating hair, within the first seconds after LCO application. At a certain time about 1h 30min after Nod factor application, a cytoplasmic dense spot at one site of the swelling forms (Fig. 4c) which subsequently increases to a cytoplasmic dense area (Fig. 4d). From this local accumulation of cytoplasm the new out-
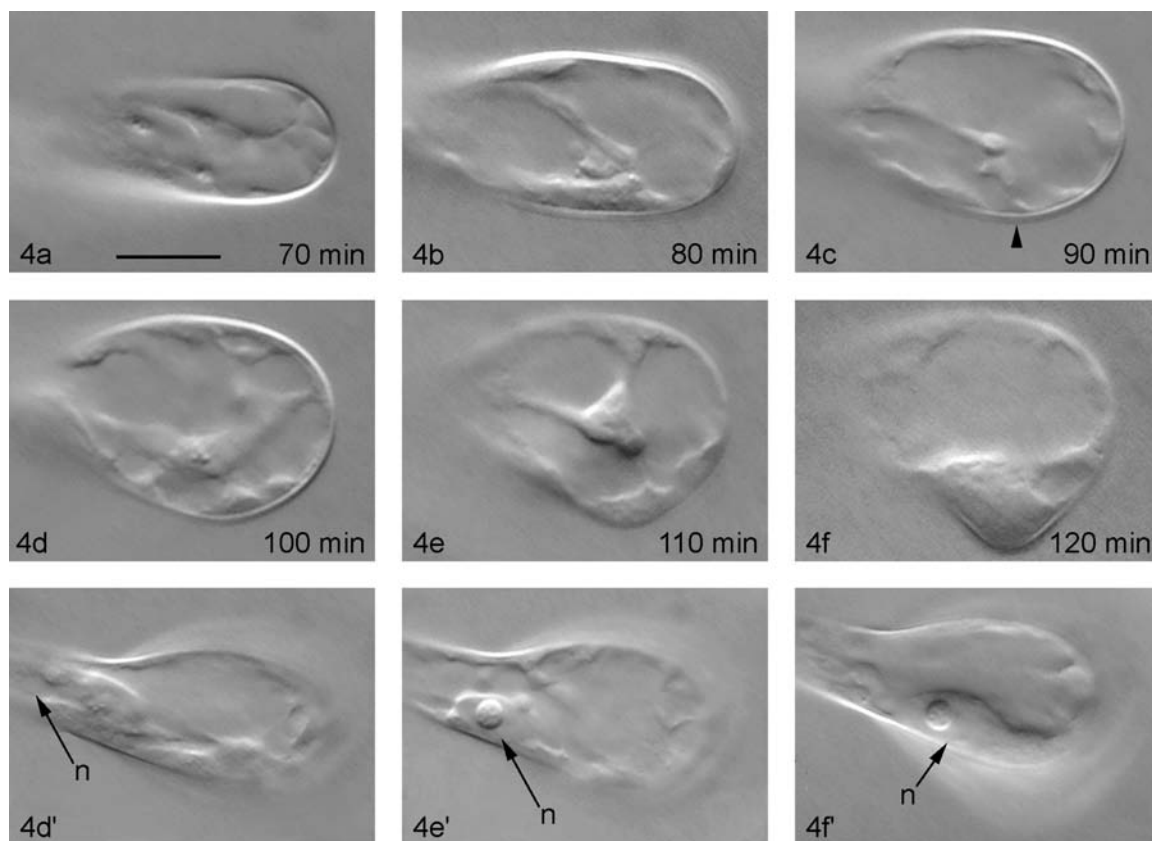
Figure 4. A-F Time series of a root hair tip 70 min after application of 10^{-9} M Nod factors. The VEC images give details of the cytoarchitecture of the cytoplasm in the swelling. The cytoplasmic dense spot (arrowhead in **C**) at one site of the swelling always is in contact with a transvacuolar cytoplasmic strand. This strand changes shape and orientation permanently. **D'-F'** resemble the situation in **D-F** with the focal plane set to the nucleus (*n*). Magnification is the same in all images, bar = 20 μm

growth is formed (Fig. 2k, 2l, Fig. 4e, 4f). Within the next 30 min a new tip with dense

cytoplasm is being built up from which tip growth starts again (Fig. 2m). The nucleus which had lost its fixed distance to the tip during growth termination moves during swelling back to the tip and maintains a position at the base or inside the swelling (Fig. 2i-l, Fig. 4d'-f'). The nucleus enters the new outgrowth when this outgrowth has reached a length of approximately 20 μm and obtains again the same position as in a growing hair (30 μm +/- 5 μm to the tip; see Figs. 2e and 2m). The development of the new outgrowth resembles the development of a polar growing root hair from a bulge. The cytoarchitecture of the new outgrowth with smooth area, sub-apical, cytoplasmic dense region and the nucleus at the bottom of the cytoplasmic dense region is the same as in a growing root hair (Fig. 2e, 2m).

Discussion

Root hair development

It is well known that in *Arabidopsis* root hairs not all root epidermal cells form a root hair (Dolan et al. 1994). The root hair forming cells, trichoblasts, arise over the intercellular space between underlying cortical cells, whereas atrichoblasts occur over a single cortical cell. Our study shows that in *M. truncatula*, like in vetch (Miller and Emons, unpublished), every root epidermal cell forms a root hair. This is not exceptional (Leavitt 1904, Schwarz 1883, reviewed by Von Guttenberg 1968). Before real polar growth starts, a bulge appears (Haberlandt 1887, Dolan et al. 1994), from which the root hair proper grows out.

Patterns of cytoplasmic streaming in root hairs

Cytoplasmic streaming is the directional movement of organelles in the cytoplasm. Why do plant cells exhibit such vigorous transport of organelles? Too few cells have been addressed to answer this question. 'Why do plant cells exploit different patterns of cytoplasmic streaming?' is a question addressed in this paper which describes these patterns in root hairs. When we compare the two patterns observed, circulation streaming and reverse fountain streaming, it is obvious that the latter is employed to obtain an unequal distribution of organelles. A third type of cytoplasmic streaming is rotation streaming. It is the streaming pattern seen in algal cells such as *Chara* (Jarosch 1956, Williamson 1992) and *Nitella* (Kamiya and Kuroda 1958, Kamiya 1959). It is not seen in root hairs at any stage and has, to our knowledge, not been reported for cells of flowering plants, which generally exhibit circulation streaming. In rotation streaming the whole

cytoplasm streams at a rather constant rate, depending on the area in the cell and in the same direction. In circulation streaming, the movement takes place in cytoplasmic strands, which lie in the cell periphery or traverse the large vacuole. In circulation streaming, movement occurs in various directions along the plasma membrane and in cytoplasmic strands that can cross the vacuole (De Win 1997). The movement of organelles in the strands is in one primary orientation, but may also be bi-directional. Organelles of different kinds move with individual and variable velocities, pass each other, may stop for a moment and reverse direction (Lichscheidl 1995).

Reverse fountain streaming in *M. truncatula* is similar to for instance this type of streaming in *Vicia* (Miller et al. 1997, 1999) and *Arabidopsis* (Ketelaar, personal communication, 2000), but a bit different from the typical reverse fountain streaming first described by Iwanami in 1956 for pollen tubes. In the wide pollen tubes of lily (Iwanami 1956), and wide root hairs of *Hydrocharis dubia* (Tominaga et al. 1998) the upward stream of organelles is at the side of the hair and the downward stream in the middle. In the thinner hairs the downward stream may be in the periphery as well. The net-velocity of streaming in the sub-apex area of the cell, where the direction of streaming reorients is slower than in the rest of the hair. This has also been reported for *Equisetum hyemale* root hairs (Emons 1987). In the *Equisetum hyemale* root hairs the area of slow transport is much longer than in *M. truncatula*, but also the total length of the hairs is almost 10 times more, up to 1 cm instead of 1 mm.

The process of cytoplasmic streaming is far from clear, and needs the study of the molecules involved, actin and its motor proteins, as well as the study of the physical aspects of this process. The hypothesis that we favor is that the actin cytoskeleton not only serves in the movement of the organelles, but as much in the organization of the cytoplasm, i.e. the formation of the cytoarchitecture. The finer and denser the actin filament bundles, the smaller the vacuoles (or extensions of the large central vacuole) and the organelles between them. An area of fine bundles of actin filaments like in the basal side of the sub-apex in growing root hairs (Miller et al. 1999, De Ruijter 1999) may not allow the nucleus to enter that area. An even finer sieve-like structure at the apical side of the sub-apical area of root hairs, formed by the finest bundles of actin filaments in that region (Miller et al. 1999) would not allow the passage of other organelles than small vesicles. The accumulation of vesicles at the tip of the root hair would occur then, if the vesicles uncouple from the actin filaments at the base of the vesicle-rich region. The sub-apical region with fine bundles of actin filaments is displaced continually in the direction of the tip, indicating that actin filament polymerization occurs continually.

Reaction of M. truncatula root hairs to Nod factors

Vetch root hairs of all developmental stages, when growing between glass slides, react to LCO application with an increase in the density of fine bundles of actin filaments (FB-actin) and in the length of the sub-apical area bearing these fine bundles (De Ruijter et al. 1999). Studies with actin filament depolymerizing drugs have indicated that this type of cytoarchitecture is a prerequisite for tip growth in such cells (Miller et al. 1999). Nod factors have different effects on the morphogenetic growth patterns of the various stages of root hairs. The growing hairs keep on growing. When the inducing principle would be applied locally, however, like we expect to happen when bacteria attach to bulges or growing hairs, the excreted Nod factors could have an effect on the site, and therefore direction of tip growth (Emons and Mulder 2000). In the hairs that are terminating growth, Nod factors induce within minutes expansion of extensions of the vacuole towards the root hair tip. At the same time the number of transvacuolar strands increases but they deviate more from the long axis of the cell than before LCO application. The insertion of the vesicles continues, though over a larger area thus giving rise to a swollen hair tip.

We explain the swelling of the tip in these hairs, an event that precedes actual new tip growth, as follows. Hairs that are terminating growth do not have a tip-directed vesicle delivery system anymore, but do still have exocytosis vesicles at the extreme tip. Though the increase in the number of fine bundles of actin filaments by LCO is as rapid as 3 min (De Ruijter et al. 1999), it takes some time before the new vesicles find an anchor in the plasma membrane from where to start new local exocytosis. In the meantime, before anchoring, the residual Golgi vesicles insert randomly in the plasma membrane of the tip, which still has only a primary expandable cell wall. This causes the tip to swell. We do not exclude that also new vesicles are exocytosed at random before the new tip has anchored itself (see also discussion about calcium in De Ruijter et al. 1998 and Esseling et al. 2000).

In *Vicia sativa* and *M. truncatula*, full-grown root hairs do not respond with root hair deformation or root hair branching. By definition, full-grown cells have a secondary cell wall, which does not expand and secondary cell wall deposition has been shown to occur in root hair tips (*Equisetum hyemale*: Emons and Wolters-Arts 1983). So, a full-grown root hair cell wall would have to be weakened before branching could occur. This does not seem to happen in our assay.

Acknowledgements

References

Allen NS and Bennett MN. 1996. Electro-optical imaging of f-actin and endoplasmic reticulum in living and fixed plant cells. Scanning Microsc Suppl 10: 177-187.

De Ruijter NCA, Rook MB, Bisseling T and Emons AMC. 1998. Lipochitooligosaccharides reinitiate root hair tip growth in *Vicia sativa* with high calcium and spectrin-like antigen at the tip. Plant J 13: 341-350.

De Ruijter NCA, Bisseling T and Emons AMC. 1999. *Rhizobium* Nod factors induce an increase in sub-apical fine bundles of actin filaments in *Vicia sativa* root hairs within minutes. MP MI 12: 829-832.

De Win AHN. 1997. Quantitative analyses of organelle movements in pollen tubes. PhD Thesis, Catholic University of Nijmegen, pp 1-19.

Dolan L, Duckett CM, Grierson C, Linstead P, Schneider K, Lawson E, Dean C, Poethig S and Roberts K. 1994. Clonal relationships and cell patterning in the root epidermis of *Arabidopsis*. Development 120: 2465-2474.

Emons AMC and Wolters-Arts AMC. 1983. Cortical microtubules and microfibril deposition in the cell wall of root hairs of *Equisetum hyemale*. Protoplasma 117: 68-81.

Emons AMC. 1987. The cytoskeleton and secretory vesicles in root hairs of *Equisetum* and *Limnobium* and cytoplasmic streaming in root hairs of *Equisetum*. Ann Bot 60: 625-632.

Emons AMC and Mulder B. 2000. Nodulation factors trigger an increase of fine bundles of subapical filaments in *Vicia* root hairs: implications for root hair curling around bacteria. In: De Wit PJGM, Bisseling T and Stiekema W (eds) Biology of plant-microbe interaction, vol. 2, pp 272-276.

Esseling J, De Ruijter NCA and Emons AMC. 2000. The root hair actin cytoskeleton as backbone, highway, morphogenetic instrument and target for signaling. In: Ridge RW and Emons AMC (eds) Cell and molecular biology of plant root hairs. Springer, Tokyo, pp 29-52.

Fåhraeus G. 1957. The infection of white clover root hairs by nodule bacteria studied by a simple glass slide technique. J Gen Microbiol 16: 374-381.

Haberlandt G. 1887 Function und Lage des Zellkernes bei den Pflanzen. Gustav Fischer, Jena, pp 45-59.

Heidstra R, Geurts R, Franssen H, Spaink HP, van Kammen A and Bisseling T. 1994. Root hair deformation activity of nodulation factors and their fate on *Vicia sativa*. Plant Physiol 105: 787-797.

Iwanami Y. 1956 Protoplasmic movement in pollen grains and tubes. Phytomorphology 6: 288-295.

Jarosch R. 1956. Plasmaströmung und Chloroplastenrotation bei Characeen. Phyton (Austria) 6: 87-107.

Kamiya N and Kuroda K. 1958. Measurement of the motive force of the protoplasmic rotation in *Nitella*. Protoplasma Bd.L/1: 144-148.

Kamiya N. 1959. Protoplasmic streaming. In: Helibrunn LV et al. (eds) Protoplasmatologia, Handbuch der Protoplasmaforschung Vol. VIII part 3a, Springer, Wien.

Kijne JW. 1992. The *Rhizobium* infection process. In: Stacey G, Burris RH, Evans HJ (eds) Biological Nitrogen Fixation. Chapman and Hall, New York, pp 349-398.

Leavitt R.G. 1904 Trichomes of the root in vascular Cryptogams and Angiosperms. Proc. of the Boston Soc of Nat Hist 3.

Lichtscheidl IK. 1995. Organelle motility in plant cells: *Allium cepa* inner epidermis. In: Wiss. Film Nr. 47: 111-125. Accompanying publication for the film C 2540 of the Austrian Federal Institute of Scientific Film.

Lichtscheidl IK and Foissner I. 1996. Video microscopy of dynamic plant cell organelles: principles of the technique and practical application. J Microsc 181:117-128.

Miller DD, De Ruijter NCA and Emons AMC. 1997. From signal to form: aspects of the cytoskeleton-plasma membrane-cell wall continuum in root hair tips. J Exp Bot 48: 1881-1896.

Miller DD, De Ruijter NCA, Bisseling T and Emons AMC. 1999. The role of actin in root hair morphogenesis: studies with lipochito-oligosaccharide as a growth stimulator and cytochalasin as an actin perturbing drug. Plant J 17: 101-113.

Schwarz F. 1883. Die Wurzelhaare der Pflanzen. Ein Beitrag zur Biologie und Physiologie dieser Organe. Untersuchungen aus dem Bot. Inst. Tübingen 1.

Tominaga M, Sonobe S and Shimmen T. 1998. Mechanism of inhibition of cytoplasmic streaming by auxin in root hair cells of *Hydrocharis*. Plant Cell Physiol 39: 1342-1349.

Von Guttenberg H. 1968. Der Primäre Bau der Angiospermenwurzel. In: Zimmermann W, Ozenda P and Wulff D (eds) Handbuch der Pflanzenanatomie VIII 5. Borntraeger, Berlin Stuttgart, pp 115.

Williamson RE. 1992. Cytoplasmic streaming in characean algae: mechanisms, regulation by Ca^{2+} and organization. In: Melkonian M (ed) Algal Cell Motility. Chapman and Hall, London, pp 73-98.

Chapter 3

Endoplasmic Microtubules Configure the Subapical Cytoplasm and are Required for Fast Growth of *Medicago truncatula* Root Hairs

B.J. Sieberer[1], A.C.J. Timmers[2], F.G.P. Lhuissier[1], and A.M.C. Emons[1]

[1] Laboratory of Plant Cell Biology, Wageningen University, Arborteumlaan 4, 6703 BD Wageningen, The Netherlands

[2] Laboratoire de Biologie Moléculaire des Relations Plantes-Microorganismes, CNRS/INRA, BP 27, 31326 Castanet-Tolosan Cedex, France

The first two authors contributed equally to the paper

Abstract

To investigate the configuration of microtubules (MTs) in tip growing *Medicago truncatula* root hairs, we used immunocytochemistry or *in vivo*-decoration by a green fluorescent protein linked to a microtubule binding domain (GFP-MBD). The two approaches gave similar results and allowed the study of MTs during hair development. Cortical MTs (CMTs) are present in all developmental stages. During the transition from bulge to a tip growing root hair, endoplasmic MTs (EMTs) appear at the tip of the young hair and remain there until growth-arrest. EMTs are a specific feature of growing hairs, forming a 3-dimensional array throughout the subapical cytoplasmic dense region. During growth-arrest, EMTs together with the subapical cytoplasmic dense region progressively disappear, while CMTs extend further towards the tip. In full-grown root hairs, CMTs, the only remaining population of MTs, converge at the tip. Upon treatment of growing hairs with 1 µM oryzalin, EMTs disappear, but CMTs remain present. The subapical cytoplasmic dense region becomes very short, the distance nucleus-tip increases, growth slows down, and the nucleus still follows the advancing tip, though at a much larger distance. Taxol has no effect on the cytoarchitecture of growing hairs; the subapical cytoplasmic dense region remains intact, the nucleus keeps its distance from the tip, but growth rate drops to the same extent as in hairs treated with 1 µM oryzalin. The role of EMTs in growing root hairs is discussed.

Introduction

Root hairs are lateral extensions of epidermal root cells involved in the uptake of water and nutrients, in anchoring the plant in the soil (Peterson and Farquhar, 1996; Gilroy and Jones, 2000), and in the interaction between nitrogen-fixing rhizobacteria and their Fabacean host plants (Mylona et al., 1995; Long, 1996). They emerge as bulges from the outer periclinal cell wall of epidermal cells and elongate almost perpendicularly to the root axis by tip growth, which reflects an underlying polarity of the cytoarchitecture (*Medicago truncatula*: Shaw et al., 2000; Sieberer and Emons, 2000).

In growing root hairs, cytoplasm, including the nucleus, is concentrated in the subapical region, whereas the basal part is highly vacuolated (*Vicia sativa*: De Ruijter et al., 1998; *Medicago trucatula*: Sieberer and Emons, 2000). The subapical cytoplasmic dense region contains endoplasmic reticulum (ER), mitochondria, plastids and Golgi bodies (*V. sativa*: Miller et al., 2000). At the base of this subapical cytoplasmic dense region is the nucleus, which follows the expanding tip at a certain distance (*M. truncatula*: Sieberer and Emons, 2000). The extreme apex of the hair looks smooth in the differential interference light microscope, and has been shown with electron microscopy to be filled with exocytotic vesicles (freeze fixation/freeze substitution: *Equisetum hyemale* Emons, 1987; *V. hirsuta*: Ridge 1988, 1993; *V. villosa:* Sherrier and VandenBosch, 1994; *Arabidobsis thaliana:* Galway et al., 1997; *V. sativa*: Miller et al., 2000).

The subapical cytoplasmic dense region is configured by FB-actin (Miller et al., 1999). FB-actin is a specific configuration of fine bundles of actin filaments. It is thought to function in the transport and/or keeping of Golgi vesicles to the vesicle rich region in the hair dome. After chemical fixation and fluorescein-phalloidin staining of growing hairs this vesicle-rich region at the very tip appears to be devoid of filamentous actin, when observed with a confocal laser-scanning microscope (CLSM) (*V. sativa*: Miller et al., 1999). The strongest indication that this typical actin cytoskeleton is involved in tip growth comes from its reaction to Nod factor, a lipochito-oligosaccharide secreted by rhizobacteria. Nod factor enhances this cytoskeleton configuration in all developmental stages of root hairs (De Ruijter et al., 1999), whereupon hair tips swell and new tip growth restarts in those that were arresting growth (De Ruijter et al., 1998). Furthermore, tip-growth in *V. sativa* root hairs is inhibited by cytochalasin D, an actin-depolymerizing drug (Miller et al., 1999).

Most of the earlier work on microtubules (MTs) in root hairs has dealt with CMTs and their role in cellulose microfibril orientation (reviewed in: Emons and Mulder, 1998; Ketelaar and Emons, 2000). Endoplasmic MTs (EMTs) have been observed only in

legume root hairs while their precise configuration and role remain unclear (Lloyd et al., 1987). Authors have proposed several functions for MTs in root hairs. They may control growth orientation (*A. thaliana*: Bibikova et al., 1999), regulate the organization of actin filaments (*Hydrocharis*: Tominaga et al., 1997), connect the nucleus to the expanding tip (*V. hirsuta*: Lloyd et al., 1987), or determine the width of the root hair tube (*E. hyemale*: Emons et al., 1990). Despite these studies, the functions of MTs in tip growth are still less clear than those of actin filaments. Furthermore, no description exists of MTs during all stages of root hair development.

We made use of green fluorescent protein (GFP) technology to visualize MTs in all developmental stages of living root hairs of *M. truncatula*, a legume well-studied for the interaction with rhizobia and mycorrhizal fungi (Cook, 1999). The dynamics of the cytoskeleton in living cells may occlude its clear observation. Compare for instance GFP-talin labeled actin (Baluska et al., 2000) with fluorescein-phalloidin stained actin (Miller et al., 1999) in root hairs. Furthermore, we wanted to know whether the same population of MTs is labeled with the GFP microtubule binding domain (GFP-MBD) fusion protein as with immuno-cytochemistry. The MBD is of animal origin and thus might not label all MTs in root hairs. Therefore, we compared the results obtained with *in vivo* labeling of MTs by GFP-MBD with results obtained with immuno-cytochemistry after rapid freeze fixation/freeze substitution (FF/FS), the most reliable fixation method for light microscopy (Baskin et al. 1996; Vos and Hepler, 1998). With both methods, we made similar observations and it was possible to monitor the configuration of MTs in all stages of root hair development.

Each stage of root hair development had a specific organization of MTs. CMTs were present in all stages of hair development in stage specific configurations, but EMTs were only present in the subapical region of vigorously growing root hairs. Studies with the microtubule inhibiting drugs oryzalin and taxol gave evidence that EMTs are essential to maintain the specific cytoarchitecture of growing root hairs as well as to keep the growth rate of these hairs at a high level.

Results

We studied the organization of MTs in *Medicago truncatula* root hairs in all developmental stages using CLSM. MTs were visualized either by immunocytochemistry after FF/FS, or *in vivo* by GFP-MBD decoration. With both methods similar results were obtained, although MTs decorated with GFP-MBD appear slightly thicker and denser than MTs labeled with antibodies. This might be due to the *in vivo* imaging technique (i.e., combination of time series and 3d imaging) for MTs in transformed root hairs. Root hairs of transformed roots developed normally and grew, with similar speed and pattern, as hairs of non-transformed roots.

Trichoblast (before bulge formation)

In *M. truncatula*, every root epidermal cell has the potential to form a bulge, and thus, in this species, all epidermal cells are trichoblasts (Sieberer and Emons, 2000). This is different from *A. thaliana*, for instance, where trichoblasts and atrichoblasts are organized in cell files (Dolan et al., 1994). A trichoblast of *M. truncatula* has one large main vacuole, which fills the cell except for a few cytoplasmic strands traversing the vacuole and a thin layer of peripheral cytoplasm containing all organelles and the nucleus. Within one cell CMTs are either oriented obliquely with different angles, and/or transversely to the long axis of the root (Fig. 1A). At the presumptive site of bulge formation, CMTs are transverse to the root axis and parallel to each other. We have not detected EMTs in transvacuolar cytoplasmic strands of trichoblasts before bulge formation; so, in this aspect they are the same as other diffuse growing plant cells (BY-2 tobacco cells: Collings et al., 1998; Granger and Cyr, 2000).

Bulge

In *M. truncatula*, root hair development starts with the formation of a bulge in the middle of the outer periclinal wall or slightly towards the root tip. Young bulges have a triangular shape with the large vacuole extending into the bulge. The nucleus is located at the site opposite to the bulge at the inner periclinal wall (Sieberer and Emons, 2000). At the site of the bulge, CMTs are mainly transverse to the long axis of the root (Fig. 1B and D). Towards both distal ends of the cell, CMTs may be slightly obliquely oriented at this stage
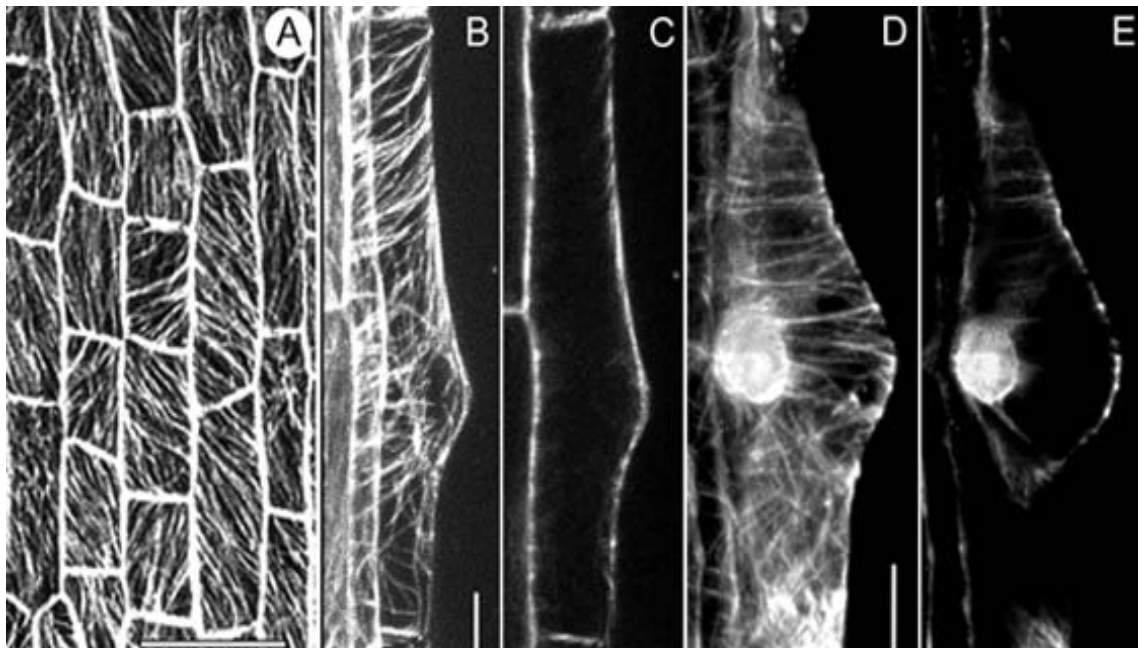
Figure 1. CMTs in trichoblasts before bulge formation (A) and during bulge formation (B – E), visualized with a CLSM in scanning steps of 1 μm. A – C GFP-MBD, D and E immunocytochemistry. **A**, CMTs are either obliquely or longitudinally oriented to the long axis of the root. Bar = 50 μm. **B**, Full-stack projection of CMTs. CMTs loop through the tip of the bulge and are transversely or slightly helically oriented to the long axis of the root in the epidermal part. Bar = 10 μm. **C**, Projection of 4 median sections. There are no detectable EMTs in this developmental stage. **D**, Full-stack projection of CMTs; for explanation see B. Bar = 10 μm. **E**, Note position of the nucleus. For explanation see C.

(Fig. 1B and D). CMTs in the bulge are continuous with CMTs in the epidermal part of the trichoblast and pass through the tip of the bulge where they loop through (Fig. 1B and D). At the tip of the bulge, the distance between CMTs increases when the bulge expands. We did not observe any EMTs between the nucleus and the tip of the bulge (Fig. 1C and E).

Initiation of polar growth

During the transition from bulge to the tip-growing root hair stage, cytoplasm accumulates at the very tip of the bulge and forms a short cytoplasmic dense region there. The nucleus is still in the epidermal part of the cell (Fig. 2A). CMTs are still oriented transversely to
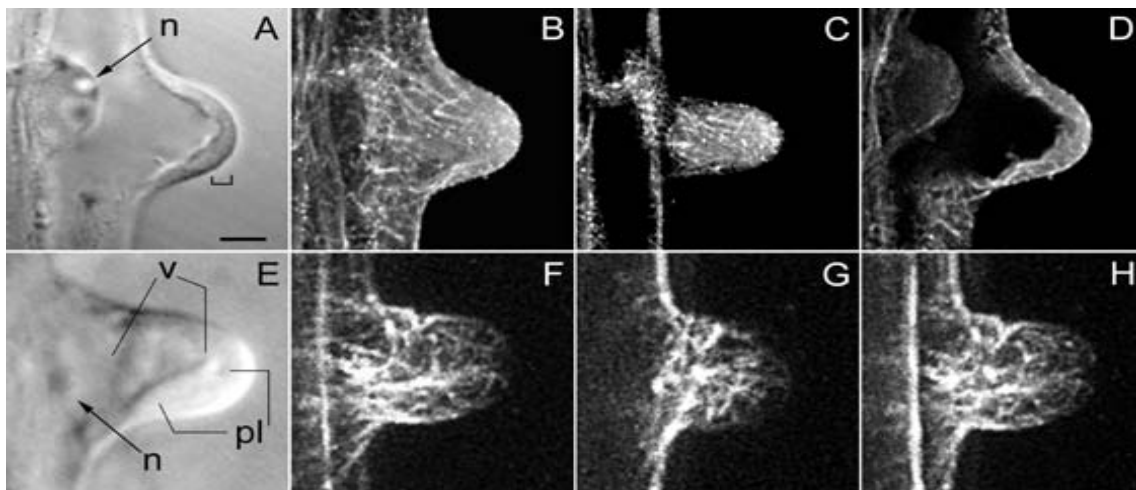
Figure 2. MTs during transition from a bulge into a growing root hair, visualized with a CLSM in scanning steps of 1 μm (B – D and F – H). B – D immunocytochemistry, F – H GFP-MBD. In this developmental stage, polar growth is initiated. **A**, Corresponding brightfield image to B – D; bracket indicates thin layer of cytoplasm at the tip. **B**, Full-stack projection of MTs. **C**, Projection of 3 peripheral sections, showing CMTs. A few CMTs still reach the very tip and are net-axially oriented below the tip region. **D**, Projection of 4 median sections; EMTs start to appear at this stage of hair development. **E**, Brightfield image of a hair at a somewhat later stage than shown in A. The cytoplasmic layer (pl) in the tip region has increased in length. **F**, Full-stack projection of MTs. **G**, Projection of 3 peripheral sections. Single CMTs still reach the very tip. **H**, Projection of 4 median sections, showing EMTs. There is a concomitant increase in both the length of the subapical cytoplasmic dense region and the density of EMTs. Images A – D show an earlier stage than images E – G. Magnification is the same in all images, bar = 20 μm, n indicates the nucleus, v the vacuole.

the root axis and a few of them still loop through the tip of the developing bulge (Fig. 2B, C, F and G). Interestingly, within the cytoplasmic layer at the tip single EMTs appear (Fig. 2D and H) and increase in density, as the subapical cytoplasmic dense region becomes larger (compare Fig. 2A with 2E and Fig. 2D with 2H). We observed EMTs both in living GFP-MBD expressing hairs and in immuno-labeled FF/FS hairs of this developmental stage.
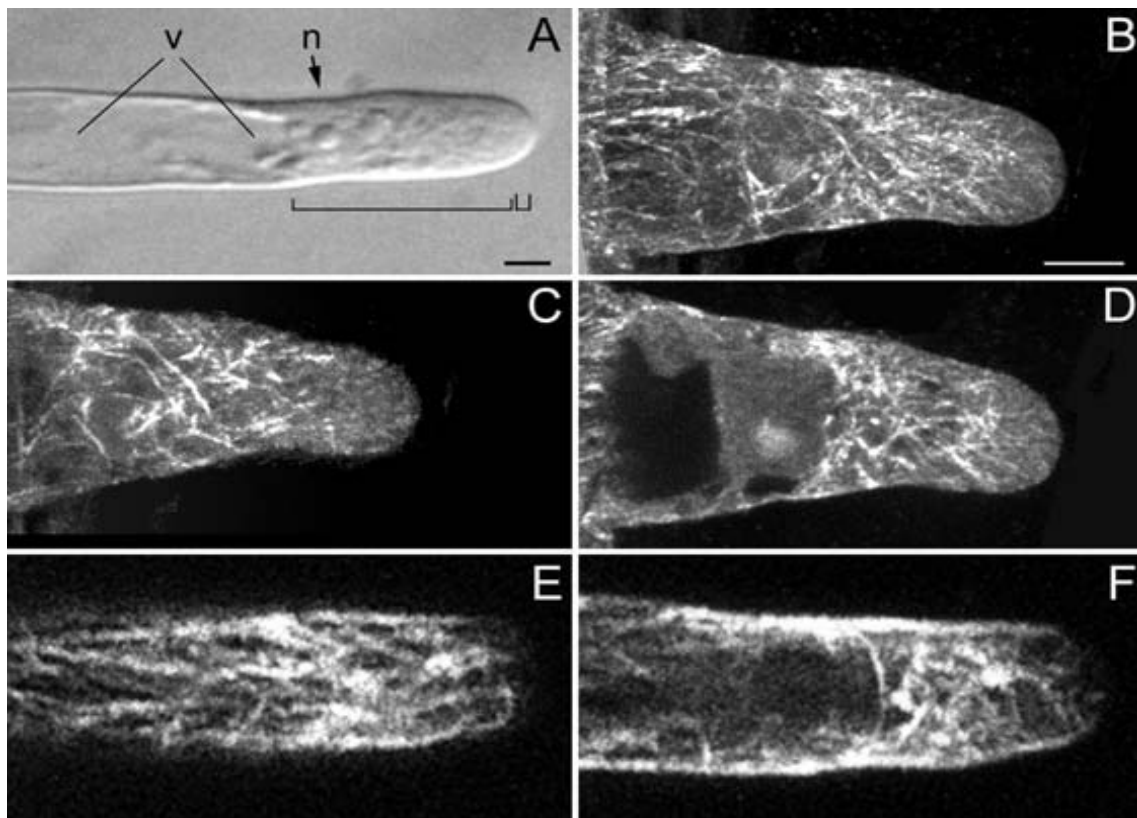
Figure 3. MTs in growing root hairs visualized with a CLSM in scanning steps of 1 µm (B – F). B – D immunocytochemistry, E and F GFP-MBD. **A**, Brightfield image of a living hair; small bracket indicates the vesicle rich region, large bracket the subapical cytoplasmic dense region, n the nucleus, v the central vacuole. Bar = 10 µm. **B**, Full-stack projection of MTs. **C**, Projection of 3 sections of the cell periphery showing net-axially aligned CMTs. CMTs do not reach the very tip. **D**, Projection of 4 median sections, showing EMTs. EMTs are abundant close to the nucleus and in the lower part of the subapical cytoplasmic dense region. The density of EMTs in the upper part of the subapical cytoplasmic dense region is low. Only a few EMTs reach the very tip. **E**, Projection of 3 sections of the cell periphery, showing CMTs. For explanation see C. **F**, Projection of 4 median sections; for explanation see D. Magnification in B – F is the same, bar in B = 10 µm.

Growing root hairs

Regularly growing root hairs exclusively elongate by tip growth. A growing root hair of *M. truncatula* has a characteristic cytoarchitecture (Sieberer and Emons, 2000). It is shown in Figure 3A and consists of an apical smooth, vesicle rich, region at the very tip,

which is followed by a subapical cytoplasmic dense region containing the nucleus. The nucleus follows the expanding tip at a distance of 30 to 40 μm, measured from the hair tip to the middle of the nucleus (see below). During this stage of vigorous tip growth, the central vacuole never enters the subapical cytoplasmic dense region, although extensions of the central vacuole may temporarily penetrate this region.

CMTs in the base of a young growing root hair are net-axially oriented to the root hair axis and continuous with CMTs in the sub-apex, which have the same orientation (Fig. 3B, C, and E). Later, still during tip growth, CMTs have different orientations along the root hair. In the basal part they are obliquely oriented and in parallel to each other, become more net-axially oriented in the upper part of the shank, and are always net-axially oriented in the subapex (Fig. 3C and E). In the CLSM images taken from living root hairs and immunolabeled FF/FS samples, the very tip of a growing root hair is devoid of CMTs (Fig. 3B, C, and E). In the shank of the root hair, the density of CMTs is higher in growing root hairs than in hairs of other developmental stages.

EMTs are located exclusively in the subapical cytoplasmic dense region between the basal part of the nucleus and the tip of the hair in a densely structured 3-dimensional array (Fig. 3D and F). We observed EMTs around and close to the nucleus in a high density. To determine whether these EMTs originate from the nuclear envelope, attach to it, or just surround it was not part of this study and would require a completely different set of experiments. EMTs in the lower part of the subapical cytoplasmic dense region occur in a higher density and deviate more from the long axis of the hair, than the EMTs close to the root hair tip. Some EMTs are reaching the very tip (Fig. 3D and F).

Growth arresting root hairs

Root hair growth-arrest starts when the main vacuole has permanently passed the nucleus (Sieberer and Emons, 2000). Thin extensions of the vacuole are reaching the very tip; subsequently growth rate drops, and eventually cell elongation stops. During growth-arrest, the nucleus does not follow the tip of the hair any longer and the cytoplasmic dense region decreases progressively in length. While the cytoplasmic dense region disappears, the central vacuole expands towards the tip (Fig. 4A). Growth-arrest is a gradual process and root hairs in this developmental stage are still growing to a certain extent before stopping growth (Sieberer and Emons, 2000). In growth-arresting hairs, CMTs (Fig. 4B, C
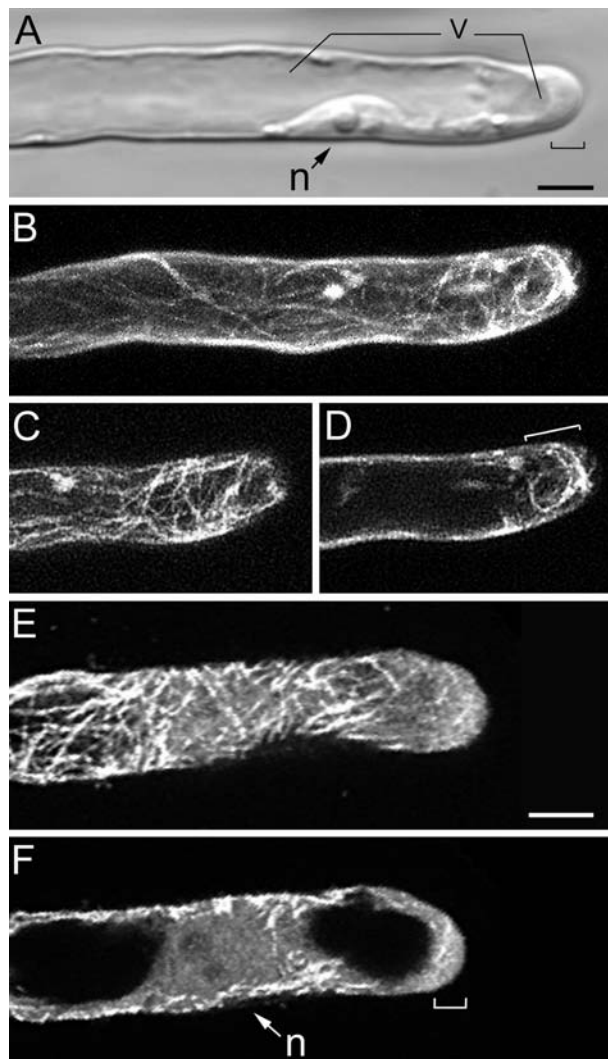
Figure 4. MTs in growth-arresting hairs visualized with a CLSM in scanning steps of 1 μm (B – F). B – D GFP-MBD, E and F immunocytochemistry. At this developmental stage the subapical cytoplasmic dense region has almost disappeared and the distance tip-nucleus has increased. **A**, Brightfield image of a living hair; bracket indicates the remaining subapical cytoplasmic dense region and the smooth (vesicle rich) region at the very tip. Bar = 10 μm (A – D). **B**, Full-stack projection of MTs. **C**, Projection of 3 peripheral sections, showing CMTs. CMTs are net-axially oriented. **D**, Projection of 4 median sections. Region of EMTs has decreased in length (bracket). **E**, Projection of 3 peripheral sections, showing CMTs. For explanation see C. Bar = 10 μm. **F**, Projection of 4 median sections; for explanation see D. n indicates the nucleus, v the vacuole.

and E) are net-axially oriented all along the root hair tube and they are reaching the very tip. As the subapical cytoplasmic dense region gets smaller the area with EMTs gets shorter, but, as long as growth continues, remains present close to the tip (Fig. 4D and F). When growth stops, all EMTs have disappeared.

Full-grown root hairs

Typically, a full-grown hair has a thin peripheral layer of cytoplasm around the large central vacuole (Fig 5A) and the nucleus has a random position within the hair (Sieberer and Emons, 2000). CMTs, the only remaining population of MTs in full-grown root hairs (Fig. 5B – F), are net-axial in the hairs that recently have stopped growth, and mainly

longitudinal in the hairs that terminated growth already some time ago (compare Fig. 5D with F). CMTs are converging at the very tip of the hair (Fig. 5B – E). In full-grown root
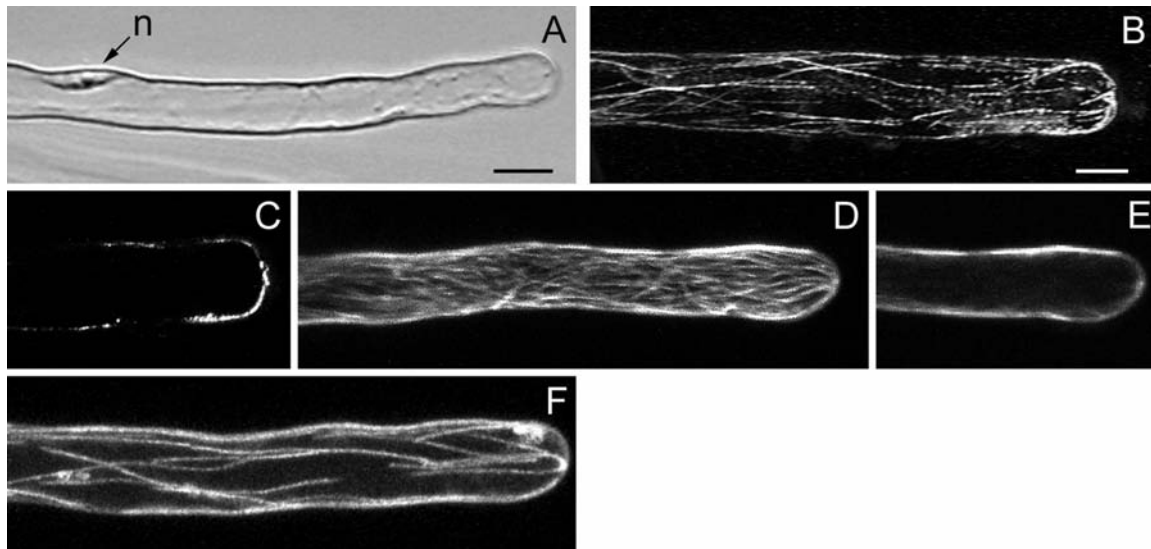

Figure 5. MTs in full-grown root hairs visualized with a CLSM in scanning steps of 1 μm. B and C immunocytochemistry, D – F GFP-MBD. A, Brightfield image of a living hair. Note position of the nucleus. Bar = 10 μm. B, Full-stack projection of CMTs. CMTs, the only remaining population of MTs in this developmental stage, are longitudinally oriented; they converge at the very tip. Bar = 10 μm (B – F). C, Projection of 2 median sections. Full-grown hairs have no EMTs. D, Full-stack projection of CMTs. The hair has stopped growth recently and the density of CMTs, which are net-axially oriented, is similar to previous developmental stages. E, Projection of 2 median sections; for explanation see C. F, Full-stack projection of CMTs in a hair of a later stage than shown in D. The density of CMTs is lower than in hairs that have just terminated growth.

hairs, the density of CMTs decreases over time (Fig. 5F), resulting in living hairs with hardly any detectable MTs left. Full-grown root hairs never have EMTs (Fig. 5C and E).

Effect of low concentrations of microtubule inhibitors on growing root hairs

To study the function of EMTs, they were depolymerized with oryzalin and stabilized with taxol. Oryzalin is a dinitroaniline herbicide, which binds rapidly and reversibly to plant tubulin with high affinity (Hugdahl and Morejohn, 1993) and depolymerizes plant

microtubules (Morejohn et al., 1987). It binds to tubulin heterodimers in the cytoplasm, and thereby prevents further growth of MTs leading to depolymerization of MTs, first the more dynamic ones (reviewed in: Anthony et al., 1999). Thus, the use of low concentrations of oryzalin, and observation of its effect in time, may enable one to dis-
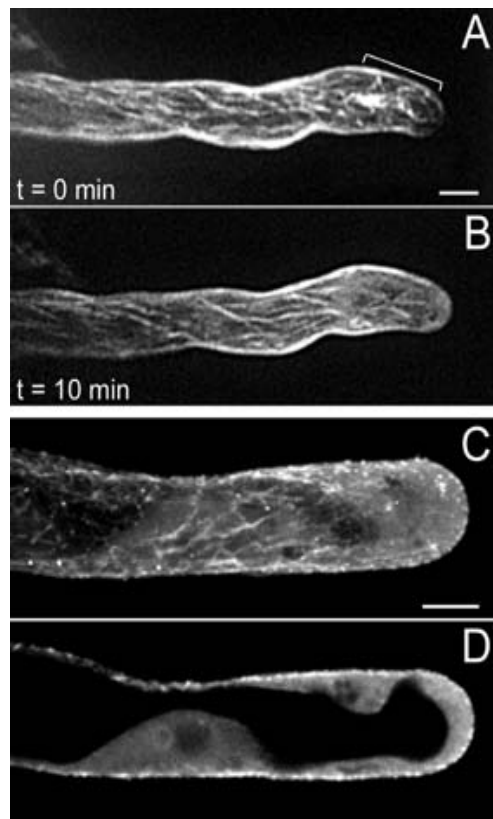

Figure 6. MTs in growing root hairs treated with 1 μM oryzalin. A and B GFP-MBD, C and D immunocytochemistry. **A**, Hair before treatment: a full-stack projection shows abundant MTs in the subapical region (bracket). **B**, 10 min after treatment. The subapical region contains less MTs and the MTs (cortical) in the shank of the hair are unchanged. **C**, 15 min after treatment. **D,** A projection of the 4 median sections shows that EMTs and the subapical cytoplasmic dense region have completely disappeared, but the vesicle rich region still is present at the very tip (also see Fig. 7B and 7C). Bar in A = 10 μm, bar in C = 10 μm.

criminate between more and less stable MTs. We applied oryzalin in concentrations of 0.25 μM, 0.5 μM, and 1 μM to growing root hairs, which had a length of 100 to 150 μm by the time of drug application. None of these concentrations affected the viability of the root hairs or the cytoplasmic streaming. In all these concentrations, oryzalin did not inhibit bulge formation (data not shown). Further, with all these concentrations, EMTs disappeared within 5 min to 10 min while CMTs remained present. Figure 6 shows this for 1 μM oryzalin in a GFP-MBD expressing root hair and an immunolabeled sample. EMTs, which normally are abundant in the subapical cytoplasmic dense region of growing hairs, were completely absent in oryzalin-treated growing root hairs while CMTs in the same hairs were not obviously affected.

Taxol, on the other hand, is a drug that binds to MTs and causes free tubulin in the cytoplasm to assemble into MTs, thus stabilizing MTs (Morejohn et al 1991). We found that the lowest concentration of a range tested (0.25 µM, 0.5 µM, and 1 µM) that had a clear effect on growth rate but did not affect cell viability, was 1 µM. We used taxol in a concentration, which had a similar effect on root hair growth rate as 1 µM oryzalin, which appeared to be 1 µM. However, in 1 µM taxol root hairs completely recovered their growth rate within 2 to 3 h. Therefore, we refreshed taxol every 120 min.

Oryzalin, at the concentration of 1 µM, had striking effects on the cytoarchitecture of growing root hairs (Fig. 7A - C). Within minutes after application of oryzalin, growing root hairs lost their typical cytoarchitecture. The subapical cytoplasmic dense region disappeared gradually within 5 to 10 min, while the vacuole passed the nucleus and expanded towards the tip of the hair. Finally, an oryzalin-treated hair had no subapical cytoplasmic dense region, the tip-nucleus distance had increased (see below), but the smooth region, containing the Golgi vesicles, was still present at the very tip and became even slightly longer over time. The smooth region in an oryzalin-treated hair could even reach a length of 15 to 20 µm in stead of the normal length of approx. 3 µm (Sieberer and Emons, 2000). As long as oryzalin was not washed out of the growth medium, the growing root hairs did not re-establish their typical cytoarchitecture. Hairs were observed up to 7 h after drug application.

The nucleus of an oryzalin treated growing root hair lost its typical position of 30 to 40 µm from the tip and moved slowly backwards in the root hair tube within the first 90 to 120 min after treatment (Fig. 8A). After that time the nucleus again was following the expanding root hair tip at a significantly larger distance (Fig. 8A). A nuclear movement at the pace with cell elongation was observed in all hairs, but the distance between the nucleus and the tip was not the same in all hairs. In approx. 70 % of the hairs, this distance was 140 ± 30 µm over a period of 4 to 5 h. The other 30 %, not represented in Fig. 8A, had a smaller (minimally 80 µm) or larger (maximally 250 µm) nucleus-tip distance, but also in these hairs the nucleus followed the tip. Relevant here is not the exact distance, but the fact that the nucleus keeps following the growing root hair tip

Taxol in a concentration of 1 µM had no effect on the cytoarchitecture (Fig. 7D – F) and the position of the nucleus (Fig. 8A). The distance nucleus-tip of 30 to 40 µm remained constant. Observed with bright - field microscopy during 7 h, the subapical cytoplasmic
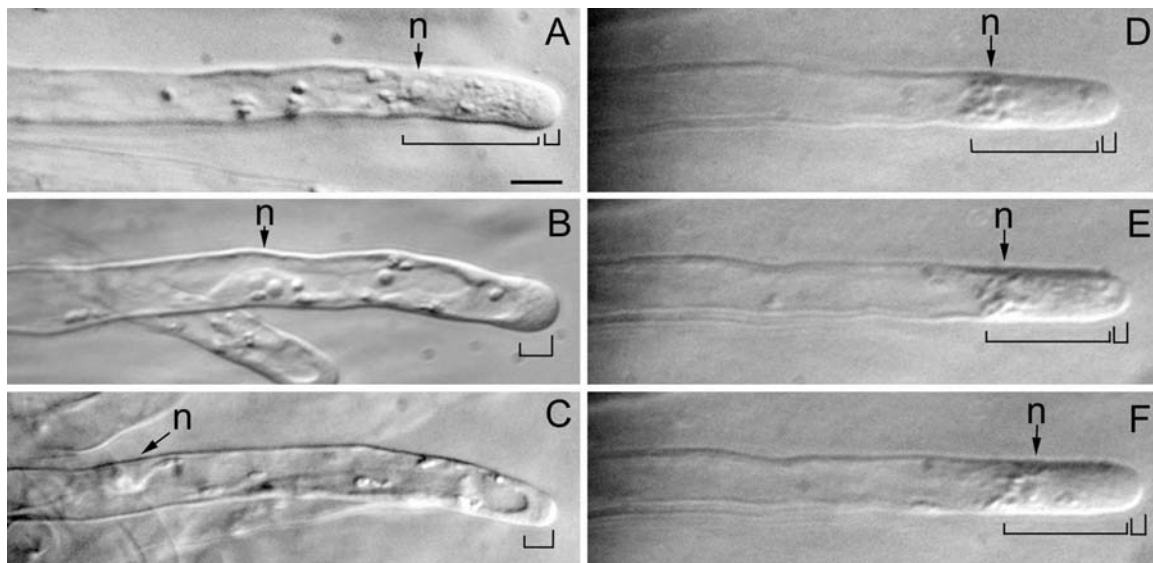
Figure 7. The effect of treatment with oryzalin or taxol on the cytoarchitecture of growing root hairs. **A**, Before treatment. **B**, 30 min 1 µM oryzalin. **C**, 60 min 1 µM oryzalin. **D**, Before treatment. **E**, 30 min 1 µM taxol. **F**, 60 min 1 µM taxol. Brightfield images from living root hairs. Large bracket indicates the subapical cytoplasmic dense region, small bracket the smooth (vesicle rich) region, n the nucleus. Magnification is the same in all images, bar = 20 µm.
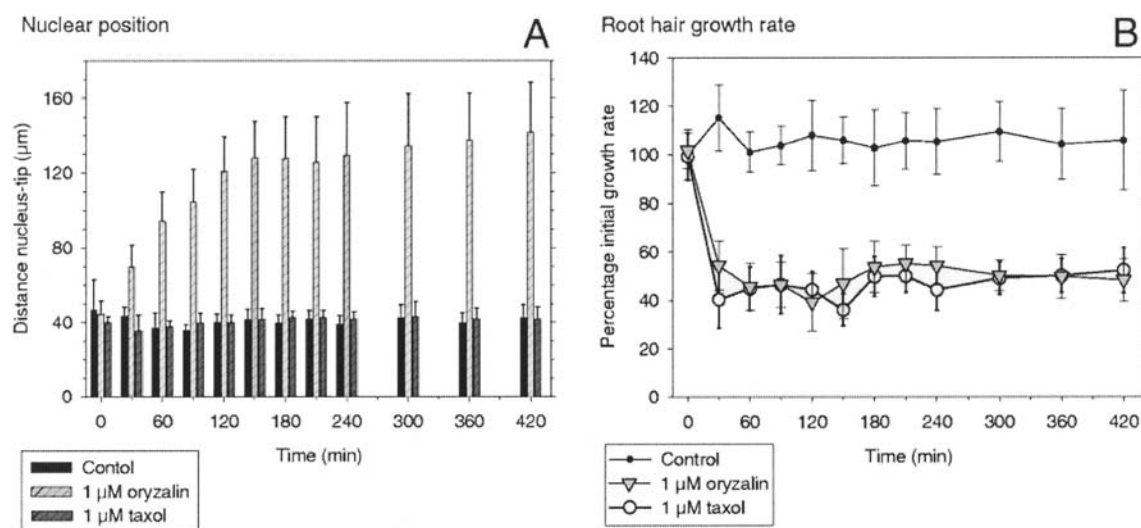
Figure 8

Figure 8 (opposite page). Nuclear position (**A**) and root hair growth rate (**B**) in growing *M. truncatula* root hairs after control treatment and treatment with 1 µM oryzalin or 1 µM taxol. While in controls and taxol-treated hairs the nucleus kept a distance of 30 – 40 µm to the tip over time, it was significantly increased in oryzalin (A). Growth rate in the hairs remained high in controls, but dropped by approx. 60 % in oryzalin and taxol (B). Results for each treatment are presented as the means of 10 hairs with their standard deviation. Results are representative for 3 independent replicates for each treatment.

dense region did not show any obvious changes in cytoarchitecture and length, compared with controls.

Oryzalin, at the above mentioned concentration of 1 µM had a significant effect on the growth rate of growing root hairs, but did not inhibit tip growth per se (Fig. 8B). Treated hairs did grow, but with a lower growth rate than untreated growing root hairs. We followed growing root hairs treated with oryzalin over a time span of 7 h. During this period, we did not observe any changes in shape and width of the root hair tube. Furthermore, these hairs always maintained one point of growth (i. e., the expanding tip). Shortly after application of 1 µM oryzalin most root hairs exhibited a single deviation from their normal growth axis, which is perpendicular to the root. In some root hairs, several deviations from the hairs' growth axis occurred irregularly over time in the presence of oryzalin. However, we never observed a wavy growth pattern of root hairs after microtubule inhibitor treatment as described for *A. thaliana* (Bibikova et al., 1999). An important difference with that work is that these authors depolymerized all MTs, while in our approach only EMTs were depolymerized and not the CMTs. It is not known whether *A. thaliana* has EMTs; they have not been reported.

When oryzalin was washed out after 7 h by replacing the medium with fresh PGM, 35 to 40 % of the growing root hairs fully recovered their cytoarchitecture, but their growth rate reached max. 70 % of the initial growth rate (data not shown). This recovery took place over a period of 4 to 6 h.

Taxol, in a concentration of 1 µM, had a similar effect on the growth rate of growing root hairs as oryzalin (Fig. 8B). While the growth rate in taxol treated growing root hairs dropped approx. to 40% of the initial growth rate, the distance nucleus-tip of 30-40 µm remained constant. In 1 µM taxol, root hairs maintained one single point of growth,

always kept the same directionality of growth, and always had the same shape as control root hairs.

Oryzalin in concentrations of 10 µM and 30 µM had the same effect on the cytoarchitecture of growing *M. truncatula* root hairs as a concentration of 1 µM had (data not shown). Growing root hairs that had a length of 100 µm to 150 µm by the time of drug application were at least observed for 5h. Within minutes upon treatment, the distance between nucleus and hair tip increased, while the subapical cytoplasmic dense region disappeared. The apical vesicle-rich region remained unchanged and tip growth itself proceeded, but growth rate dropped in a similar way as in hairs treated with 1 µM oryzalin. Using immunocytochemistry after a 30 min treatment with 30 µM oryzalin, we could not detect EMTs or intact CMTs in these hairs, while they were kept on growing for hours.

Discussion

In this paper we report changes in the spatial configuration of the microtubule cytoskeleton during development of *M. truncatula* root hairs and the effect of microtubule-inhibitors on the structure of the microtubule cytoskeleton, the cytoarchitecture, the nuclear position, and growth rate of growing hairs. The results obtained with the two used approaches, cells expressing a GFP-MBD fusion protein (Marc et al., 1998) and immuno-labeled fixed whole-mount samples, were similar. Thus, we conclude that the GFP-MBD construct decorates the same set of MTs as the anti-a-tubulin mouse monoclonal antibody clone DM 1a does. We identified two different populations of MTs in root hairs: CMTs, present in all developmental stages, and more dynamic and labile EMTs, unique for growing root hairs. Further, we did not observe any measurable effect on root hair development, the cytoarchitecture, growth pattern, and growth rate in GFP-MBD expressing root hairs. Taken together, it again has been proven that GFP-MBD is a suitable tool for studying MTs in living plant cells (Marc et al., 1998; Granger and Cyr, 2000).

Cortical microtubules during root hair development

All diffuse growing interphase plant cells have cortical microtubules, which are transverse to the direction of elongation of the cell. They become less frequent and obliquely aligned when cell elongation decelerates (Traas et al., 1985; review: Cyr, 1994; Wasteneys, 2000). These microtubules are involved in cell elongation and appear often, but not always, in the same orientation as nascent cellulose microfibrils (Sugimoto et al., 2000; review: Wasteneys, 2000). As expected, the diffuse growing trichoblasts have CMTs transverse to the root axis. The time of bulge formation seems to be the time these cells begin to stop growing. At their upper and lower edges, microtubules are becoming helical when bulges first appear. However, at the site of bulge formation, the CMTs are transverse, and after bulge appearance, they are still in this orientation running over the tip of the bulge. During bulge formation the distance between CMTs increases; they seem to passively part at the bulge tip. In the presence of oryzalin, bulges are being formed normally. Also from studies on the cytoskeleton (actin: Miller et al., 1999; actin and MTs: Baluska et al., 2000), ultrastructure (*V. sativa:* Miller et al., 2000), cytoplasmic [Ca^{2+}] gradients in wild type *A. thaliana*, and the rhd-2 mutant (Wymer et al., 1997), it was concluded that bulge formation is a distinctly different process than tip growth of the root hair proper.

CMTs have been found in root hairs of all species examined in either helical or mostly net-axial orientations (reviewed in: Ketelaar and Emons, 2000 and 2001). The function of CMTs in root hairs is still not clear. *A. thaliana* root hairs with depolymerized MTs (Bibikova et al., 1999) or a mutant with disorganized CMTs (Whittington et al., 2001), continue to elongate by tip growth, but in a slightly wavy pattern. Thus, CMTs do not seem to be required for growth per se, but may have to do with direction of elongation. Since CMTs are often found to be aligned with microfibrils, it is often thought that CMTs are responsible for directing nascent cellulose microfibrils. However, contradictory examples have been reported and other mechanisms have been proposed (reviewed in Emons and Mulder, 2000). The configuration of CMTs we now found in growing root hairs is net-axial in the upper part of growing root hairs and helical in the basal part. A cell wall study has yet to be performed for *M. truncatula*.

In *M. truncatula* root hairs, CMTs are absent from the extreme tip, both in the GFP-MBD plant and after FF/FS immunolabeling. In electron microscopy images of FF/FS root hairs of other species, CMTs were very close to the tip. They have been observed in the area where the Golgi vesicles are located (*E. hyemale*: Emons, 1989, *A. thaliana*: Galway et al., 1997). The absence of CMTs from the very tip could be explained with insufficient

labeling of MTs at this place. The specific binding sites of CMTs close to the tip of a growing root hair may not be fully accessible for GFP-MBD or antibodies, because CMTs at this site are highly decorated with microtubule binding proteins. Therefore, the absence of CMTs in *M. truncatula* should be confirmed with electron microscopy.

Endoplasmic microtubules during root hair development

EMTs are unique for the subapical region in tip-growing root hairs of *M. truncatula*. From our experiments with low concentrations of oryzalin, it is clear that EMTs are far more sensitive to depolymerization than CMTs and thus might be more dynamic than CMTs (Anthony and Hussey, 1999).

Until now, EMTs have only been reported for legume root hairs, not for any other species. Lloyd et al. (1987) found EMTs in growing root hairs of *V. hirsuta* that were hypothesized to connect the migrating nucleus to the root hair tip, where they fountain out upon the cortex. We have not seen similar structures in *M. truncatula*. Lloyd et al. used chemical fixation and immunolocalization to visualize MTs and due to the limited resolving power of the fluorescence microscope as compared to a CLSM, the precise configuration of EMTs still was a matter of speculation. In our hands, EMTs appear at the root hair tip when tip growth starts from bulges and they remain present in the tip region during cell elongation and disappear upon growth arrest. In growing root hairs, EMTs form a densely structured 3-dimentional-array close to, and in front of, the nucleus. They extend throughout the subapical cytoplasmic dense region towards the tip-region, appearing less dense there. What is the function of these EMTs? Are they involved in cell elongation or the determination of growth direction, nuclear positioning, regulation of tube width or actin filament configuration? In the following, we discuss the function of EMTs in cell elongation and in configuring cell architecture including nuclear position.

Function of EMTs in configuring the subapical cytoplasm including the localization of the nucleus at a certain distance from the hair tip

The MT depolymerizing drug oryzalin at a concentration of 1 µM caused a dramatic change in the cytoarchitecture of the subapex of growing *M. truncatula* root hairs, while taxol, a MT stabilizing drug, left the cytoarchitecture intact. EMTs, but not CMTs, were

depolymerized by 1 µM oryzalin. EMTs, but not CMTs, were depolymerized by 1 µM oryzalin. The most straightforward conclusion from these experiments is that EMTs must contribute directly or indirectly to the cytoarchitecture of growing root hairs. Therefore, we conclude that EMTs are involved in supporting the organization and maintenance of the subapical cytoplasmic dense region. The question then arises what the relationship is with the actin cytoskeleton. The actin cytoskeleton forms a specific configuration of fine bundles of actin filaments, FB-actin, in the subapical cytoplasmic dense region (Miller et al., 1999). An interesting option for the function of EMTs is the one suggested by Tominaga et al. (1997) for *Hydocharis morsus-ranae* root hairs. From their experiments in which they combined actin and microtubule drugs, these authors suggest that MTs regulate the organization of actin filaments in the cortex of root hairs. In diverse cell types functional interactions may exist between the actin and microtubule cytoskeleton (reviewed in: Goode et al., 2000) and have been suggested for tip growing plant cells (reviewed in: Kropf et al., 1998).

Related to the role of EMTs in the formation of the subapical cytoarchitecture, is their role in the positioning of the nucleus at a distance of 30 to 40 µm to the growing root hair tip. In an oryzalin treated hair, the nucleus first loses its position, but after a period of backward movement, it again is actively following the (now more slowly) growing tip at a larger but again fixed distance. For *A. thaliana* root hairs it has been reported that microtubule inhibitors such as oryzalin and taxol had no effect on nuclear movement (Chytilova et al., 2000). The question, not only for drug-treated cells but also for control cells, is: "what keeps the nucleus following the root hair tip?" Apparently, this is not only the cytoskeleton of EMTs.

Function of EMTs in cell elongation

Oryzalin, in a concentration at which only EMTs are depolymerized, caused a completely different cytoarchitecture, but have the same effect on growth rate as taxol in a concentration that kept the cells viable. Oryzalin caused the disappearance of the subapical cytoplasmic dense region, but in taxol the cytoarchitecture of apex and subapex remained unaltered. After treatment with oryzalin the smooth vesicle rich region at the very tip remained present and even increased in length. What is the same in both treatments is that the vesicle rich region at the root hair tip remains present. This is the one and most important prerequisite for tip growth. The fusion of the vesicles with the plasma

membrane is the actual cell elongation process, which of course cannot take place if the vesicles are not there. We conclude that exocytotic vesicles are still being produced, and delivered to the vesicle rich region, and fuse with the plasma membrane in growing root hairs treated with oryzalin or taxol. Tip growth proceeds, though at a low rate. From electronmicroscopy experiments we know that the subapical region of legume root hairs contains longitudinal cisternae of the endoplasmic reticulum and also mitochondria and Golgi bodies (vetch: Miller et al., 2000). Actin labeling has shown the occurrence of subapical net-axial fine bundles of actin filaments, called FB-actin (vetch; Miller et al., 1999). Since hairs in which the subapical cytoplasm is not present anymore (oryzalin) or stabilized (taxol) do still grow, we hypothesize that EMTs, possibly together with or in relation to FB-actin, configure the subapical cytoplasm, but that the vesicle transport system is actin-based. The combined EMTs, FB-actin, and ER cell structure may form a subapical buffer reservoir for exocytotic vesicles in transit to the apical vesicle rich region.

In the presence of both oryzalin and taxol, the growth rate of root hairs drops by 60%. The simplest explanation for this in the case of oryzalin is that the delivery of exocytotic vesicles to the vesicle rich region is inefficient, because there is no buffer of vesicles. Along the same line, this delivery may be inefficient in the presence of taxol, because the EMTs are not functioning properly. In addition, there are root hairs of for instance *Limnobium stoloniferum* (Emons, unpublished) or *H. morsus ranae* (see images of Tominaga et al., 1997) that do not have a subapical cytoplasmic dense region or that have an extremely short one. Of course, they do possess a vesicle rich region. Growth rates of root hairs of species, with and without a subapical cytoplasmic dense region, have not been compared.

One should have an open mind for other possible explanations. One of the important observations is that, though in oryzalin treated hairs the subapical cytoplasmic dense region disappears, the vesicle rich region remains present and even enlarges. The fact that upon oryzalin treatment the vesicle rich region enlarges, while growth rate is tempered, suggests that the drug may interfere with the growth process, exocytosis, itself. In that case, taxol should interfere with exocytosis in a similar fashion.

Relevance of endoplasmic microtubules for legumes

It is striking that EMTs have only been reported for legume root hairs, though MTs in root hairs of several species have been studied (reviewed in Ketelaar and Emons, 2000). Several of these studies were designed to investigate the relationship of CMTs with cellulose microfibrils. Therefore, only the cell cortex was investigated and EMTs may have been missed.

However, we should consider that legume root hairs might be special. Legumes have developed symbiosis with rhizobia. During the root hair curling around rhizobia, one of the first steps during the infection process, the cytoplasm with its contents (e.g. cytoskeleton, ER, Golgi bodies, etc.) mediates the curling and the formation of an infection thread through which the bacteria traverse the hair towards the root cortex. One can imagine that for both processes EMTs are important.

Material and Methods

Plant Culture

Seeds of *Medicago truncatula* cv Jemalong (Fabaceae) were scarified with 97% sulfuric acid for 10 min and surface sterilized with a mixture of 96% (v/v) ethanol and 30% (v/v) hydrogen peroxide (ethanol:hydrogen peroxide [1:1, v/v]) for 3 min. After rinsing with sterile water, seeds were imbibed for 4 h at 30°C in sterile water and placed on 1% (w/v) agarose-plates. Plates were sealed and stored upside down in the dark for 2 to 4 days at 4ºC to synchronize germination. During germination for 6 to 8 h at 24ºC the seeds were protected from light. Seedlings were transferred on wet filter paper and grown in vertical orientation for 24 to 48 h under sterile conditions at 24ºC and 16 h day length. The plant growth medium (PGM) which was used to humidify the filter paper contained 1.36 mM $CaCl_2$, 0.97 mM $MgSO_4$, 1.12 mM Na_2PO_4, 1.36 mM KH_2PO_4 and 20 µM Fe-citrate, pH 6.5 (Miller et al. 1999).

In a different set-up seedlings were grown at an angle of 45° for 24 to 30h in micro-chambers in between a cover slip and a glass slide (Fåhraeus slides: Fåhraeus 1957; Heidstra et al., 1994) in sterile conditions at 24ºC and 16 h day length. Each Fåhraeus slide contained two seedlings and 3 ml PGM.

Whole mount immunocytochemistry of MTs

For rapid freeze-fixation, seedlings were plunged into liquid propane cooled to -180°C with liquid nitrogen and kept there at least for 20 sec. Roots were excised and transferred into cryogenic vials, freeze substituted in water-free methanol containing 0.05% [v/v] glutaraldehyde for 48 h at -90°C and allowed to warm to room temperature over a 24 h period. Samples were re-hydrated in a graded series of methanol in phosphate-buffered saline (PBS, 137 mM NaCl, 2.7 KCl, 1.5 mM KH_2PO_4, 8.1 mM Na_2HPO_4, pH 7.4) containing fixative (0.1% glutaraldehyde [v/v] and 4% [w/v] paraformaldehyde). After re-hydration, a partial cell wall digestion was carried out in a saturated suspension of driselase (Fluka, Buchs, Switzerland) and macerocyme R10 (Serva, Heidelberg, Germany) in 100 mM 2-morpholinoethanesulfonic acid (MES) for 40 min at 35°C and pH 6.15). The specimens were then washed two times for 5 min in PBS and to block unspecific sites incubated for 5 min in PBS containing 0.1% (w/v) acetylated bovine serum albumin ([BSA$_{ac}$] Aurion, Wageningen, Netherlands) and 0.05% (v/v) Triton X-100 (BDH Laboratory Supplies, Poole, UK). The samples were incubated in the monoclonal primary antibody anti-a-tubulin mouse, clone DM 1a (Sigma Chemical Co., St. Louis, USA) diluted 1:300 (v/v) in PBS containing 0.1% (w/v) BSA$_{ac}$ and 0.05% (v/v) Triton X-100 for 12h at 4°C. After washing three times for 5 min in PBS the samples were incubated in the secondary antibody goat against mouse/IgG/Alexa 488 (Molecular Probes, Eugene, USA) diluted 1:300 (v/v) in PBS containing 0.1% (w/v) BSA$_{ac}$ and 0.05% (v/v) Triton X-100 for 12h at 4°C. Specimens were washed twice for 5 min with PBS and for 5 min with CITIFLUOR PBS solution (Citifluor Ltd., London, UK), and mounted in an antifading medium (PROLONG ANTIFADE, Molecular Probes).

Microscopic observation

Anti-a-tubulin labeled microtubules were visualized with a BIO-RAD MCR 600 confocal laser-scanning microscope (CLSM) (Bio-Rad Laboratories Ltd., Hertfordshire, UK) with an argon-krypton ion laser attached to a NIKON DIAPHOT 300 (Nikon Europe B.V., Badhoevedorp, The Netherlands) inverted microscope equipped with a 60x FL 1.4 n.a. oil immersion objective (Nikon). Samples were scanned in subsequent steps of 1 μm. Images were taken and projected with Confocal Assistant Version 4.02 (Bio-Rad, written by Todd Clark Brelje) and processed with Scion Image Beta 4.0.2. (Scion Corporation, Frederick, Maryland, USA) and Adobe Photoshop 5.5 (Adobe Systems Incorporated, Mountain View, CA, USA).

GFP-MBD decoration of MTs / Transgenic *Medicago truncatula* plants

Used plasmids

The GFP-MBD fusion gene with expression under the control of the 35S promotor was provided in a pUC18 vector by Richard Cyr (Marc et al. 1998). The complete insert from this plasmid was transferred to pCambia1390 (CAMBIA, PO Box 3200, Canberra ACT 2601, Australia) by using the HindIII-EcoRI sites, and was kindly provided by Theodorus WJ Gadella Jr. (Wageningen University).

Plant transformation and culture

Transformed roots of *M. truncatula* cv Jemalong were obtained by using *Agrobacterium rhizogenes* according to the protocol described by Boisson-Dernier et al. (2001). About 3 to 4 weeks later plants with transformed roots were put into square 12 cm plastic dishes (Greiner Labortechnik, Kremsmünster, Austria) with one of the 4 sides containing in the middle a round perforation of about 5 mm in diameter. Each individual plant was put in the perforation in such a way that the root was inside on Fåhraeus medium containing 0.8 % agar and the stem part outside the plate. Plates were put vertically in a culture room at 25°C and 18-h day length.

Microscopic observations

For observation, the roots growing on agar were submerged in sterile water and covered with a gas permeable plastic foil (bioFOLIE 25, Sartorius AG, Vivascience Support Center, Göttingen, Germany) to prevent them from drying. The opened dish was put on the microscope stage of a ZEISS LSM510 (Carl Zeiss SA, Le Pecq, France) and observations were carried out either with a 40x/0.8 WPH2 Achroplan or 63x/0.9 WPH3 Achroplan objective. In general, optical sections were made of whole root hairs with a separating distance of 1 μm between subsequent sections. Image projections were made with ZEISS LSM Image Examiner and images were processed with Image-Pro plus (Media Cybernetics, L.P.).

Light Microscopy

Root hairs were observed with a 20x 0.4 n.a. or a 40x 0.55 n.a. objective (Nikon) on an inverted microscope with Hoffman modulation contrast system (DIAPHOT 200, Nikon), equipped with a CCD camera (DXC-95OP, Sony, Tokyo, Japan). Image recording and processing, and quantitative live-measurements were done with a real time digital contrast

and low light enhancement image processor (ARGUS-20, Hamamatsu Photonics, Hamamatsu City, Japan). To prevent light-induced stress, low light and green filters were used during quantitative live-measurements and related image recording.

Drugstudies

Oryzalin (Greyhound Chromatography, Birkenhead, UK) was dissolved in dimethyl sulfoxide ([DMSO] Merck, Darmstadt, Germany) as 10 mM stock solution and used at 0.25 µM, 0.5 µM, 1 µM, 10 µM, and 30 µM in PGM. Taxol ([paclitaxel] Sigma Chemical Co.) was dissolved in DMSO as 10 mM stock solution and used at 0.25 µM, 0.5 µM, 1 µM and 5 µM in PGM.

In Fåhraeus slides, drug solutions were applied on the microscope stage with a constant flow of 1 ml min^{-1}, replacing gradually the PGM in the slides. The final volume in each slide was 3 ml. While oryzalin was applied only once, taxol was refreshed every 120 min in the same way as applied for the first time (see above). To prevent evaporation of water during observation, slides were covered on the microscope stage with a large plastic Petri dish. Measurements on growth rate and nuclear position were done on growing root hairs of non transformed *Medicago truncatula* cv Jemalong roots. Growing root hairs had a length of 100 µm to 150 µm when measurements were started.

Control roots were treated with PGM only, containing the same amount of DMSO as the drug solutions.

Upon request, all novel materials described in this publication will be made available in a timely manner for non-commercial research purposes, subject to the requisite permission from any third-party owner of all parts of the material. Obtaining any permission will be the responsibility of the requestor.

Acknowledgments

Literature Cited

Anthony RG, Hussey PJ. 1999. Dinitroaniline herbicide resistance and the microtubule cytoskeleton. Trend Plant Sc 4: 112-116.

Baluška F, Salaj J, Mathur J, Braun M, Jasper F, Samaj J, Chua NH, Barlow PW, Volkmann D. 2000. Root hair formation: F-actin-dependent tip growth is initiated by local assembly of profilin-supported F-actin meshworks accumulated within expansin-enriched bulges. Dev Biol 227: 618-632.

Baskin TI, Miller DD, Vos JW, Wilson JE, Hepler PK. 1996. Cryofixing single cells and multicellular speciments enhances structure and immunocytochemistry for light microscopy. J Microsc 182: 149-161.

Bibikova TN, Blancaflor EB, Gilroy S. 1999. Microtubules regulate tip growth and orientation in root hairs of *Arabidopsis thaliana*. Plant J 17: 657-665.

Boisson-Dernier A, Chabaud M, Garcia F, Bécard G, Rosenberg C, Barker DG. 2001. *Agrobacterium rhizogenes*-transformed roots of *Medicago truncatula* for the study of nitrogen-fixing and endomycorrhizal symbiotic associations. Mol Plant Microbe Interact 14: 695-700.

Chytilova E, Macas J, Sliwinska E, Rafelski SM, Lambert GM, Galbraith DW. 2000. Nuclear dynamics in Arabidopsis thaliana. Mol Biol Cell 11: 2733-2741.

Collings DA, Asada T, Allen NS, Shibaoka H. 1998. Plasma membrane-associated actin in bright yellow 2 tobacco cells. Plant Physiol 118: 917-928.

Cook D. 1999. *Medicago truncatula*: a model in the making! Curr Opin Plant Biol 2: 301-304.

Cyr RJ. 1994. Microtubules in plant morphogenesis: role of the cortical array. Annu Rev Cell Biol 10: 153-180.

De Ruijter NCA, Bisseling T, Emons AMC. 1999. *Rhizobium* Nod factors induce an increase in sub-apical fine bundeles of actin filaments in vicia sativa root hairs within minutes. Mol Plant Microbe Interact 12: 829-832.

De Ruijter NCA, Rook MB, Bisseling T, Emons AMC. 1998. Lipochito-oligosaccharides re-initiate root hair tip growth in *Vicia sativa* with high calcium and spectrin-like antigen at the tip. Plant J 13: 341-350.

Dolan L, Duckett CM, Grierson C, Linstead P, Schneider K, Lawson E, Dean C, Poethig S, Roberts K. 1994. Clonal relationships and cell patterning in the root epidermis of *Arabidopsis*. Development 120: 2465-2474.

Emons AMC, Mulder BM. 2000. How the deposition of cellulose microfibrils builds cell wall architecture. Trends Plant Sci 5: 35-40.

Emons AMC, Mulder BM. 1998. The making of the architecture of the plant cell wall: how cells exploit geometry. Proc Natl Acad Sci USA 95: 7215-7219.

Emons AMC, Wolters-Arts AMC, Traas JA, Derksen J. 1990. The effect of colchicine on microtubules and microfibrils in root hairs. Acta Bot Neerl 39: 19-28.

Emons AMC. 1989. Helicoidal microfibril deposition in a tip-growing cell and microtubule alignment during tip morphogenesis: a dry-cleaving and freeze-substitution study. Can J Bot 67: 2401-2408.

Emons AMC. 1987. The cytoskeleton and secretory vesicles in root hairs of *Equisetum* and *Limnobium* and cytoplasmic streaming in root hairs of *Equisetum*. Ann Bot 60: 625-632.

Fåhraeus G. 1957. The infection of white clover root hairs by nodule bacteria studied by a simple glass slide technique. J Gen Microbiol 16: 374-381.

Galway ME, Heckman Jr. JW, Schiefelbein JW. 1997. Growth and ultrastructure of Arabidopsis root hairs: the rhd 3 mutation alters vacuole enlargement and tip-growth. Planta 201: 209-218.

Goode BL, Drubin DG, Barnes G. 2000. Functional cooperation between the microtubule and actin cytoskeletons. Curr Op Cell Biol 12: 63-71.

Gilroy S, Jones DL. 2000. Through form to function: root hair development and nutrient uptake. Trends Plant Sci 5: 56-60.

Granger CL, Cyr RJ. 2000. Microtubule reorganization in tobacco BY-2 cells stably expressing GFP-MBD. Planta 210: 502-509

Heidstra R, Geurts R, Franssen H, Spaink HP, van Kammen A, Bisseling T. 1994. Root hair deformation activity of nodulation factors and their fate on *Vicia sativa*. Plant Physiol 105: 787-797.

Hugdahl JD, Morejohn LC. 1993. Rapid and reversible high-affinity binding of the dinitroanaline herbicide oryzalin to tubulin from *Zea mays* L. Plant Physiol 102: 725-740.

Ketelaar T, Emons AMC. 2001. The cytoskeleton in plant cell growth: lessons from root hairs. New Phytol 152: 409-418.

Ketelaar T, Emons AMC. 2000. The role of microtubules in root hair growth and cellulose microfibril deposition. In Ridge RW, Emons AMC, eds, Root hairs. Cell and molecular biology, Springer-Verlag, Tokyo, pp 17-28.

Kropf DL, Bisgrove SR, Hable WE. 1998. Cytoskeletal control of polar growth in plant cells. Cur Opin Cell Biol 10: 117-122.

Long SR. 1996. *Rhizobium* symbiosis: Nod factor in perspective. Plant Cell 8: 1855-1898.

Lloyd CW, Pearce KJ, Rawlins DJ, Ridge RW, Shaw PJ. 1987. Endoplasmic microtubules connect the advancing nucleus to the tip of legume root hairs, but F-actin is involved in basipetal migration. Cell Motil Cytosk 8: 27-36.

Marc J, Granger CL, Brincat J, Fisher DD, Kao T, McCubbin AG, Cyr RJ. 1998. A GFP-MAP4 reporter gene for visualizing cortical mirotubule rearrangements in living epidermal cells. Plant Cell 10: 1927-1939.

Miller DD, Leferink-ten Klooster HB, Emons AMC. 2000. Lipochito-Oligosaccharide nodulation factors stimulate cytoplasmic polarity with longitudinal endoplasmic reticulum and vesicles at the tip in vetch root hairs. Mol Plant Microbe Interact 13: 1385-1390.

Miller DD, De Ruijter NCA, Bisseling T, Emons AMC. 1999. The role of actin in root hair morphogenesis: studies with lipochito-oligosaccharide as a growth stimulator and cytochalasin as an actin perturbing drug. Plant J 17: 141-154.

Morejohn LC. 1991. The molecular pharmacology of plant tubulin and microtubules. In Lloyd CW, ed, The cytoskeletal basis of plant growth and form, Academic Press, New York, pp 29-43.

Morejohn LC, Bureau TE, Molé-Bajer AS, Fosket DE. 1987. Oryzalin, a dinitroaniline herbicide, binds to plant tubulin and inhibits microtubule polymerization in vitro. Planta 172, 252-264.

Mylona P, Pawlowski K, Bisseling T. 1995. Symbiotic nitrogen fixation. Plant Cell 7: 869-885.

Peterson LR, Farguhar ML. 1996. Root hairs: specialized tubular cells extending root surfaces. Bot Rev 62: 1-35.

Ridge RW. 1993. A model of legume root hair growth and Rhizobium infection. Symbiosis 14: 359-373.

Ridge RW. 1988. Freeze-substitution improves the ultrastructural preservation of legume root hairs. Bot Mag Tokyo 101: 427-441.

Shaw SL, Dumais J, Long SR. 2000. Cell surface expansion in polarly growing root hairs of *Medicago truncatula.* Plant Physiol 124: 959-969.

Sherrier DJ, Van den Bosch KA. 1994. Secretion of cell wall polysaccharides in *Vicia* root hairs. Plant J 5: 185-195.

Sieberer B, Emons AMC. 2000. Cytoarchitecture and pattern of cytoplasmic streaming in root hairs of *Medicago truncatula* during development and deformation by nodulation factors. Protoplasma 214: 118-127.

Sugimoto K, Williamson RE, Wasteneys GO. 2000. New techniques enable comparative analysis of microtubule orientation, wall texture, and growth rate in intact roots of Arabidopsis. Plant Physiol 124: 1493-1506.

Timmers ACJ, Auriac M-C, Truchet G. 1999. Refined analysis of early symbiotic steps of the *Rhizobium-Medicago* interaction in relationship with microtubular cytoskeleton rearrangements. Development 126: 3617-3628.

Tominaga M, Morita K, Sonobe S, Yokota E, Shimmen T. 1997. Microtubules regulate the organization of actin filaments at the cortical region in root hair cells of *Hydrocharis*. Protoplasma 199: 83-92.

Traas JA, Braat P, Emons AMC, Meekes H, Derksen J. 1985. Microtubules in root hairs. J Cell Sci 76: 303-320.

Wasteneys GO. 2000. The cytoskeleton and growth polarity. Cur Opin Plant Biol 3: 503-511.

Whittington AT, Vugrek O, Wei KJ, Hasenbein NG, Sugimoto K, Rashbrooke MC, Wasteneys GO. 2001. MOR1 is essential for organizing cortical microtubules in plants. Nature 411: 610-613.

Wymer C, Bibikova TN, Gilroy S. 1997. Cytoplasmic free calcium distributions during the development of root hairs of *Arabidopsis thaliana*. Plant J 12: 427-439.

Vos JW, Hepler PK. 1998. Calmodulin is uniformly distributed during cell division in living stamen hair cells of *Tradescantia virginata*. Protoplasma 201: 158-171.

Chapter 4

Nod factors alter the microtubule cytoskeleton in *Medicago truncatula* root hairs to allow root hair reorientation

B.J.. Sieberer[1], A.C.J. Timmers[2], and A.M.C. Emons[1]

[1] Laboratory of Plant Cell Biology, Wageningen University, Arborteumlaan 4, 6703 BD Wageningen, The Netherlands

[2] Laboratoire des Interactions Plantes Microorganismes, CNRS/INRA, BP 27, 31326 Castanet-Tolosan Cedex, France

The first two authors have contributed equally to this work.

Abstract

The microtubule cytoskeleton is an important part of the tip-growth machinery in legume root hairs. Here we report the effect of Nod factor (NF) on microtubules (MTs) in root hairs of *Medicago truncatula*. In tip-growing hairs, the ones that typically curl around rhizobia, NF caused a subtle shortening of the endoplasmic MT array, which recovered within 10 minutes, whereas cortical MTs were not visibly affected. In growth-arresting root hairs, endoplasmic MTs disappeared shortly after NF application, but reformed within 20 minutes, whereas cortical MTs remained present in a high density. After NF treatment, growth-arresting hairs were swelling at their tips, whereafter a new outgrowth formed that deviated with a certain angle from the former growth axis. Microtubule depolymerisation with oryzalin caused a growth deviation similar to NF, while combined with NF, oryzalin increased and the microtubule-stabilizing drug taxol suppressed NF-induced growth deviation. The NF-induced disappearance of the endoplasmic MTs correlated with a loss of polar cytoarchitecture and straight growth directionality whereas the reappearance of EMTs correlated with the new set up of polar cytoarchitecture. Drug studies showed that microtubules are involved in determining root hair elongation in a new direction after NF treatment.

Introduction

The symbiosis between leguminous plants and rhizobia leads to the formation of a new organ, the N_2 fixing root nodule. The different steps involved in the establishment of the symbiosis between these two organisms are tightly controlled through a complex network of signaling cascades (Cullimore and Dénarié 2003; Endre et al. 2002; Geurts 2003; Limpens et al. 2003; Madsen et al. 2003; Radutoiu et al. 2003; Stracke et al. 2002; for review see: Parniske and Downie 2003). Nod factors (NFs) are signal molecules secreted by rhizobia and have been shown to be essential for successful symbiosis (Fisher and Long 1992; Lerouge et al. 1990; Roche et al. 1991; Spaink et al. 1991; Truchet et al. 1991). One of the first essential steps in the infection process is the curling of root hairs around the bacteria (Esseling et al. 2004; Hadri and Bisseling 1998; Kijne 1992). Van Batenburg et al. (1986) proposed that root hair tip growth is essential for root hair curling. Recently, hair curling has been described as iterative tip growth reorientation (Esseling et al. 2003).

It has been shown that the actin cytoskeleton is a target of NFs (*M. sativa*: Allen et al., 1994; *Phaseolus vulgaris*: Cárdenas et al. 1998, 2003; *Vicia sativa*: De Ruijter et al. 1998; Miller et al. 1999; Ridge 1992). During root hair curling of *Medicago* root hairs inoculated with *Sinorhizobium meliloti*, endoplasmic microtubules (EMTs) are present between the nucleus and the root hair tip of the curl, concentrate at the infection site where bacteria enter the root hair, and are present between the nucleus and the tip of the infection thread during infection thread growth in the root hair shank (Timmers 2000). Despite these findings, the responses of the MT cytoskeleton shortly after application of NF and their function in the early infection process remained elusive.

Elongating legume root hairs have endoplasmic microtubules (EMTs) in their sub-apex (*Vicia hirsuta*: Lloyd et al. 1987) that are organized in an extensive array (*M. truncatula*: Sieberer et al. 2002; *M. sativa*: Weerasinghe et al. 2003), which they acquire when tip growth begins and retain until growth stops (Sieberer et al. 2002). In contrast to legume root hairs, in growing *Arabidopsis* hairs the subapical array of EMTs consists of a few bundles of microtubules (Van Bruaene et al. 2004).

In the root hair deformation assay, in which NFs are globally applied to roots in a glass microchamber, the so-called Fåhraeus slides (Fåhraeus 1957), only growth-arresting root hairs respond with root hair deformation (*Vicia sativa*: Heidstra et al. 1994; de Ruijter et al. 1998; *M. truncatula*: Sieberer and Emons 2000), which is swelling of the root hair tip (i.e. temporary switch to isodiametric growth) and formation of a new outgrowth from the swelling (i.e. reinitiation of tip-growth) (*V. sativa*: de Ruijter et al. 1998; *M. truncatula*:

Sieberer and Emons 2000). In *Arabidopsis* root hairs, a pulse application of actin depolymerizing drugs causes swelling, from which tip growth resumes in the original growth orientation (Ketelaar et al., 2003). When the same treatment with actin depolymerizing drugs is performed in *Arabidopsis* hairs where microtubules were experimentally ablated, the new axis of cell elongation deviates from the original growth axis by a certain angle (Ketelaar et al. 2003). The newly formed outgrowth after NF induced root hair swelling also deviates at a certain angle from the original growth axis. This is an indication that MTs are NFs effectors. Here we report the effect of NFs, the microtubule depolymerizing drug oryzalin, the microtubule stabilizing drug taxol, and combinations of these agents on microtubule arrays and cell growth of *M. truncatula* root hairs. MTs were visualized by immunocytochemistry after rapid freeze fixation as well as with a GFP microtubule binding domain (GFP-MBD) fusion protein decoration in living root hairs.

Our findings show that the microtubule cytoskeleton contributes to root hair morphology, determines cytoplasmic polarity in elongating hairs, and therefore is an essential part of the tip-growth machinery. It appears to be a direct or indirect target of early NF signaling, and its dynamics a prerequisite for root hair reorientation upon NF perception.

Results

Effects of Nod factor on the microtubule cytoskeleton and the cytoarchitecture of elongating root hairs

Within 3 to 5 min after NF application we observed a subtle and transient shortening of the three-dimensional and dense EMT array in the subapex of tip-growing hairs (compare Fig. 1, B with C, F, and H) that completely restored within 10 – 15 min. The restored EMT array remained present until regular growth termination (data not shown), which was the same as in control root hairs. Five minutes after NF treatment the EMT array at the basal part of the subapical region had almost completely disappeared (Fig. 1, C) or become less dense (Fig. 1, F H) in approx. 76% of the observed hairs (Table 1), whereas EMTs closer to the hair tip remained present (Fig. 1, C, and E through H). The percentage of root hairs with disturbed EMT array 5 min after NF application was higher than 10 min after NF application (significantly different at the 0.05 level, $p = 0.021589$, independent student's t-test analysis). The effect on the EMT array was subtle and could be observed only when a successive sequence of optical sections taken with CLSM was investigated. While the EMT array or the cytoarchitecture in one section appeared normal (Fig. 1, E and G), in the next section the EMT array was shorter and vacuole extensions penetrated the sub-apex (Fig. 1, F and H). To find out whether this was a true effect of NF and not just medium refreshment or the freeze fixation method, we compared NF-challenged root hairs with control hairs subjected to medium refreshment and freeze fixation. In the latter, only 45% of the hairs responded with a temporarily disturbed EMT array 5 min after treatment with plant growth medium (Table 1), which was lower than 5 min after NF treatment (significantly different at the 0.05 level, $p = 0.010104$). CMTs in a tip-growing hair treated with NF were not obviously affected (Fig. 1 D) at any time after NF application and their over-all patterning was similar to control root hairs treated with plant growth medium (PGM).

The temporary and partial shortening of the EMT array in elongating root hairs after NF application could only be observed in single optical planes taken with CLSM from immunolabeled root hairs after freeze fixation and freeze substitution, but not in GFP-MBD expressing root hairs. This could be due to a lack in resolving power (number and optical depth of z-scans) of the applied imaging technique to observe GFP-MBD decorated MTs in living root hairs (Sieberer et al. 2002), and the fact that the microtubules in the living hairs, especially the EMTs, are highly dynamic (Sieberer et al., 2002; Vos et al,

2003; Timmers A.C.J., unpublished results), which makes it difficult to visualize their precise configuration in a still image of the dense three-dimensional EMT array in a tip-growing root hair.
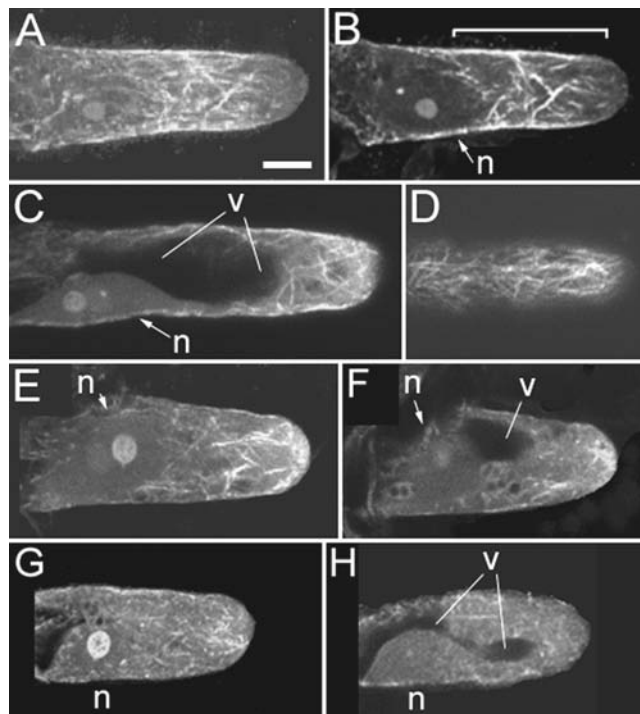

Figure 1. MTs in untreated and NF treated tip-growing *M. truncatula* root hairs. A and B, 5 min after control treatment. C through H, 5 min after treatment with 10^{-9}M NF. MTs were decorated with immunocytochemistry and visualized with a CLSM in scanning steps of 1 μm. n, nucleus; v, vacuole. Magnification is the same in all images. Bar = 10 μm. **A**, Full-stack projection; CMTs are net-axially oriented and do not reach the very tip of the hair. **B**, A median section of the same hair shows EMTs in the sub-apex of the hair (bracket). **C**, The projection of two median scans shows a short EMT array in the sub-apex (compare with Fig. 1 B). The vacuole has overtaken the nucleus and occupies a large part of the space between nucleus and tip, where normally the EMT array spreads. **D**, The projection of two cortical scans of the hair in C shows that CMTs are not obviously affected shortly after NF treatment. **E**, In a single optical section the EMT array and the cytoarchitecture appear to be undisturbed. **F**, The next successive section of the hair in E shows that the EMT array has almost completely disappeared. Close to the tip a few EMTs are present. The vacuole has started with overtaking the nucleus. **G**, Projection of two median scans. The EMT array has decreased in density; EMTs in the vicinity of the nucleus are short and fragmented. **H**, The next successive section of the hair in G reveals that a thin tubular extension of the central vacuole is penetrating the subapical plasma. EMTs are present in a low density.

Together with the temporary shortening of the subapical EMT array after NF treatment went a transient vacuolization of the cytoplasmically dense subapical region in elongating root hairs. Within 5 minutes after NF application in approx. 80% of the observed hairs

extensions from the central vacuole temporarily entered the dense subapical cytoplasm (Fig 2 B). Tip-growth did not stop during the temporary disturbance of the subapical region caused by NF and the cytoarchitecture recovered within 10 to 15 min (Fig. 2 C). Further, we compared the cytoarchitecture of tip-growing *M. truncatula* root hairs treated with NF with those treated with oryzalin, a microtubule-depolymerizing drug. Also in tip-growing hairs treated with 1 µM oryzalin thin extensions of the central vacuole started penetrating the dense cytoplasm within 5 min after application (Fig. 2 E). In contrast to NF treated hairs these vacuolar extensions increased in volume until the dense cytoplasm in the sub-apex had completely disappeared within 10 to 20 min, except for a cortical layer in the hair tube and a smooth, vesicle rich, region at the very tip of the hair (Fig. 2 F). In the presence of oryzalin, both the subapical dense cytoplasm and the EMT-array never recovered in elongating hairs and tip-growth proceeded, though at a lower growth rate (Sieberer et al. 2002). Control medium refreshment did not, or only slightly, affect the subapical cytoarchitecture of tip-growing hairs (Fig. 2, G – I).

Minutes after treatment	Percentage of tip-growing hairs with temporarily disturbed EMT array	
	NF	PGM
5 min	76.5% SD = 2.12	45% SD = 2.83
10 min	33.5% SD = 4.95	31% SD = 2.83
30 min	27% SD = 1.41	23.5% SD = 2.12

Table 1. Short term effects of 10^{-9}M NF and medium refreshment (PGM) on the EMT array of tip-growing root hairs. Samples were cryo-fixed 5, 10, and 30 min after NF treatment. EMTs were labeled with immunocytochemistry and visualized with confocal laser scanning microscopy. Forty root hairs per time point (4 different roots; 10 hairs per root) for each treatment were observed. The number of root hairs with disturbed EMT arrays (see Fig. 1C, F, and H) was scored. The results are presented as the mean percentages with SD of two independent repeats of the experiment.
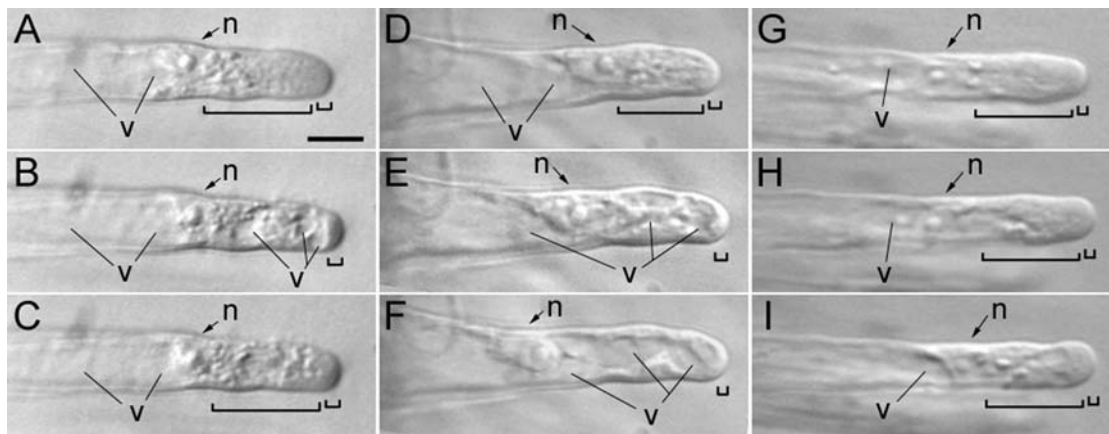
Figure 2. Short-term effect of 10^{-9}M NF, 1 µM oryzalin, and medium refreshment on the cytoarchitecture of tip-growing *M. truncatula* root hairs. Time series of living root hairs obtained with bright-field microscopy. Large bracket indicates the subapical region rich in cytoplasm; the small bracket indicates the clear zone (vesicle rich region). n, nucleus; v, vacuole. Magnification is the same in all images. Bar = 20 µm. **A,** Before treatment. **B,** Five minutes after NF. The subapical cytoarchitecture is heavily disturbed. **C,** Fifteen minutes after NF. The cytoarchitecture has almost completely recovered. **D,** Before treatment. **E,** Five minutes after oryzalin. The subapical cytoarchitecture is heavily disturbed. **F,** Fifteen minutes after oryzalin. Except for the vesicle rich region at the very tip the vacuole almost completely fills the sub-apex. In the presence of oryzalin the cytoarchitecture is not recovering. **G,** Before treatment. **H,** Five minutes after medium refreshment. **I,** Fifteen minutes after medium refreshment.

Effects of NF on the microtubule cytoskeleton and the cytoarchitecture of growth-arresting root hairs

Since the observed changes of the MT cytoskeleton in elongating root hairs upon NF treatment were subtle and short-termed, we studied the MTs in growth-arresting hairs after NF application as well. Differently from younger tip-growing hairs, growth-arresting hairs respond to globally applied NF with a distinct change in hair morphology called root hair deformation. Several cellular responses of the initial effects of NF can be elucidated by studying root hair deformation (for review see: Lhuissier et al. 2001), allowing the researcher the more black and white evaluation of the pronounced cellular responses to NF, which in our case are NF-induced changes of the MT cytoskeleton.
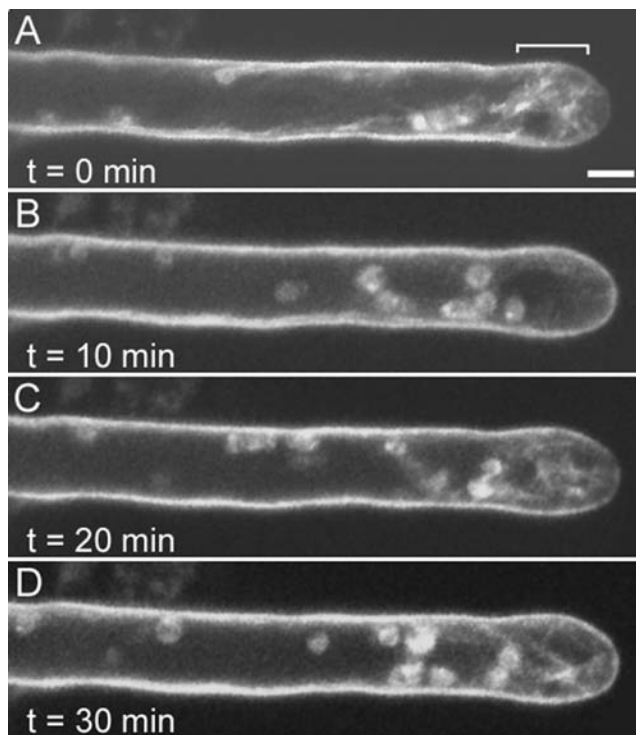
Figure 3. Time series of EMTs in a growth-arresting *M. truncatula* root hair treated with 10^{-9}M NF. MTs were decorated with GFP-MBD and visualized with a CLSM in scanning steps of 1 μm; for each image, 3 median sections were projected. Magnification is the same in all images. Bar = 10 μm. **A**, Before treatment; in the sub-apex there still is a short EMT array present (bracket). **B**, Ten minutes after treatment. The EMT array has disappeared. **C**, Twenty minutes after treatment. Single EMTs have reappeared inside a cytoplasmic strand in the sub-apex of the hair. **D**, Thirty minutes after treatment. EMTs within transvacuolar cytoplasmic strands have increased in density, but a dense EMT array as seen in A has not been rebuilt yet.

During growth-arrest the EMT array gradually shortens, as the dense cytoplasm in the sub-apex decreases in length, and eventually disappears after growth-termination (Sieberer et al., 2002). However, as long as tip-growth continues, EMTs are present. We have defined growth arrest as the time between the moment the vacuole permanently overtakes the nucleus and stop of hair elongation (Sieberer and Emons 2000). This process can take as long as 2 to 3 h.

Upon application of 10^{-9}M NF, the short EMT array of a growth-arresting hair disappeared within 5 to 10 min (Fig 3). Twenty to 30 min later, subapical EMTs reappeared inside a single or multiple transvacuolar cytoplasmic strand(s) (Fig. 3, C and D). During root hair tip swelling these cytoplasmic strands were constantly changing shape and volume, and, depending on their volume, contained various amounts of EMTs (Fig. 4, A, B and E). CMTs were extending to and reaching the very tip of growth-arresting hairs within 5 to 10 minutes after NF application. This is usually a sign that tip-growth is ceasing (Sieberer et al. 2002), but in contrast to a fully grown hair CMT density did not decrease over time (Fig. 4, C and D) and CMTs did not converge at the root hair tip (compare Fig. 6, A with

B) after NF application. As expected, also in growth-arresting hairs the prime effect of NFs on MTs was a rapid shortening of EMTs, while CMTs are not, or to a lesser extent, affected.
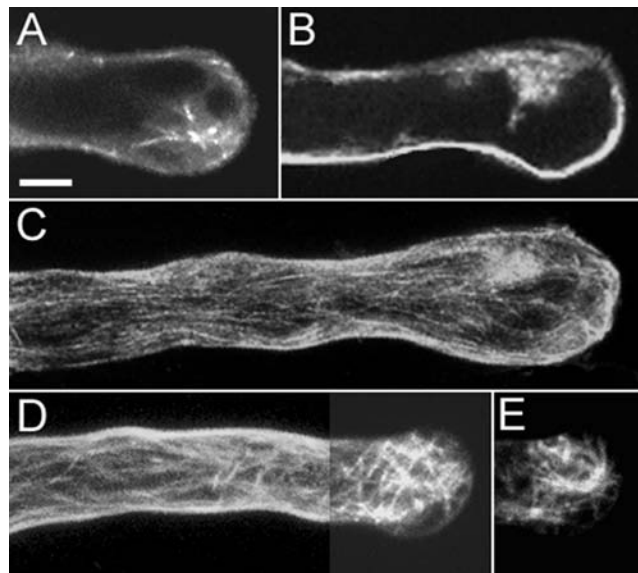

Figure 4. MTs in the swellings of growth-arresting root hairs treated with 10^{-9}M NF. MTs where visualized with CLSM in scanning steps of 1?m. A through C, Immunocytochemistry; D and E, GFP-MBD. Magnification is the same in all images. Bar = 20 μm. **A,** Sixty minutes after NF; a projection of 2 median sections shows EMTs inside the swelling. **B,** Seventy minutes after NF; a projection of 2 median sections shows EMTs inside the swelling. EMTs are located in cytoplasmic strands that constantly change shape, size, and orientation. **C,** Seventy minutes after NF; a full stack projection shows that CMTs remain present in a high density. **D,** Seventy minutes after NF; a full stack projection shows CMTs in a high density and a net-axial orientation in the shank of the hair and in a random pattern in the swelling. **E,** A projection of 3 median sections of the hair in D shows that EMTs appear in different densities within cytoplasmic strands inside the swelling.

A new root hair outgrowth emerged from the swollen tip between 90 to 120 min after application of NF. The dense three-dimensional EMT array described for a tip-growing root hair progressively reappeared (Fig. 5) and the newly formed outgrowth had a polarized cytoarchitecture (Fig. 7 D). Once tip-growth had reinitiated, the very tip of the newly formed outgrowth was devoid of detectable CMTs (Fig. 5, A through D), the same situation as in a tip-growing root hair (Sieberer et al. 2002; see also Fig. 1 A). In Table 2, cellular responses of growth-arresting hairs to NF application are summarized.

Oryzalin in a concentration of 10 μM has been reported to cause bulging and branching of alfalfa root hairs (Weerasinghe et al., 2003). In growth-arresting root hairs that respond to

	Growth-arresting root hairs	Fully grown root hairs	Growth-arresting root hairs treated with 10⁻⁹M NF
Tip-growth	Gradually decreasing growth rate until growth stops.	No cell elongation.	Tip-growth switches to isodiametric growth within 5 min. Re-initiates within 90 – 120 min.
Dense cytoplasm in sub-apex	Gradually shortening until disappearance at growth-arrest	Absent.	Disappearance within 5 min. Reappearance within 90 – 120 min.
EMT array	Gradually shortening until disappearance at growth-termination.	Absent.	Disappears within 5 min. Reappears in transvacuolar cytoplasmic strands within 20 - 30 min.
CMTs	Start reaching the hair tip. Net-axially aligned.	Converge at hair tip. Low density. Net-axially aligned.	Single CMTs reach the hair tip. High density. Net-axially aligned in hair tube. Randomly aligned in swelling.
Distance nucleus-tip	Gradually increasing.	Random position in root hair.	Larger than 30 – 40 µm for 60 min. Distance of 30 – 40 µm from tip in new outgrowth.

Table 2. NF effects on growth-arresting *M. truncatula* root hairs.

NF with root hair deformation, we found that 1 µM oryzalin triggers swelling and outgrowth of root hair tips in a similar fashion as NF do (see below). Therefore, we compared the effect of 1 µM oryzalin on the microtubule cytoskeleton in hairs of this developmental stage with the effect of NF. In growth-arresting hairs treated with 1 µM oryzalin, EMTs did not reappear during root hair swelling at any time after treatment (Fig. 6, D and F). Further, no EMTs were found in the sub-apex of the outgrowth that emerged from the oryzalin induced swelling (data not shown). CMTs did not converge at the very tip of the hair, but appeared to be fragmented (Fig. 6, C and E). CMTs in the shank of the hairs were not obviously affected by 1 µM oryzalin (Fig. 6, C and E). They also remained present in the swelling, but were completely absent in the newly formed outgrowth (data not shown). Thus, although NF and oryzalin both induced swelling and outgrowth, the behavior of the MT cytoskeleton is different.
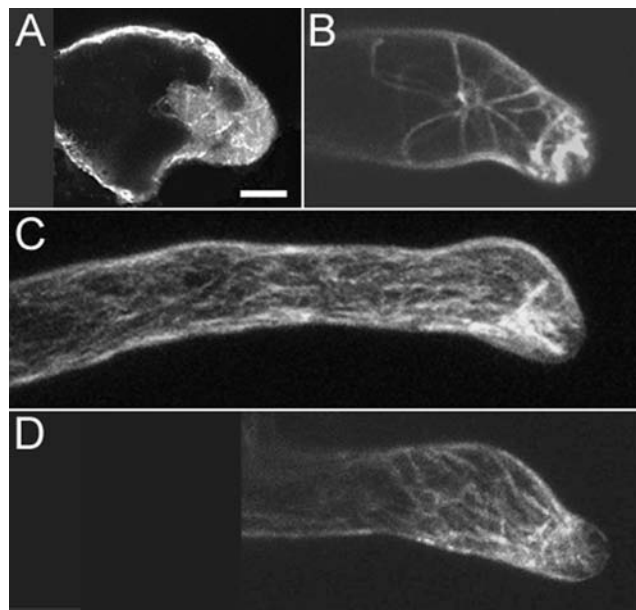
Figure 5. MTs in the newly formed outgrowth after application of 10^{-9}M NF to growth-arresting *M. truncatula* root hairs. A, Immunocytochemistry. B through D, GFP-MBD. Magnification is the same in all images. Bar = 10 μm. **A,** 120 minutes after NF; a projection of 2 median sections shows EMTs in the emerging outgrowth. **B,** 150 minutes after NF; a projection of 2 median sections shows EMTs in the sub-apex of the newly formed outgrowth. EMTs are located inside cytoplasmic strands. **C,** 120 minutes after NF; a full-stack projection shows a dense EMT array in the sub-apex of the outgrowth. In the shank and in the swelling CMTs are net-axially oriented. The very tip of the outgrowth is devoid of detectable MTs. **D,** 150 minutes after NF; full-stack projection. The MT array has been almost completely rebuilt.

Microtubules determine the angle with which the new outgrowth deviates from the former growth axis during root hair deformation

After application of 10^{-9}M NF, growth-arresting hairs responded within minutes and their tips started to swell. Between 90 and 120 min after NF application, a tip growing tube reinitiated from the swelling. Important to note, NF-treated growth arresting root hairs can become longer than control root hairs (Sieberer and Emons 2000). The newly formed outgrowth had a fully recovered polarized cytoarchitecture similar to a young tip-growing hair with a smooth vesicle rich region at the very tip, a tip-nucleus distance of 30 – 40 μm, and accumulated cytoplasm in the sub-apex (compare Fig. 7, A with D). The growth axis of the newly formed outgrowth deviated from the original growth axis of the hair on average by 23.3° (Table 3).

The tips of elongating *M. truncatula* root hairs were swelling after treatment with low concentrations of actin-depolymerizing drugs and subsequent recovery of tip-growth occurred in the original growth orientation (Fig. 7 B and C, Table 3), which was in the

case of cytochalasin D significantly different at the 0.05 level from NF (p = 0.004164) or oryzalin-induced growth reorientation (p = 2.16183E-05) (independent student's t-test analysis).
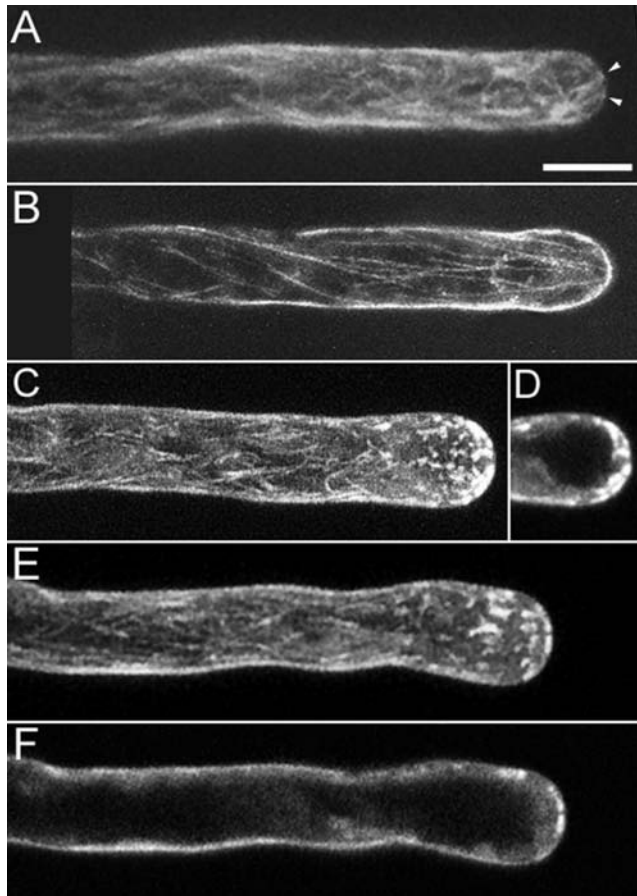

Figure 6. MTs in a growth-arresting hair treated with 10^{-9} M NF, in a fully grown hair, and a growth-arresting hair treated with 1 µM oryzalin. A, and C through F, GFP-MBD; B, immunocytochemistry. Magnification is the same in all images. Bar = 20 µm. **A,** Twenty-five minutes after NF; full-stack projection. CMTs appear in the very tip (arrowheads), but do not converge. In the shank CMTs remain present in a high density (compare with B). **B,** Fully grown hair; full-stack projection. CMTs have decreased in density. The sub-apex is devoid of EMTs. **C,** Thirty minutes after oryzalin. In a full-stack projection CMTs appear fragmented in the hair tip. **D,** A projection of two median sections of the hair in C shows that EMTs have completely disappeared. **E,** Sixty minutes after oryzalin. A full-stack projection shows that in the swelling the tip-region still is devoid of a CMT array; CMTs in the shank remain present. **F,** A projection of two median sections of the hair in E shows that EMTs are completely absent in the swelling.

Oryzalin had a similar effect on the morphogenesis of a growth-arresting hair than NF. After root hair swelling, a new outgrowth formed between 90 and 120 min upon application of 1 µM oryzalin. The newly formed outgrowth deviated on average by 29.5° from the original growth orientation of the hair (Fig. 7 E; Table 3), which was similar to NF-induced growth deviation (not significantly different at the 0.05 level, p = 0.102237184). However, in oryzalin treated hairs, the newly formed outgrowth did not re-
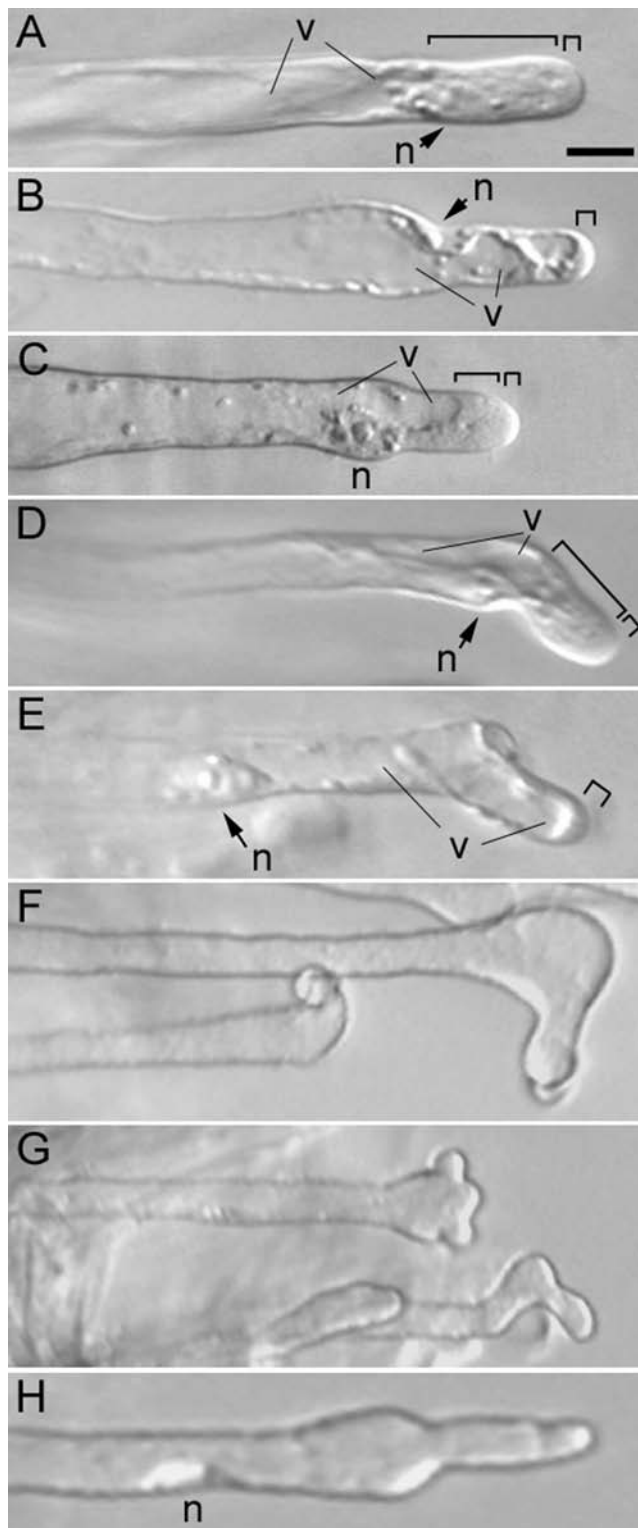
Figure 7. Root hair deformation of growth-arresting root hairs after treatment with actin inhibitors, NF and/or microtubule inhibitors. Bright-field images of living root hairs. Large bracket indicates the subapical region that is rich in cytoplasm; small bracket indicates the smooth (vesicle-rich) region. N, nucleus; v, vacuole. Magnification is the same in all images. Bar = 20 μm. **A,** Sixty minutes after growth medium refreshment, showing undisturbed tip-growth pattern **B,** Sixty minutes after recovery from a 45 min pulse treatment with 1 μM cytochalasin D; the newly formed outgrowth shows no deviation from the original growth. **C,** Sixty minutes after recovery from a 45 min pulse treatment with 10 nM latrunculin; the newly formed outgrowth shows no deviation from the original growth axis. **D,** 120 min after 10^{-9}M NF; the newly formed outgrowth deviates by approx. 35° from the original growth axis and has a similar cytoarchitecture as a tip-growing hair. **E,** 180 min after 1 μM oryzalin; the newly formed outgrowth deviates by approx. 36° from the original growth axis and has not regained the cytoarchitecture of a tip-growing root hair. **F,** 140 min after a combination of 10^{-9}M NF and 1 μM oryzalin; the newly formed outgrowth deviates by approx. 100° from the original growth axis and has not regained the polar cytoarchitecture of a tip-growing root hair. **G,** Same treatment as in F; some of the hairs had problems with restricting tip-growth to...(continued on next page)

gain the same cytoarchitecture as in NF treated hairs. The tip-region contained a thin layer of cytoplasm (small bracket in Fig. 7 E), in the sub-apex no dense cytoplasm accumulated and the nucleus did not obtain a distance to the tip of 30 to 40 μm (compare Fig. 7, A with D and E). Indeed, oryzalin treated growth-arresting hairs did not get new growth potential but stopped elongating at, or before, the time and length normal for the species (data not shown).

When a combination of 10^{-9}M NF and 1 μM oryzalin was applied to growth-arresting hairs, the hair tips formed a swelling. A new outgrowth emerged from the swelling between 90 and 120 min after application (Fig. 7 F). However, the polarized cytoarchitecture was not restored, which was the same after oryzalin treatment alone. The sub-apex in such hairs was devoid of dense cytoplasm (compare Fig. 7, A with D and F). Interestingly, the newly formed outgrowth deviated on average with a steeper angle of 68.5° (Table 3) from the original growth axis of the hair than the outgrowth of hairs treated either with 1 μM oryzalin (significantly different at the 0.05 level, p = 8.19477E-17) or NF alone (significantly different at the 0.05 level, p = 6.08777E-24) (Table 3). The NF and 1 μM oryzalin effects were additive, showing that the (partial) impairment of microtubules leads to an increase of the angle at which the newly formed outgrowth deviates from the original growth axis.

When oryzalin was applied within 60 min to hairs initially treated with NF only, the deviation of the outgrowth was similar to that of hairs exposed to a combination of NF and oryzalin, whereas an application of oryzalin later than 60 min after NF treatment caused a similar deviation than NF alone (data not shown).

These findings indicate that microtubules serve in determining growth directionality of *M. truncatula* hairs. This was exemplified further by the approx. 12% of the root hairs that showed problems with restricting tip-growth to only one site (Fig. 7 G). To find out whether MTs have to be dynamic for NF to alter them such that the directionality of root hair elongation changes, we applied NF to root hairs in which the MTs were stabilized with taxol.

(legend to Figure 7 continued)…one site (upper hair), and/or with maintaining one growth directionality (hair below). Root hairs have not regained the polar cytoarchitecture of tip-growing hairs. **H,** 140 min after a combination of 10^{-9}M NF and 1 μM taxol; the newly formed outgrowth shows no deviation from the original growth axis and has not regained the polar cytoarchitecture of a tip-growing hair.

Treatment	Deviation from original growth axis of the hairs in degrees
1 µM CD	15.8° SD = 14.9
10^{-9}M NF	23.3° SD = 18.4
1 µM oryzalin	29.5° SD = 14.2
10^{-9}M NF + 1 µM oryzalin	68.5° SD = 20.8
10^{-9}M NF + 1µM taxol	16.4° SD = 13.1

Table 3. Deviations from the original growth axis of root hairs after 180 min of NF and/or microtubule inhibitor treatment. The values are averages of 40 hairs with their SD. Three independent replicates for each treatment were performed.

In growth-arresting root hairs treated with a combination of 10^{-9}M NF and 1 µM taxol tip-growth ceased within minutes upon application and hair tips started to swell. Tip-growth reinitiated between 90 to 120 min after application. The newly formed outgrowth deviated with a smaller angle of approx. 16.4° from the original growth axis (Fig. 7 H, Table 3) when compared with NF (significantly different at the 0.05 level, $p = 0.001002$), oryzalin ($p = 6.54436E-06$), or a combination of NF and oryzalin ($p = 8.19477E-17$). Taxol alone did not cause changes in root hair morphology, but slowed down elongation speed (Sieberer et al., 2002).

Discussion

Endoplasmic microtubules are a target for Nod factor signaling and involved in NF induced root hair reorientation

Our study shows that a treatment with Nod factor (NF) causes a rapid, subtle, and transient shortening of the subapical endoplasmic MT array in tip-growing *Medicago truncatula* root hairs. The effect of NF on the EMTs is more severe than on cortical MTs. The short EMT array of growth-arresting hairs completely disappeared after NF application, but started to reappear after 20 to 30 min, after which growth resumed albeit in a different orientation. This deviation of the new outgrowth from the original growth axis was larger when NF and the microtubule depolymerizing drug oryzalin were applied together and reduced when NF was applied in combination with taxol, a MT-stabilizing drug. In addition, the oryzalin-induced absence of EMTs, as well as their stabilization by taxol, suppressed the NF-induced new growth potential in growth-arresting hairs. Together, these findings demonstrate that the microtubule cytoskeleton contributes to the tip-growth process and to the determination of growth direction of elongating hairs, and that it is a direct or indirect target of early NF signaling. The latter two features are crucial for root hair curling around rhizobia.

Our results on changes of the microtubule cytoskeleton in root hairs after NF challenge differ substantially from those reported by Weerasinghe et al. (2003). These authors describe in elongating *M. sativa* root hairs a complete disintegration of the microtubule cytoskeleton after NF perfusion, starting at the base of the hair within 3 min with the EMTs and within 10 min with the CMTs. The disintegration of the CMTs has completed within 30 min. The MT network reforms 60 min after NF exposure, though in hairs longer than 150 – 180 μm the recovery is incomplete. In *M. truncatula* root hairs we never observed such a dramatic change in MT organization at any time after NF application. Species specific differences in the NF response of MTs may explain the different observations made in *M. sativa* and *M. truncatula*, but are not very likely, since the organization of the MT cytoskeleton in elongating root hairs and the pattern of root hair deformation after NF application appear to be similar in the two species (this paper; Weerasinghe et al. 2003). The different method of NF application Weerasinghe et al. (2003) used, and/or a not fully optimized chemical fixation protocol could be the reason for the unlike results. Gentle application of NF was described to be crucial for an undisturbed cytoarchitecture of root hairs (Esseling et al. 2004), and thus the cytoskeleton.

Further it has been shown that a not optimized chemical fixation can cause severe artifacts of the actin cytoskeleton - and hence the cytoarchitecture - in root hairs (Esseling et al. 2000; Ketelaar and Emons 2001) and pollen tubes (Lovy-Wheeler et al. 2005), reasons why we used freeze fixation and GFP-technology.

The subtle changes in the MT pattern after NF treatment that we report here could point towards a transient change in the dynamic instability parameters of EMTs. In tip-growing *M. truncatula* root hairs EMTs are highly dynamic (Vos et al. 2003) and more sensitive to microtubule depolymerizing drugs than CMTs (Sieberer et al. 2002), which could explain why EMTs are more severely affected by NF than CMTs. A NF-induced increase in MT dynamic instability parameters could be a prerequisite for the changes in the MT cytoskeleton that are needed to redirect root hair growth for obtaining root hair curling around rhizobia. Measurements of MT dynamic instability parameters have been successfully performed in the plant cell cortex (Donukshe and Gadella 2003; Shaw et al. 2003; Vos et al. 2004), including the cortex of *Arabidopsis* root hairs (Van Bruaene et al. 2004). In the large volume of the sub-apex of *M. truncatula* root hairs with its dense EMT array analysis of the behavior of individual MTs was impossible to carry out with current methods. As often in cell biology, new instrumentation should bring further answers.

The question rises, how the dynamic instability could be altered by NF. MT depolymerization can be triggered, for instance, by increased cytoplasmic calcium levels (Cyr 1991, 1994). Elongating root hairs have a tip-focused Ca^{2+} gradient, which increases in legumes within minutes upon application of NF (Allen et al. 1994; Cárdenas et al. 1998; de Ruijter et al. 1998; Felle et al. 1998, 1999a, 1999b), leading to several downstream events affecting the cytoskeleton (for review see: Lhuissier et al. 2001). The *Arabidopsis* ton mutant has high calcium-channel activity and constitutively disorganized CMTs (Thion et al 1998). These findings could imply that NF influences the MT organization in the root hair tip of legumes via transiently increased calcium levels.

The effect of NF on the microtubule cytoskeleton differs from that of oryzalin

The effect of oryzalin on microtubules partly resembles the effect of NF: in both cases the EMT array shortens. Further, NF and oryzalin cause a similar deformation phenotype in growth-arresting hairs and when applied together they have an additive effect on root hair deformation. This indicates that although both NF and oryzalin cause depolymerisation of

EMTs, their mode of action is different. If NF would have the same mode of action on MTs as oryzalin, a higher concentration of NF or oryzalin alone should lead to a similar deformation phenotype as a combination of NF and oryzalin. This is not the case (data not shown). Oryzalin binds to tubulin heterodimers, preventing further growth of MTs, which eventually leads to MT depolymerization as long as oryzalin is present (Anthony and Hussey, 1999). The action mechanism of NF on MTs is unknown. The most important difference between NF and oryzalin is the fact that EMTs start to reappear in a NF treated hair, eventually forming a dense three-dimensional EMT array in the sub-apex of the new outgrowth.

Microtubules and actin filaments are early targets of Nod factor signaling

Recovery of tip-growth in *M. truncatula* root hairs from actin depolymerizing drugs after tip swelling takes place in the original orientation of hair elongation (Fig 7 B, C). The same has been observed in *A. thaliana* root hairs that were treated with F-actin depolymerizing drugs (Ketelaar et al. 2003). In terms of root hair morphogenesis, NF-induced root hair deformation resembles hair deformation after microtubule depolymerization by oryzalin and not after fine F-actin depolymerization. The NF-induced deformation phenotype in *M. truncatula* root hairs can be mimicked in *A. thaliana* by a pulse treatment with F-actin depolymerizing drugs in root hairs where microtubules were experimentally ablated (Ketelaar et al. 2003). Thus, it can be concluded that in addition to a signaling pathway towards the actin cytoskeleton (*V. sativa*: Ridge 1992; De Ruijter et al. 1999; *M. sativa*: Allen et al. 1994; *Phaseolus vulgaris*: Cárdenas et al. 1998, 2003), NF induces a signal transduction pathway towards microtubules. If NF would signal only towards the actin cytoskeleton, the newly formed outgrowth in a NF challenged hair should occur in the same direction as after treatment with actin-depolymerizing drugs that is, without a deviation from the original growth axis. This clearly is not the case.

From our results it cannot be concluded whether either MTs or actin filaments are the prime target of NF signaling, or if one of the two cytoskeleton compounds influences the other, or else if they respond simultaneously to NF. Even though the importance of the actin cytoskeleton in NF signaling is paramount, we have demonstrated that also the microtubule component of the cytoskeleton is essential for setting up the interaction between rhizobia bacteria and legumes.

Material and Methods

Plant transformation with GFP-MBD

The GFP-MBD fusion gene, linked to an upstream 35S promotor was provided in a pUC18 vector by Richard Cyr (Marc et al. 1998). The complete insert from this plasmid was transferred to pCambia1390 (CAMBIA, Canberra, Australia; kindly provided by Theodorus WJ Gadella Jr. (University of Amsterdam, The Netherlands), by using the HindIII-EcoRI sites. Transformed roots of *M. truncatula* cv Jemalong were obtained by using *Agrobacterium rhizogenes* according to the protocol described by Boisson-Dernier et al. (2001).

Plant Culture

Seeds of *Medicago truncatula* cv Jemalong (Fabaceae) were germinated as described before (Sieberer et al., 2002). For live observation and immunocytochemistry of wild type root hairs after NF or drug treatment, seedlings were grown at an angle of approx. 25° for 24 to 30h in between a cover slip and a glass slide (Fåhraeus slides: Fåhraeus 1957; Heidstra et al., 1994) in sterile conditions at 24ºC and 16 h day length. The space in between cover slip and glass slide was 1.2 mm. Each of these microchambers contained two seedlings and 2.4 ml plant growth medium (PGM; 1.36 mM $CaCl_2$, 0.97 mM $MgSO_4$, 1.12 mM Na_2PO_4, 1.36 mM KH_2PO_4 and 20 µM Fe-citrate, pH 6.5). The plants with transgenic roots were transferred 3 to 4 weeks after transformation into square 12 cm plastic dishes (Greiner Labortechnik, Kremsmünster, Austria) with a round perforation of about 5 mm in diameter in the middle of one of the 4 sides. Each individual plant was put in the perforation in such a way that the root was inside on PGM containing 0.8 % agar and the stem part outside the plate. Plates were put vertically in a culture room at 25°C and 18-h day length.

NF treatment and drugstudies

Before any treatment, the Fåhraeus slides were gently placed on the microscope stage and plants were left to recover for at least half an hour.

NF [NodRm-IV(C16:2, Ac, S)] was used in a concentration range of 10^{-8}M to 10^{-11}M in PGM. All concentrations used gave similar results. Presented are results obtained with 10^{-9}M NF, since this concentration was used by us in previous work on *M. truncatula* root hairs (Sieberer and Emons 2000; Esseling et al. 2004). NF application was done on stage of the microscope at room temperature in Fåhraeus slides with a constant flow of 800 µl min^{-1}, replacing gradually the PGM in the slides. The final volume in each slide was 2.4

ml. For rapid freeze-fixation, roots were taken out of the Fåhraeus slides 5, 10, 20, 30, 70, and 120 min after NF application and within two to three seconds directly plunged into liquid propane.

Oryzalin (Greyhound Chromatography, Birkenhead, UK) was dissolved in dimethyl sulfoxide ([DMSO] Merck, Darmstadt, Germany) as 10 mM stock solution and used at 1 µM in PGM. Taxol ([paclitaxel], Sigma-Aldrich Chemie B.V., Zwijndrecht, The Netherlands) was dissolved in DMSO as 10 mM stock solution and used at 1 µM in PGM.

For combination treatments of NF and microtubule inhibitors the final concentrations were 10^{-9}M NF and 1 µM oryzalin, or 10^{-9}M NF and 1 µM taxol in PGM.

In Fåhraeus slides, drug solutions or a combination of NF and drugs were applied on the microscope stage with a constant flow of 800 µl min^{-1}, replacing gradually the PGM in the slides. The total volume washed through each slide was 2.4 ml. The drug- and/or NF-induced deviations from the original growth axis were measured in growth-arresting hairs with a length of at least 400 µm by the time treatment started.

Drugs were applied to GFP-MBD expressing root hairs by submerging the roots growing on agar in a 10^{-9} NF and/or a 1 µM oryzalin solution in PGM. After submerging, roots were covered with a gas permeable plastic foil (bioFOLIE 25, Sartorius AG, Vivascience Support Center, Göttingen, Germany) to prevent them from drying, and observed as described below.

Bright-field Microscopy

Root hairs were observed with a 20x 0.4 n.a. or a 40x 0.55 n.a. objective (Nikon) on an inverted microscope with Hoffman modulation contrast system (DIAPHOT 200, Nikon), equipped with a CCD camera (DXC-95OP, Sony, Tokyo, Japan). Image recording and processing were done with a real time digital contrast and low light enhancement image processor (ARGUS-20, Hamamatsu Photonics, Hamamatsu City, Japan). Quantitative measurements of root hair growth directionality were done with ImageJ (Wayne Rasband, National Institutes of Health, USA; http://rsb.info.nih.gov/ij). Only root hairs with the swelling and the newly formed outgrowth in one optical plane have been taken to determine the deviation of the new outgrowth from the original growth axis. To prevent light-induced stress, low light and green filters were used during quantitative live-measurements and related image recording.

Whole mount immunocytochemistry of MTs

For rapid freeze-fixation, seedlings were taken from the Fåhraeus slides and directly plunged into liquid propane and kept there at least for 20 sec. Roots were excised and

transferred into cryogenic vials, containing water-free methanol with 0.05% [v/v] glutaraldehyde. In this solution, roots were freeze substituted for 48 h at -90°C and allowed to warm to room temperature over a 24 h period. Samples were re-hydrated in a graded series of methanol in phosphate-buffered saline (PBS, 137 mM NaCl, 2.7 KCl, 1.5 mM KH_2PO_4, 8.1 mM Na_2HPO_4, pH 7.4) containing fixative (0.1% glutaraldehyde [v/v] and 4% [w/v] paraformaldehyde). After re-hydration, a partial cell wall digestion was carried out in a saturated suspension of driselase (Fluka, Buchs, Switzerland) and macerocyme R10 (Serva, Heidelberg, Germany) in 100 mM 2-morpholinoethanesulfonic acid (MES; pH 6.15) for 40 min at 35°C. The specimens were then washed two times for 5 min in PBS and to block unspecific sites incubated for 5 min in PBS containing 0.1% (w/v) acetylated bovine serum albumin ([BSA_{ac}] Aurion, Wageningen, Netherlands) and 0.05% (v/v) Triton X-100 (BDH Laboratory Supplies, Poole, UK). The samples were incubated in monoclonal anti-a-tubulin clone DM 1a (Sigma Chemical Co., St. Louis, USA) diluted 1:300 (v/v) in PBS containing 0.1% (w/v) BSA_{ac} and 0.05% (v/v) Triton X-100 for 12h at 4°C. After washing three times for 5 min in PBS the samples were incubated in anti mouse/IgG/Alexa 488, raised in goat (Molecular Probes, Eugene, USA), diluted 1:300 (v/v) in PBS containing 0.1% (w/v) BSA_{ac} and 0.05% (v/v) Triton X-100 for 12h at 4°C. Specimens were washed twice for 5 min with PBS and for 5 min with CITIFLUOR PBS solution (Citifluor Ltd., London, UK), whereafter they were mounted in an antifading medium (PROLONG ANTIFADE, Molecular Probes).

Microscopic observation of MTs after immunocytochemistry
Antibody labeled microtubules were visualized with a BIO-RAD MCR 600 confocal laser-scanning microscope (CLSM) (Bio-Rad Laboratories Ltd., Hertfordshire, UK) with an argon-krypton ion laser attached to a NIKON DIAPHOT 300 (Nikon Europe B.V) inverted microscope equipped with a 60x FL 1.4 n.a. oil immersion objective (Nikon) or with a 100x FL 1.2 n.a. water immersion objective (Leitz, Wetzlar, GER). Z-stacks were collected with Z-steps of 1 μm. Images were acquired and projected with Confocal Assistant Version 4.02 (Bio-Rad) and processed with Scion Image Beta 4.0.2. (Scion Corporation, Frederick, Maryland, USA) and Adobe Photoshop 5.5 (Adobe Systems Incorporated, Mountain View, CA, USA).
To compare early effects of NF vs. PGM on the microtubule cytoskeleton, for each time point per treatment the endoplasmic microtubules (EMTs) and the cortical microtubules (CMTs) of 40 root hairs were compared with the microtubule cytoskeleton of untreated young tip-growing *M. truncatula* hairs. Only root hairs with similar fluorescent signal

intensity and evenly distributed fluorescent signal were imaged. The experiment was repeated twice.

Microscopic observations of GFP-MBD expressing root hairs

For observation, the roots growing on agar were submerged in sterile water and covered with a gas permeable plastic foil (bioFOLIE 25, Sartorius AG, Vivascience Support Center, Göttingen, Germany) to allow direct observation and to prevent them from drying. The opened dish was put on the microscope stage of a ZEISS LSM510 (Carl Zeiss SA, Le Pecq, France) and observations were carried out either with a 40x/0.8 WPH2 Achroplan or 63x/0.9 WPH3 Achroplan objective. In general, Z-stacks were made of whole root hairs with a Z-step of 1 μm between subsequent optical sections. Image projections were made with ZEISS LSM Image Examiner and images were processed with Image-Pro plus (Media Cybernetics, L.P.).

Acknowledgements

Literature cited

Anthony RG and Hussey PJ. 1999. Dinitroaniline herbicide resistance and the microtubule cytoskeleton. Trend Plant Sc 4:112-116.

Allen NS, Bennett MN, Cox DN, Shipley A, Ehrhardt DW and Long SR. 1994. Effects of Nod factors on alfalfa root hair Ca^{++} and H^+ currents on cytoskeleton behavior. Pages 107-114 in: Advances in molecular genetics of plantmicrobe interactions, vol 3. M.J. Daniels, J.A. Downie, A.E. Osbourn, eds. Kluwer Academic Publishers, Dordrecht, The Netherlands.

Boisson-Dernier A, Chabaud M, Garcia F, Bécard G, Rosenberg C and Barker DG. 2001. *Agrobacterium rhizogenes*-transformed roots of *Medicago truncatula* for the study of nitrogen-fixing and endomycorrhizal symbiotic associations. Mol. Plant-Microbe Interact. 14:695-700.

Cárdenas L, Vidali L, Domínguez J, Pérez H, Sánchez F, Hepler PK and Quinto C. 1998. Rearrangement of actin microfilaments in plant root hairs responding to *Rhizobium etli* nodulation signals. Plant Physiol. 116:871-877.

Cárdenas, L., Thomas-Oates, J.E., Nava, N., Lopez-Lara, I.M., Hepler, P.K., and Quinto, C. 2003. The role of nod factor substituents in actin cytoskeleton rearrangements in *Phaseolus vulgaris*. Mol. Plant-Microbe Interact. 16:326-334.

Cullimore J and Dénarié J. 2003. Plant Sciences: How legumes select their sweet talking symbionts. Science 302:575-578.

Cyr RJ. 1991. Calcium calmodulin affects microtubule stability in lysed protoplasts. J Cell Sci. 100:311–317.

Cyr RJ. 1994. Microtubules in plant morphogenesis: role of the cortical array. Annu. Rev. Cell Biol. 10:153–180.

De Ruijter NCA, Rook MB, Bisseling T and Emons AMC. 1998. Lipochito-oligosaccharides re-initiate root hair tip growth in *Vicia sativa* with high calcium and spectrin-like antigen at the tip. Plant J. 13:341-350.

De Ruijter NCA, Bisseling T and Emons AMC. 1999. *Rhizobium* Nod factors induce an increase in sub-apical fine bundles of actin filaments in *Vicia sativa* root hairs within minutes. Mol. Plant-Microbe Interact. 12:829-832.

Dhonukshe P and Gadella TWJ Jr. 2003. Alteration of microtubule dynamic instability during preprophase band formation revealed by yellow fluorescent protein–CLIP170 microtubule plus-end labeling. Plant Cell 15:597–611.

Endre G, Kereszt A, Kevei Z, Mihacea S, Kalo P and Kiss GB. 2002. A receptor kinase gene regulating symbiotic nodule development. Nature 417:962-966.

Esseling JJ, de Ruijter NCA and Emons AMC. 2000. The root hair cytoskeleton as backbone, highway, morphogenetic instrument and target for signaling. Pages 29-52 in: Root hairs. Cell and molecular biology. R.W. Ridge, and A.M.C. Emons, eds. Springer-Verlag, Tokyo, Japan.

Esseling JJ, Lhuissier FGP and Emons AMC. 2003. Nod factor-induced root hair curling: Continuous polar growth towards the point of Nod factor application. Plant Physiol. 132:1982-1988.

Esseling JJ, Lhuissier FGP and Emons AMC. 2004. A nonsymbiotic root hair tip growth phenotype in NORK-mutated legumes: Implications for nodulation factor–induced signaling and formation of a multifaceted root hair pocket for bacteria. Plant Cell 16:933-944.

Fåhraeus G. 1957. The infection of white clover root hairs by nodule bacteria studied by a simple glass slide

technique. J. Gen. Micobiol. 16:374-381.

Felle HH, Kondorosi E, Kondorosi A and Schultze M. 1998. The role of ion fluxes in Nod factor signaling in *Medicago sativa*. Plant J. 13:453–463.

Felle HH, Kondorosi E, Kondorosi A and Schultze M. 1999a. Nod factors modulate the concentration of cytosolic free calcium differently in growing and non-growing root hairs of *Medicago sativa* L. Planta 209:207–212.

Felle HH, Kondorosi E, Kondorosi A and Schultze M. 1999b. Elevation of the cytosolic free $[Ca^{2+}]$ is indispensable for the transduction of the Nod factor signal in alfalfa. Plant Physiol. 121:273–280.

Fisher RF and Long SR. 1992. Rhizobium-plant signal exchange. Nature 357:655–660.

Geurts R. 2003. LysM domain receptor kinases regulating rhizobial nod factor-induced infection. Science 302:630–633.

Hadri AE and Bisseling T. 1998. Responses of the plant to Nod factors. Pages 403-416 in: The Rhizobiaceae: Molecular Biology of Model Plant-Associated Bacteria. H.P. Spaink, A. Kondorosi, and P.J.J. Hooykaas, eds. Kluwer Academic Publishers, Dordrecht, The Netherlands.

Heidstra R, Geurts R, Franssen H, Spaink HP, van Kammen A and Bisseling T. 1994. Root hair deformation activity of nodulation factors and their fate on *Vicia sativa*. Plant Physiol. 105:787-797.

Ketelaar T and Emons AMC. 2001. The cytoskeleton in plant cell growth: Lessons from root hairs. New Phytol. 152:409-418.

Ketelaar T, de Ruijter NCA and Emons AMC. 2003. Unstable f-actin specifies the area and microtubule direction of cell expansion in *Arabidopsis* root hairs. Plant Cell 15:285-292.

Kijne JW. 1992. The *Rhizobium* infection process. Pages 349-398 in: Biological Nitrogen Fixation. G. Stacey, R. Burris, and H. Evans, eds. Chapman and Hall, New York and London.

Lerouge P, Roche P, Faucher C, Maillet F, Truchet G, Promé JC and Dénarié J. 1990. Symbiotic host specificity of *Rhizobium meliloti* is determined by a sulphated and acetylated glucosamine oligosaccharide signal. Nature 344:781–784.

Lhuissier FGP, de Ruijter NCA, Sieberer BJ, Esseling JJ and Emons A.M.C. 2001. Time course of cell biological events evoked in legume root hair by *Rhizobium* Nod factors: State of the art. Annals of Botany 87: 289-302.

Limpens E, Franken C, Smit P, Willemse J, Bisseling T and Geurts R. 2003. LysM domain receptor kinases regulating rhizobial Nod factor-induced infection. Science 302:630-633.

Lloyd CW, Pearce KJ, Rawlins DJ, Ridge RW and Shaw PJ. 1987. Endoplasmic microtubules connect the advancing nucleus to the tip of legume root hairs, but F-actin is involved in basipetal migration. Cell Motil. Cytosk. 8:27-36.

Lovy-Wheeler A, Wilsen KL, Baskin TI, and Hepler PK. Published online 4 March 2005. Enhanced fixation reveals the apical cortical fringe of actin filaments as a consistent feature of the pollen tube. Planta Online First, DOI: 10.1007/s00425-004-1423-2.

Madsen EB, Madsen LH, Radutoiu S, Olbryt M, Rakwalska M, Szczyglowski K, Sato S, Kaneko T, Tabata S, Sandal N and Stougaard J. 2003. A receptor kinase gene of the LysM type is involved in legumeperception of rhizobial signals. Nature 425:637-640.

Marc J, Granger CL, Brincat J, Fisher DD, Kao T, McCubbin AG and Cyr RJ. 1998. A GFP-MAP4 reporter gene for visualizing cortical mirotubule rearrangements in living epidermal cells. Plant Cell 10:1927-1939.

Miller DD, De Ruijter NCA, Bisseling T and Emons AMC. 1999. The role of actin in root hair morphogenesis: studies with lipochito-oligosaccharide as a growth stimulator and cytochalasin as an actin perturbing drug. Plant J. 17:141–154.

Radutoiu S, Madsen LH, Madsen EB, Felle HH, Umehara Y, Grønlund M, Sato S, Nakamura Y, Tabata S, Sandal N and Stougaard J. 2003. Plant recognition of symbiotic bacteria requires two LysM receptor-like kinases. Nature 425:585-592.

Parniske M and Downie JA. 2003. Plant biology: Locks, keys and symbioses. Nature 425:569-570.

Ridge RW. 1992. A model of legume root hair growth and Rhizobium infection. Symbiosis 14:359-373.

Roche P, Debelle F, Maillet F, Lerouge P, Faucher C, Truchet G, Dénarié J and Promé JC. 1991. Molecular basis of symbiotic host specificity in *Rhizobium meliloti*: nodH and nodPQ genes encode the sulfation of lipo-oligosaccharide signals. Cell 67:1131-1143.

Shaw SL, Kamyar R, Ehrhardt DW. 2003. Sustained microtubule treadmilling in *Arabidopsis* cortical arrays. Science 300:1715-1718.

Sieberer B and Emons AMC. 2000. Cytoarchitecture and pattern of cytoplasmic streaming in root hairs of *Medicago truncatula* during development and deformation by nodulation factors. Protoplasma 214:118-127.

Sieberer BJ, Timmers ACJ, Lhuissier FGP and Emons AMC. 2002. Endoplasmic microtubules configure the subapical cytoplasm and are required for fast growth of *Medicago truncatula* root hairs. Plant Physiol. 130:977-988.

Spaink HP, Sheeley DM, van Brussel AAN, Glushka J, York WS, Tak T, Geiger O, Kennedy EP, Reinhold VN and Lugtenberg BJJ. 1991. A novel highly unsaturated fatty acid moiety of lipo-oligosaccharide signals determines host specificity of *Rhizobium*. Nature 354:125-130.

Stracke S, Kistner C, Yoshida S, Mulder L, Sato S, Kaneko T, Tabata S, Sandal N, Stougaard J, Szczyglowski K and Parniske M. 2002. A plant receptor-like kinase required for both bacterial and fungal symbiosis. Nature 417:959-962.

Thion L, Mazars C, Nacry P, Bouchez D, Moreau M, Ranjeva R, Thuleau P. 1998. Plasma membrane depolarization-activated calcium channels, stimulated by microtubule depolymerizing drugs in wild-type Arabidopsis thaliana protoplasts, display constitutively large activities and longer half life in ton2 mutant cells affected in the organization of cortical microtubules. Plant J. 13:603–610.

Timmers ACJ. 2000. Infection of root hairs by Rhizobia: Infection thread development with emphasis on the microtubular cytoskeleton. Pages 223-239 in: Root hairs. R.W. Ridge, and A.M.C. Emons, eds. Springer-Verlag, Tokyo,Japan.

Truchet G, Roche P, Lerouge P, Vasse J, Camut S, de Billy F, Promé JC and Dénarié J. 1991. Sulphated lipo-oligosaccharide signals of *Rhizobium meliloti* elicit root nodule organogenesis in alfalfa. Nature 351:670-673.

Van Batenburg FHD, Jonker R, Kijne JW. 1986. *Rhizobium* induces marked root hair curling by redirection of tip growth: a computer simulation. Physiol. Plant 66:476-480.

Van Bruaene, N., Greg, J., and van Oostveldt, P. 2004. Reorganization and *in vivo* dynamics of microtubules during *Arabidopsis thaliana* root hair development. Plant Physiol. 136:3905-3919. First published on November

19, 2004; 10.1104/pp.103.031591.

Vos, J.W., Sieberer, B., Timmers, A.C.J., and Emons, A.M.C. 2003. Microtubule dynamics during preprophase band formation and the role of endoplasmic microtubules during root hair elongation. Cell Biol. Int. 27:295.

Vos, J.W., Dogterom, M, and Emons, A.M.C. 2004. Microtubules become more dynamic but not shorter during preprophase band formation: A possible "Search-and-Capture" mechanism for microtubule translocation. Cell Motil Cytoskeleton 57:246–258.

Weerasinghe, R.R., Collings, D.A., Johannes, E., Allen, N.S. 2003. The distributional changes and role of microtubules in Nod factor-challenged *Medicago sativa* root hairs. Planta 218:276-287.

Chapter 5

Microtubules guide root hair tip growth

B.J. Sieberer, T. Ketelaar, J.J. Esseling and A.M.C. Emons

Department of Plant Sciences, Laboratory of Plant Cell Biology, Wageningen University, Arboretumlaan 4, 6703 BD, Wageningen, The Netherlands

Summary

The ability to establish cell polarity is crucial to form and function of an individual cell. Polarity underlies critical processes during cell development, such as cell growth, cell division, cell differentiation, and cell signalling. Interphase cytoplasmic microtubules in tip-growing fission yeast cells have been shown to play a particularly important role in regulating cell polarity. By placing proteins that serve as spatial cues in the cell cortex of the expanding tip, microtubules determine the site where excocytosis, and therefore growth, takes place. Transport and the targeting of exocytotic vesicles to the very tip depend on the actin cytoskeleton. Recently, endoplasmic microtubules have been identified in tip-growing root hairs, which are an experimental system for plant cell growth. We will review the data that demonstrate involvement of microtubules in hair elongation and polarity of the model plants *Medicago truncatula* and *Arabidopsis thaliana*. Differences and similarities between the microtubule organisation and function in these two species are discussed and we will compare the observations in root hairs with the microtubule based polarity mechanism in fission yeast.

Introduction

Root hairs are lateral extensions of root epidermal cells. They elongate as cylindrical, uniaxilar structures, which reach an enormous length compared to their width. Root hairs enlarge the surface of the roots, and by this they support the absorption of water and nutrients (for review see: Gilroy & Jones, 2000). Especially under low nutrient availability, root hairs facilitate an increased uptake of nutrients (phosphorus uptake in *Arabidopsis*: Bates & Lynch, 2000). Further, root hairs may serve in the anchoring of plants into the soil (Peterson & Farquhar, 1996; Gilroy & Jones, 2000), although Bailey et al. (2002) have shown in a mutant study that rather lateral roots than root hairs are crucial for anchorage. Finally, root hairs are sites for interaction of host plants with a range of soil-living symbiotic micro-organisms (Clarkson, 1985; Dolan et al., 1994; Peterson & Farquhar, 1996; Ridge, 1996) such as nitrogen-fixing rhizobacteria that infect legume roots (Mylona et al., 1995; Long, 1996).

The shape of root hairs is produced by a very special form of polarized growth, called tip growth. In tip growing cells, the actual growth process is restricted to the very tip (Derksen & Emons, 1990; Shaw et al., 2000; Dumais et al., 2004), also known as apex or apical dome. Tip growth is a precisely orchestrated process characterized by the maintenance of a cylindrical shape with a constant diameter and a uniaxial extension pattern (Shaw et al., 2000). Tip-growing root hairs have a highly polarized cytoarchitecture. The tip-growth machinery localizes in abundance in the apex and sub-apex of an elongating hair and consists of a tip-focused gradient of calcium ions, actin filaments, microtubules, Golgi-derived and endocytotic vesicles, Golgi bodies, endoplasmic reticulum, mitochondria, the nucleus, and the exo-/endocytosis molecules such as snare proteins and clathrin. The growth mechanism primarily consists of the fusion of vesicle membranes with the plasma membrane and exocytosis of cell wall material at the hair tip (Miller et al., 1997; Wasteneys & Galway, 2003), leading to an irreversible increase in cell surface. The cytoskeleton has been identified to be a key-player in the tip-growth process.

Comprehensive reviews that emphasize to a large extent on the actin cytoskeleton in tip-growing plant cells have recently been published (Geitmann & Emons, 2000; Hepler et al., 2001; Wasteneys & Galway, 2003). Although recent reviews by Grierson & Ketelaar (2003) and Hussey et al. (2004) give a good and detailed overview on the microtubule cytoskeleton in tip-growing plant cells, recent work (*Medicago truncatula*: Sieberer et al.,

2002, submitted; Vos et al., 2003; *M. sativa*: Weerashinge et al., 2003; *Arabidopsis thaliana*: van Bruaene et al., 2004) allows us now to better understand the role microtubules play in tip-growing root hairs. In addition, one may gain insight in microtubule functioning by studying another tip-growing organism: fission yeast. A microtubule based cell polarity mechanism in fission yeast has been identified; here we will discuss this mechanism and the possibility that microtubules perform a homologous function in setting up cell polarity in root hairs.

Root hair tip-growth

Root hair development exhibits two fascinating aspects of the regulation of positional information during plant cell growth. (1) Before bulge formation starts, the root epidermal cell that will give rise to the root hair must break its symmetric growth pattern and (2) initiate cell growth at a very confined area. Root hairs emerge as bulges from root epidermal cells, the so called trichoblasts, when intercalary cell elongation of these cells ceases (*Arabidopsis*: Sugimoto et al., 2000; *Medicago*: Sieberer et al., 2002). Unlike *Medicago*, where all epidermal root cells are trichoblasts (Sieberer & Emons, 2000), *Arabidopsis* has, in addition to trichblasts, atrichoblasts, epidermal cells that do not produce root hairs (Dolan et al., 1994). Studies on the cytoskeleton (actin: Miller et al., 1999; actin and MTs: Baluska et al., 2000), ultrastructure (*Vicia sativa*: Miller et al., 2000), and cytoplasmic calcium gradients in *Arabidopsis* (Wymer et al., 1997), support the conclusion that bulge formation is a distinctly different process than tip growth (for review see: Grierson & Ketelaar, 2003).

Once tip growth has initiated, a cylindrically shaped tube develops with a more or less constant diameter (*Medicago*: approx. 10 − 14 μm; *Arabidopsis*: approx. 6 - 10 μm), which elongates uniaxially, perpendicular to the root axis until the mature length of the hair has been reached (*Medicago*: up to 1 mm; *Arabidopsis*: up to at least 1 mm). When grown in liquid medium, root hair growth occurs with a growth rate of 0.8 − 1.4 μm min^{-1} in *Medicago* (Sieberer & Emons, 2000) and 0.93 - 2 μm min^{-1} in *Arabidopsis* (Wymer et al., 1997; Bibikova et al., 1999; Ketelaar et al., 2002). Root hair diameter and growth rate rely on the precisely orchestrated exocytosis process of tip growth. This growth pattern reflects the underlying polarity of the cytoarchitecture. The sub-apex of tip growing root hairs is filled with dense cytoplasm, whereas the basal part of the hair contains an enlarging vacuole, surrounded by a thin layer of cortical cytoplasm (*Arabidopsis*: Galway

et al., 1997; *Vicia sativa*: de Ruijter et al., 1998; *M. truncatula*: Sieberer & Emons 2000).

For a better understanding of the role MTs play in cell polarity and tip-growth, we give a short description of common and different cytoarchitectural features in elongating root hairs of the model species for root hair growth: the legumes *Medicago* and *Vicia*, and *Arabidopsis*. Common to all tip-growing root hairs is, as stated above, the accumulation of cytoplasm in the subapical region. The subapical cytoplasm contains a high number of organelles such as endoplasmic reticulum, mitochondria, plastids, and Golgi bodies (*Vicia sativa*: Miller et al., 2000). The nucleus is positioned at the base of the subapical, cytoplasmic dense area and follows the growing hair tip at a fixed distance, which is 30 to 40 μm in *Medicago* (Sieberer & Emons, 2000; Sieberer et al., 2002) and 40 to 75 μm in *Arabidopsis* (Ketelaar et al., 2002). The cytoplasm in the extreme apex is devoid of large organelles but packed with vesicles, as transmission electron microscopic images reveal (*Equisetum hyemale*: Emons, 1987; *Vicia hirsuta*: Ridge, 1988, 1993; *V. villosa*: Sherrier & van den Bosch, 1994; *Arabidopsis*: Galway et al., 1997; *V. sativa*: Miller et al., 2000). A category of these vesicles are Golgi-derived and contain cell wall matrix material that will be deposited in the expanding cell wall upon exocytosis. Other vesicles are of endocytotic origin (Emons & Traas, 1986). In *Medicago* and *Vicia* the cytoplasmic dense subapical region is more compact than in *Arabidopsis*: Not only is the tip-nucleus distance shorter, but also the cytoplasm is only penetrated temporarily by thin extensions of the central vacuole, whereas in *Arabidopsis* these extensions are bigger, and occupy the subapical region for a longer time. The significance of these differences is not known.

Microtubule organization and dynamics in elongating root hairs

During the transition from a bulge into an elongating root hair, the very tip of the bulge progressively gets devoid of detectable CMTs; they seem to passively part at the bulge tip (*M. truncatula*: Sieberer et al., 2002). At this developmental stage cytoplasm is accumulating at the tip of the bulge and forms a short cytoplasmic dense region. Endoplasmic MTs start to appear within this region (*Medicago*: Sieberer et al., 2002; *Arabidopsis*: van Bruaene et al., 2004). An indication that MTs could be involved in the initiation of tip-growth comes from transgenic *Arabidopsis* lines with reduced a-tubulin expression (Bao et al., 2001). Occasionally, multiple root hairs emerge from a single swelling in these lines. Although this is likely to be caused by a defective initiation of tip growth, alternatively bulge formation or tip growth itself may be defective, as all these

defects could cause identical phenotypes.

Cortical MTs (CMTs) are present in all stages of root hair growth in all species examined (for review, see Ketelaar & Emons, 2000, 2001). In this respect, root hairs are not different from other interphase plant cells. CMTs appear as dense arrays in growing root hairs and are oriented either net-axially (more or less longitudinally; *Equisetum hyemale*: Emons & Wolters-Arts, 1983; Traas et al., 1985; *Medicago*: Sieberer et al., 2002; *M. sativa*: Weerasinghe et al., 2003; *Arabidopsis*: van Bruaene et al., 2004), or helically (*Allium cepa*: Lloyd, 1983; Traas et al., 1985). Whether or not CMTs reach the very tip – the site of actual cell growth – in elongating root hairs has been under debate for a long time. CMTs have not been detected in root hair apices with immunocytochemistry after freeze fixation and freeze substitution, and with *in vivo* decoration by GFP, fused to the microtubule binding domain of mouse Microtubule Associated Protein (MAP) 4 (GFP-MBD; Marc et al., 1998) (*M. truncatula*: Sieberer et al., 2002; *M. sativa*: Weerasinghe et al., 2003; *Arabidopsis*: van Bruaene et al., 2004). However, CMT have been found in the extreme tips of elongating root hairs in transmission electron microscopy (TEM) images after freeze fixation/freeze substitution (*Equisetum hyemale*: Emons, 1989; *Arabidopsis*: Galway et al., 1997). There are several explanations for these contradicting observations. (1) CMTs are highly dynamic at the very tip (see below) and may therefore be difficult to visualize in a still image of a 4D confocal microscopy scan. (2) CMTs may be present in the tip region but not be fully accessible for antibodies or the GFP-MBD fusion protein since CMTs at this site might be decorated with MAPs (see below). (3) The CMTs in the TEM images may be freeze fixation or freeze substitution artefacts. Even though this seems unlikely, the absence of CMTs in the extreme apex may be explained by the tip-focused Ca^{2+} gradient in growing root hairs (*Arabidopsis*: Schiefelbein et al., 1992; Bibikova et al., 1997; Wymer et al., 1997; *Vicia sativa*: de Ruijter et al., 1998; *Phaseolus vulgaris*: Cárdenas et al., 1999; *Medicago sativa*: Felle et al., 1999a,b). MTs are sensitive to elevated Ca^{2+} level concentrations (Cyr, 1991, 1994), and the high Ca^{2+} concentration in the apex of growing root hairs may cause depolymerisation or inhibit polymerisation. As the organisation of putative CMTs in the apex of growing root hairs may give us indications about their function in tip growth, clarification of their organisation by newly developed techniques or detailed transmission electron microscopic analysis will be of interest.

After growth-arrest, root hairs of *Medicago* and *Arabidopsis* show a decrease in CMT density. In fully-grown root hairs CMTs are either longitudinally (*Medicago*: Sieberer et al., 2002; *Arabidopsis*: van Bruaene et al., 2004) or helically (*Arabidopsis*: van Bruaene et

al., 2004) oriented and appear to be longer and better aligned than CMTs in growing hairs (Van Bruaene et al., 2004). After growth arrest CMTs reach the tip and converge there.

Endoplasmic MTs (EMTs), microtubules that are not located in the cell cortex, are atypical for interphase plant cells. However, recently they have been shown to be present in the subapical cytoplasmically dense region in elongating root hairs. Root hairs acquire endoplasmic microtubules (EMTs) when tip growth begins and retain these EMTs until growth stops (*M. truncatula*: Sieberer et al., 2002; *A. thaliana*: van Bruaene et al., 2004). In *Medicago* and *Arabidopsis*, EMTs were observed around and close to the nucleus in a high density (Sieberer et al., 2002; van Bruaene et al., 2004). Bakhuizen (1988) showed in a TEM study on growing *Vicia sativa* and *Pisum sativum* root hairs that EMTs are present in the vicinity of the nuclear envelope, and that bundles of EMTs run axially towards the hair tip. Van Bruaene et al. (2004) described in young tip-growing *Arabidopsis* hairs distinct sites in the vicinity of the surface of the nucleus where EMTs appear. They hypothesise that these locations are microtubule nucleation sites and that in elongating *Arabidopsis* root hairs EMTs may be involved in the transport of new MT nucleation complexes from the nucleus to other places in the root hair. In tip-growing root hairs of the legumes *M. truncatula* (Sieberer et al., 2002; see also Fig. 1a), *M. sativa* (Weerashinge
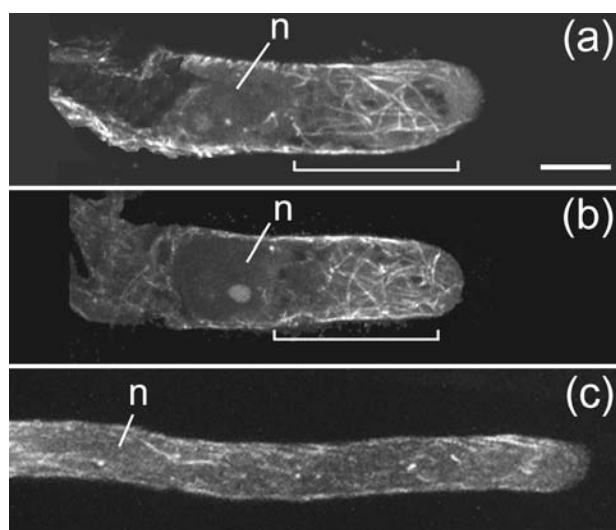
Figure 1. Endoplasmic microtubules in tip-growing root hairs. (**a**) *Medicago truncatula*, (**b**) *Lotus japonicus*, (**c**) *Arabidopsis thaliana*. Brackets in (a) and (b) indicate the subapical region containing a dense array of endoplasmic microtubules. Endoplasmic microtubules in the subapex of *Arabidopsis* root hairs do not form a vast array (c). Microtubules were visualized with a confocal laser scanning microscope in scanning steps of 1 µm after rapid freeze fixation – freeze substitution and immunocytochemistry. All images are projections of three median sections. Magnification is the same in all images. Bar = 10 µm. n, nucleus.

et al., 2003), *Vicia hirsuta* (Lloyd et al., 1987), and *Lotus japonicus* (Fig. 1b) the EMTs

are organized into a vast three dimensional array that spreads throughout the entire subapex between the nucleus and the very tip (Fig. 1a,b). EMTs in the lower part of the subapical cytoplasmic dense region occur in a higher density and deviate more from the long axis of the hair than the EMTs close to the root hair tip (Sieberer et al., 2002). Some EMTs are reaching into the very tip (*M. truncatula*: Sieberer et al., 2002), where microtubule ends make contact with the plasma membrane (*Vicia sativa*: Bakhuizen, 1988). In contrast to legumes, EMTs in growing *Arabidopsis* root hairs do not form a dense array in the sub-apex, but consist, at most, of a few bundles of endoplasmic microtubules between hair tip and the nucleus, as studies with GFP-MBD decorated MTs revealed (Van Bruaene et al., 2004). With immunocytochemisty after rapid freeze fixation EMTs could either not be detected in *Arabidopsis* hairs (Ketelaar et al., 2002) or this method gave a much weaker signal on EMTs than in legume root hairs (Fig. 1c). The absence/low density of EMTs in these samples may indicate that immunocytochemistry is not sensitive enough to detect EMTs for the reasons given above. Alternatively, this may indicate that expression of GFP-MBD in *Arabidopsis* induces polymerization/bundeling of EMTs. TEM analysis of EMTs may clarify these contradicting results.

MTs in elongating and fully grown root hairs of both species, *Medicago* and *Arabidopsis*, are highly dynamic. Especially the EMTs in elongating root hairs constantly change their orientation and configuration, whereas CMTs in the root hair shank appear to be less dynamic (Van Bruaene et al., 2004). Experiments with low concentrations of the microtubule depolymerizing drug oryzalin showed that EMTs are less stable than CMTs (*M. truncatula*: Sieberer et al., 2002). Real time 4D confocal microscopy revealed that EMT dynamics are caused by alternating phases of MT growth and shrinkage (*Medicago*: Vos et al., 2003; *Arabidopsis*: van Bruaene et al., 2004). Moreover, in *Medicago* EMTs were observed to grow from the sub-apical region into the very tip of the root hair (Vos et al., 2003), where they remain only for a few seconds upon which they shrink again. Because of the high density and the unsynchronized dynamics of EMTs in *Medicago* root hairs, quantitative analysis proved difficult to be performed. Future studies of 4D confocal microscopy images should give more insights on EMT dynamics in these root hairs. A quantitative analysis of CMT dynamics in fully grown root hairs of *Arabidopsis* (Van Bruaene et al., 2004) suggests a process called hybrid tread milling with dynamic instability at the MT plus ends that mainly point towards the hair tip, and slow depolymerization at the MT minus ends. This is similar to what recently has been described in *Arabidopsis* epidermal cells (Shaw et al., 2003) and in tobacco bright yellow 2 cells (Vos et al., 2004). Van Bruaene et al. (2004) further suggest that this process

would allow MTs in root hairs first to nucleate and then to get ordered: Upon contact with other MTs, MTs partly depolymerize followed by polymerization/reorientation, finally resulting in the alignment of CMTs. A similar observation has been made by Dixit & Cyr (2004 a, b) in tobacco bright yellow 2 cells. In elongating *Arabidopsis* root hairs, dispersed nucleation sites of MTs have been identified in the subapical cytoplasmic dense region and the cortex (Van Bruaene et al., 2004). Although MT density is too high to allow quantification of MT behaviours in these regions of elongating hairs with current methods, one can imagine a similar MT organizing mechanism in these hairs as described for fully grown hairs (Van Bruaene et al., 2004). It is likely that microtubule dynamics are at least partially under control of MAPs; however, the regulation of MT dynamics by specific proteins has not been studied in root hairs.

MTs and their role in root hair cell polarity

Root hairs of both species, *Medicago* and *Arabidopsis* do have subapical EMTs during tip-growth – though with differences in patterning and abundance. Do these differences reflect a difference in function of the EMTs? Experiments with the MT depolymerizing drug oryzalin show that EMTs in elongating *Medicago* root hairs contribute to cell polarity. Upon application of 1 µM oryzalin, EMTs, but not CMTs, disappear within minutes, the polar distribution of the cytoplasm in the subapex of the hairs is lost, and the nucleus-tip distance increases over time (Sieberer et al., 2002). However, the smooth region (i.e., the vesicle rich zone) at the very tip remains present and even increases in length over time and consequently tip-growth continues, though the growth rate is reduced by approx. 60% (Sieberer et al., 2002). *M. truncatula* root hairs treated with oryzalin do not reach their mature length. *Arabidopsis* root hairs treated with up to 10 µM oryzalin continue to grow at a normal growth-rate, but in a wavy pattern (Bibikova et al., 1999; Ketelaar et al., 2002), which has not been described for *Medicago* (Sieberer et al., 2002; Weerashinge et al., 2003). It is not clear whether the absence of EMTs, CMTs or both is responsible for this wavy growth pattern. The nucleus-tip distance in *Arabidopsis* remains the same as without oryzalin treatment. Nuclear movement in *Arabidopsis* has been demonstrated to exclusively depend on the actin cytoskeleton (Ketelaar et al., 2002; van Bruaene et al., 2003), whereas in elongating *Medicago* root hairs the EMTs clearly are needed in keeping the nucleus at a position of 30 to 40 µm to the tip, but perhaps not for nuclear movement per se, which depends on an intact actin cytoskeleton (*V. hirsuta*: Lloyd et al., 1987; *M. truncatula*: Sieberer et al., 2002).

Paclitaxel (taxol) is an anti-cancer drug that binds to microtubules rather than to tubulin dimers, thereby inhibiting MT dynamics, eventually leading in a dose dependent manner to stabilization and bundling of MTs (for review see: Blagosklonny & Fojo, 1999). Paclitaxel has also been shown to affect MTs in plant cells (Collings et al., 1998). In elongating *Medicago* and *Arabidopsis* root hairs (*M. truncatula*: Sieberer et al., 2002; *A. thaliana*: Bibikova et al., 1997), paclitaxel does not obviously affect polar distribution of the cytoplasm in the subapex. However, the effect of paclitaxel on tip-growth is, similar to that of oryzalin, different in the two species. In *Medicago*, tip growth continues without a deviation from the orginal growth axis, but growth rate drops in a similar manner as after oryzalin treatment (Sieberer et al., 2002). Tip-growth in paclitaxel treated *Arabidopsis* root hairs continues in a wavy pattern with even steeper deviations from the straight growth axis than in oryzalin treated hairs, and without a significant drop in growth rate (Bibikova et al., 1999; Ketelaar et al., 2002). Could there be functional differences of the EMT array that cause the different response of the root hair on microtubule depolymerisation or stabilisation?

In *Arabidopsis*, microtubules control growth direction, since inhibition of microtubule dynamics, both by depolymerization and stabilization cause a wavy growth phenotype. Although microtubules maintain the uniaxial expansion direction, there is no major physiological significance of altering growth direction. In legumes, however, the vast EMT array in elongating root hairs may have a specific role in the early interactions between legumes and soil-living rhizobacteria. Legume roots infected with rhizobia form new plant organs, the root nodules, where rhizobia fix atmospheric nitrogen and make it accessible for the plant. One of the first steps in the plant-bacteria interaction is the curling of root hairs around the bacteria (Kijne, 1992; Hadri & Bisseling, 1998; Esseling et al., 2004). Root hair curling has been described as iterative growth reorientation (Esseling et al., 2003).

MTs in elongating *Medicago* root hairs respond to rhizobacterial signal molecules, the nodulation factors or Nod factors (Weerashinge et al., 2003; Sieberer et al., submitted). Sieberer et al. (submitted) report a short-termed and subtle shortening of the EMT array in tip-growing *M. truncatula* hairs. Growth arresting hairs respond to globally applied Nod factors with root hair deformation, that is swelling of the hair tips (i.e., isodiametric growth) after which tip-growth resumes, albeit in a deviant orientation. Oryzalin causes a deformation phenotype similar to Nod factors in growth arresting root hairs; combined with Nod factors it increases while taxol suppresses Nod factor-induced growth deviation. Interestingly, the root hair deformation phenotype caused by NF in *Medicago* root hairs

can be mimicked by depolymerization and recovery of filamentous actin in *Arabidopsis* hairs where MTs got experimentally ablated with oryzalin (Ketelaar et al., 2003). Also in growth arresting *Medicago* hairs EMTs are affected by Nod factors. The short EMT array in these hairs completely disappears within minutes after application, but reappears after 20 to 30 min. The NF-induced depolymerization of the EMTs correlates with a loss of polar cytoarchitecture and straight growth directionality, while their site of reappearance predicted the new direction of hair elongation. These findings indicate that in addition to the actin cytoskeleton (*M. sativa*: Allen et al., 1994; *Phaseolus vulgaris*: Cárdenas et al., 1998, 2003; *Vicia sativa*: De Ruijter et al., 1998; Miller et al., 1999; Ridge, 1992) also the MT cytoskeleton in *Medicago* root hairs is a target of Nod factor signalling. These observations indicate that both in legumes and in *Arabidopsis*, microtubules are involved in determining growth directionality, possibly by defining in a yet unknown manner the place where exocytosis takes place. In doing so, microtubules could steer polar cell expansion without interfering with actin based tip-growth itself. The major difference between *Arabidopsis* and legume species is that microtubules just fine-tune the growth direction in *Arabidopsis* (and perhaps also in other non-legumes), whereas they are an essential element in the initial stages of symbiosis between legumes and rhizobacteria. It is tempting to speculate that the specific function of EMTs in the symbiotic process may explain the more extended EMT array in legumes compared to *Arabidopsis*, and that the differential response of legumes and *Arabidopsis* root hairs to disturbance of microtubules could be caused by the evolution of the EMT array to facilitate symbiosis. However, there may be specific properties of the EMT array for different species, independent on whether they are legumes or not.

How could microtubules control the direction of tip growth? Bibikova et al. (1999) showed that in *Arabidopsis* taxol-stabilized MTs loose the ability to restrict tip-growth to only one site by applying an intracellular artificial Ca^{2+} gradient (local uncaging of a caged Ca^{2+} ionophore). In untreated hairs local uncaging of Ca^{2+} led only to a transient and limited reorientation towards the artificial Ca^{2+} gradient, whereas root hairs with taxol-stabilized MTs showed a pronounced redirection of growth. (Bibikova et al., 1999). In *Medicago* root hairs Nod factor treatment leads to elevated cytosolic Ca^{2+} levels (Allen et al., 1994; de Ruijter et al 1998; Cárdenas et al., 1999; Felle et al., 1999a, b), which in turn lead to several downstream events affecting the cytoskeleton (for review see: Lhuissier et al., 2001). Nod factors may affect MTs in *Medicago* root hairs via transiently increased Ca^{2+} levels, since MT depolymerization can be triggered by elevated cytoplasmic Ca^{2+} levels (Cyr, 1991, 1994). Additional evidence that elevated calcium

levels affect MTs is available from studies on the *Arabidopsis* ton mutant, which has high calcium-channel activity. CMTs of this mutant are disorganized (Thion et al., 1998). These findings point towards an interaction between MTs and the tip-focused cellular machinery that maintains a high Ca^{2+} gradient at the root hair tip. A possible candidate involved in transferring the Nod factor signal to microtubules may be phospholipase D (PLD), since activation of PLD causes microtubule disruption (Dhonukshe et al., 2003; Gardiner et al., 2003) and PLD is involved in Nod factor-induced root hair deformation (Den Hartog et al., 2001).

MTs and their putative role in targeting exocytosis markers to the very tip of elongating root hairs

Interesting observations concerning the role of MTs in the tip-growth process were made in the tip growing fission yeast *Schizosaccharomyces pombe*. Similarly to root hairs, the direction of polar growth in *S. pombe* is dependent on microtubules. From the nucleus, which is in the middle of the cell, three to four bundles of dynamic microtubules radiate with their plus ends toward both tips of the cells. Mutations in the microtubule associated proteins (MAPs) Tip1p, Tea1p, Tea2p and Mal3p lead to short microtubules and bent/wavy cells or cells with multiple tips (Beinhauer et al., 1997; Browning et al., 2000; Brunner & Nurse, 2000; Behrens & Nurse, 2002). From a combination of mutant analysis and GFP techniques, it is clear that it is the linear transport and the delivery of the MAPs via the microtubules toward the cell tips, which is the crucial process in setting up the cells' polarity. Tea2p is a kinesin-like motor protein that, along the microtubules, interacts with at least the Clip170 homolog Tip1p (Busch & Brunner, 2004) and Tea1p, and moves toward the growing microtubule plus-ends. Mal3p is an End Binding (EB1) homologue that labels the microtubules and also moves, independent of Tea2p, to the microtubule plus ends. Once there, Mal3p directly interacts with Tip1p via a CAP-Gly domain containing region and associates with Tea2p, and therefore, Tea2p and Tea1p stay associated with the growing microtubule plus end. When the plus ends with the proteins reach the tip of the cell via microtubule polymerisation, Mal3p plus end labelling of the microtubules disappears (Busch & Brunner, 2004), the microtubules undergo catastrophe and Tip1p, Tea1p and Tea2p stay in the growing tip. For Tea1p, it has been observed that it attaches to the membrane associated protein Mod5p (Morphology defective 5; Snaith & Sawin, 2003), and forms a complex with Bud6p and For3p, a formin that assembles actin cables (Feierbach et al., 2004). This could be a direct link between the polarity complex

and actin polymerization, and thus, the location of exocytosis and direction of growth.
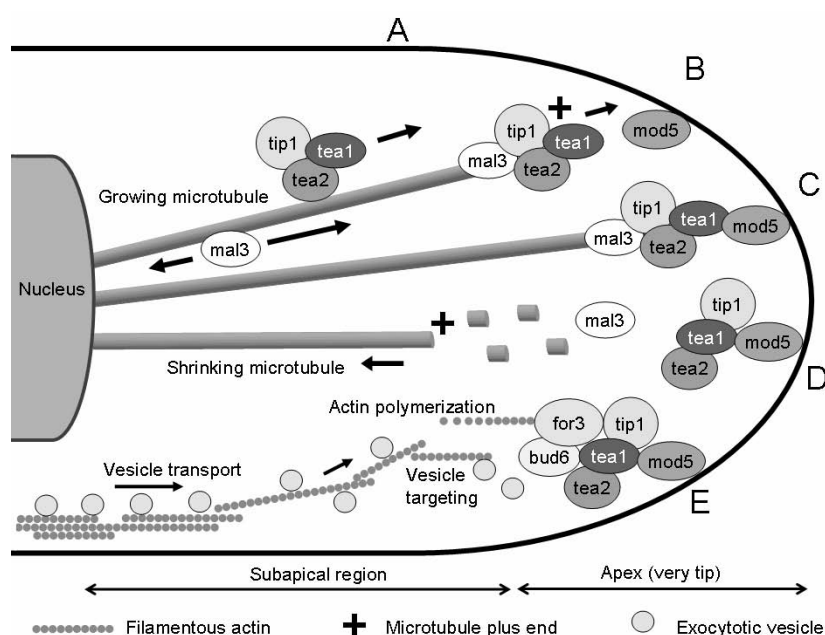

Figure 2. Scheme of putative microtubule regulation of tip-growth in root hairs, based on what has been described in *Schizosaccharomyces pombe*. **A**, The kelch-repeat protein tea1 interacts with the kinesin-like motor protein tea2 and the Clip170 homolog tip1, thereby moving towards the growing microtubule plus end. The EB1 homolog mal3 moves independently of tea2 to the microtubule plus end. A protein complex of mal3, tip1, tea2, and tea1 associates with the growing microtubule plus end and gets delivered to the hair tip by microtubule growth (**B** and **C**). **D**, tip1, tea1, and tea2 may remain at the tip after mal3 dissociation and microtubule depolymerization. Tea1 attaches to the membrane associated protein mod5 and (**E**) forms a complex with bud6 and for3, a formin that assembles actin filaments. The actin filaments facilitate the transport and targeting of exocytotic vesicles to the very tip.

A homology search for the proteins involved in setting up polarity in *S. pombe* reveals that the *Arabidopsis* genome contains 3 EB1 homologues At3g47690 (AtEB1a), At5g62500 (AtEB1b) and At5g67270 (AtEB1c), and that in *M. truncatula* at least 4 expressed EB1 homologues are present (MtD20746, MtD20502 and MtD05012). GFP-AtEB1 has been shown to decorate the plus ends of growing microtubules in *Arabidopsis* (Chan et al., 2003; Mathur et al., 2003). Other proteins from the cell polarity pathway in which EB1 is active in fission yeast appear not to be present in the *Arabidopsis* genome, but their function may be performed by yet unidentified proteins. Even though not all proteins in the EB1 pathway have been found in plants, EB1 homologues are present in plant cells and their localisation to microtubule plus ends is similar to that in fission yeast. Therefore, EB1 proteins may perform the same function in plants as in *S. pombe*. Since growing *M.*

truncatula root hairs have an array of highly dynamic EMTs (Sieberer et al., 2002), which can grow from the sub-apical region into the very root hair tip (Vos et al., 2003), and determine root hair elongation direction (Sieberer et al., submitted) linear transport of polarity markers via microtubules like in *S. pombe* could exist in plants, and have a role in root hair growth direction.

Conclusion

Microtubules are essential in determining the direction of root hair growth. In legumes, they determine the growth direction of a new outgrowth in growth terminating root hairs, treated with Nod factors. Since an essential element of the legume rhizobacterium symbiosis is the entrapment of bacteria in a root hair pocket, formed by iterative changes in growth direction, it is likely that microtubules are important in the initiation of symbiosis. Interesting work on fission yeast shows that a microtubule based polarity mechanism is present in this organism. One of the main proteins in this mechanism is EB1, of which homologues are present in plants. Future research in our exciting field will reveal if there is a microtubule based polarity mechanism in plants as in fission yeast and identify the proteins that are involved in this mechanism.

References

Allen NS, Bennett MN, Cox DN, Shipley A, Ehrhardt DW, Long SR. 1994. Effects of Nod factors on alfalfa root hair Ca^{++} and H^+ currents on cytoskeleton behavior. In: Daniels MJ, Downie JA, Osbourn AE, eds. *Advances in molecular genetics of plant microbe interactions*. Dordrecht, the Netherlands: Kluwer Academic Publishers, Vol 3, 107–114.

Bailey PHJ, Currey JD, Fitter AH. 2002. The role of root system architecture and root hairs in promoting anchorage against uprooting forces in Allium cepa and root mutants of *Arabidopsis thaliana*. Journal of Experimental Botany 53: 333-340.

Bakhuizen R. 1988. *The plant cytoskeleton in the rhizobium-legume symbiosis*. PhD thesis, Leiden University, the Netherlands.

Baluška F, Salaj J, Mathur J, Braun M, Jasper F, Samaj J, Chua N-H, Barlow PW, Volkman D. 2000. Root hair formation: F-actin-dependent tip growth is initiated by local assembly of profilin-supported F-actin meshworks accumulated within expansin-enriched bulges. Developmental Biology 227: 618–632.

Bao YQ, Kost B, Chua NH. 2001. Reduced expression of a-tubulin genes in *Arabidopsis thaliana* specifically affects root growth and morphology, root hair development and root gravitropism. Plant Journal 28: 145–157.

Bates TR, Lynch JP. 2000. The efficiency of *Arabidopsis thaliana* (Brassicaceae) root hairs in phosphorus

acquisition. American Journal of Botany 87: 964–970.

Behrens R, Nurse P. 2002. Roles of fission yeast tea1p in the localization of polarity factors and in organizing the microtubular cytoskeleton. Journal of Cell Biology 157: 783-793.

Beinhauer JD, Hagan IM, Hegemann JH, Fleig U. 1997. Mal3, the fission yeast homolog of the human APC-interacting protein EB-1 is required for micorotubule integrity and the maintenance of cell form. Journal of Cell Biology 139: 717-728.

Bibikova TN, Zhigilei A, Gilroy S. 1997. Root hair growth in *Arabidopsis thaliana* is directed by calcium and an endogenous polarity. Planta 203: 495– 505.

Bibikova TN, Blancaflor EB, Gilroy S. 1999. Microtubules regulate tip growth and orientation in root hairs of *Arabidopsis thaliana*. Plant Journal 17: 657-665.

Blagosklonny MV, Fojo T. 1999. Molecular effects of paclitaxel: myths and reality (a critical review). International Journal of Cancer 83:151-156.

Browning H, Hayles J, Mata J, Aveline L, Nurse P, McIntosh JR. 2000. Tea2p is a kinesin-like protein required to generate polarized growth in fission yeast. Journal of Cell Biology 151: 15-2.

Brunner D, Nurse P. 2000. CLIP170-like tip1p spatially organizes microtubular dynamics in fission yeast. Cell 102: 695-704.

Busch KE, Brunner D. 2004. The microtubule plus end-tracking proteins mal3p and tip1p cooperate for cell-end targeting of interphase microtubules. Current Biology 14: 548-559.

Cárdenas L, Vidali L, Domínguez J, Pérez H, Sánchez F, Hepler PK, Quinto C. 1998. Rearrangement of actin microfilaments in plant root hairs responding to *Rhizobium etli* nodulation signals. Plant Physiology 116: 871-877.

Cárdenas L, Feijo JA, Kunkel JG, Sanchez F, Holdaway-Clarke T, Hepler PK, Quinto C. 1999. Rhizobium nod factors induce increases in intracellular free calcium and extracellular calcium influxes in bean root hairs. Plant Journal 9: 347-352.

Cárdenas L, Thomas-Oates JE, Nava N, Lopez-Lara IM, Hepler PK, Quinto C. 2003.
The role of nod factor substituents in actin cytoskeleton rearrangements in *Phaseolus vulgaris*. Molecular Plant Microbe Interaction 16: 326-334.

Chan J, Calder GM, Doonan JH, Lloyd CW. 2003. EB1 reveals mobile microtubule nucleation sites in Arabidopsis. Nature Cell Biology 5: 967-971.

Clarkson DT. 1985. Factors affecting mineral nutrient acquisition by plants. Annual Review of Plant Physiology 36: 77–115.

Collings DA, Asada T, Allen NS, Shibaoka H. 1998. Plasma membraneassociated actin in bright yellow 2 tobacco cells: evidence for interaction with microtubules. Plant Physiology 118: 917–928.

Cyr RJ. 1991. Calcium/calmodulin affects microtubule stability in lysed protoplasts. Journal of Cell Science 100:311–317.

Cyr RJ. 1994. Microtubules in plant morphogenesis: role of the cortical array. Annual Review in Cell Biology 10: 153–180.

Den Hartog M, Musgrave A, Munnik T. 2001. Nod factor-induced phosphatidic acid and diacylglycerol pyrophosphate formation: a role for phospholipase C and D in root hair deformation. Plant Journal 25: 55-65.

Derksen J, Emons AMC. 1990. Microtubules in tip growth systems. In: Heath IB, ed. *Tip growth in plant and fungal cells*. San Diego, USA: Academic Press, 147-181.

De Ruijter NCA, Rook MB, Bisseling T, Emons AMC. 1998. Lipochito-oligosaccharides reinitiate root hair tip growth in *Vicia sativa*, with high calcium and spectrin-like antigen at the tip. Plant Journal 13: 341-350.

Dhonukshe P, Gadella TW Jr. 2003. Alteration of microtubule dynamic instability during preprophase band formation revealed by yellow fluorescent protein-CLIP170 microtubule plus-end labeling. Plant Cell 15:597-611.

Dixit, R, Cyr RJ. 2004a. Encounters between dynamic cortical microtubules promote ordering of the cortical array through angle-dependent modifications of microtubule behavior. Plant Cell 16: 3274-3284.

Dixit R, Cyr R. 2004b. The cortical microtubule array: From dynamics to organization. Plant Cell 16: 2546-2552.

Dolan L, Duckett CM, Grierson C, Linstead P, Schneider K, Lawson E, Dean C, Poethig S, Roberts K. 1994. Clonal relationships and cell patterning in the root epidermis of Arabidopsis. Development 120: 2465–2474.

Dumais J, Long SR, Shaw SL. 2004. The mechanics of surface expansion anisotropy in *Medicago truncatula* root hairs. Plant Physiology 136:3266-3275.

Emons AMC, Wolters-Arts AMC. 1983. Cortical microtubules and microfibril deposition in the wall of root hair of *Equisetum hyemale*. Protoplasma 117: 68-81.

Emons AMC, Traas JA. 1986. Coated pits and coated vesicles on the plasma membrane of plant cells. European Journal of Cell Biology 41: 57-64.

Emons, AMC. 1987. The cytoskeleton and secretory vesicles in root hairs of *Equisetum* and *Limnobium* and cytoplasmic streaming in root hairs of *Equisetum*. Annals of Botany 60: 625–632.

Emons, AMC. 1989. Helicoidal microfibril deposition in a tip-growing cell and microtubule alignment during tip morphogenesis: a dry-cleaving and freeze-substitution study. Canadian Journal Botany 67: 2401–2408.

Esseling JJ, Lhuissier FGP, Emons AMC. 2003. Nod factor-induced root hair curling: continuous polar growth towards the point of Nod factor application. Plant Physiology 132: 1982–1988.

Esseling JJ, Lhuissier FGP, Emons AMC. 2004. A nonsymbiotic root hair tip growth phenotype in NORK-mutated legumes: implications for nodulation factor–induced signaling and formation of a multifaceted root hair pocket for bacteria. Plant Cell 16: 933–944.

Feierbach B, Verde F, Chang F. 2004. Regulation of a formin complex by the microtubule plus end protein tea1p. Journal of Cell Biology 165: 697-707.

Felle HH, Kondorosi E, Kondorosi A, Schultze M. 1999a. Elevation of the cytosolic free $[Ca^{2+}]$ is indispensable for the transduction of the Nod factor signal in alfalfa. Plant Physiology 121: 273-279.

Felle HH, Kondorosi E, Kondorosi A, Schultze M. 1999b. Nod factors modulate the concentration of cytosolic free calcium differently in growing and non-growing root hairs of *Medicago sativa* L. Planta 209:207-212.

Galway ME, Heckman JW, Schiefelbein JW. 1997. Growth and ultrastructure of *Arabidopsis* root hairs: the rhd3 mutation alters vacuole enlargement and tip growth. Planta 201: 209–218.

Gardiner J, Collings DA, Harper JD, Marc J. 2003. The effects of the phospholipase D-antagonist 1-butanol

on seedling development and microtubule organisation in Arabidopsis. Plant Cell Physiology 44: 687-96.

Geitmann A, Emons AMC. 2000. The cytoskeleton in plant and fungal cell tip growth. Journal of Microscopy 198: 218-245.

Gilroy S, Jones DL. 2000. Through form to function: root hair development and nutrient uptake. Trends in Plant Science 5:56-60.

Grierson CS, Ketelaar T. 2004. Development of root hairs. In: Hussey PJ, ed. *The plant cytoskeleton in cell differentiation and development*. Annual Plant Reviews Series, Oxford, UK: Blackwell Publishers.

Hadri AE, Bisseling T. 1998. Responses of the plant to Nod factors. In: Spaink HP, Kondorosi A, and Hooykaas PJJ, eds. *The Rhizobiaceae: Molecular Biology of Model Plant-Associated Bacteria.* Dordrecht, the Netherlands: Kluwer Academic Publishers, 403-416.

Hepler PK, Vidali L, Cheung AY. 2001. Polarized cell growth in higher plants. Annual Review of Cell and Developmental Biology 17:159-87.

Hussey PJ, Deeks MJ, Hawkins TJ Ketelaar T. 2004. Polar cell growth and the cytoskeleton biology. In: Lindsey K, ed. *Polarity in Plants.* Annual Plant Reviews Series. London, UK: Blackwell Publishers.

Ketelaar T, Emons AMC. 2000. The role of microtubules in root hair growth and cellulose microfibril deposition. In: Ridge RW, Emons AMC, eds. *Root hairs. Cell and molecular biology.* Tokyo, Japan: Springer-Verlag, 17–28.

Ketelaar T, Emons AMC. 2001. The cytoskeleton in plant cell growth: lessons from root hairs. New Phytologist 152: 409–418.

Ketelaar T, Faivre-Moskalenko C, Esseling JJ, de Ruijter NCA, Grierson CS, Dogterom M, Emons AMC. 2002. Positioning of nuclei in Arabidopsis root hairs: an actin-regulated process of tip growth. Plant Cell 14: 2941–2955.

Ketelaar T, de Ruijter NCA, Emons AMC. 2003. Unstable F-actin specifies the area and microtubule direction of cell expansion in Arabidopsis root hairs. Plant Cell 15: 285–292.

Kijne JW. 1992. The Rhizobium infection process. In: Stacey G, Burris R, Evans H, eds. *Biological nitrogen fixation*. New York and London: Chapman and Hall, 349–398.

Lhuissier FGP, de Ruijter NCA, Sieberer BJ, Esseling JJ, Emons AMC. 2001. Time course of cell biological events evoked in legume root hair by Rhizobium Nod factors: State of the art. Annals of Botany 87: 289-302.

Long SR. 1996. Rhizobium symbiosis: Nod factor in perspective. Plant Cell 8: 1855 1898.

Lloyd C. 1983. Helical microtubular arrays in onion root hairs. Nature 305: 311–313.

Lloyd CW, Pearce KJ, Rawlins DJ, Ridge RW, Shaw PJ. 1987. Endoplasmic microtubules connect the advancing nucleus to the tip of legume root hairs, but F-actin is involved in basipetal migration. Cell Motility and Cytoskeleton 8: 27–36.

Marc J, Granger CL, Brincat J, Fisher DD, Kao T, McCubbin AG, Cyr RJ. 1998. A GFP-MAP4 reporter gene for visualizing cortical microtubule rearrangements in living epidermal cells. Plant Cell 10: 1927–1939.

Mathur J, Mathur N, Kernebeck B, Srinivas BP, Hulskamp M. 2003. A novel localization pattern for an EB1-like protein links microtubule dynamics to endomembrane organization. Current Biology 13:1991-1997.

Miller DD, de Ruijter NCA, Emons AMC. 1997. From signal to form: Aspects of the cytoskeleton-plasma membrane-cell wall continuum in root hair tips. Journal of Experimental Botany 48: 1881–1896.

Miller, DD, de Ruijter NCA, Bisseling T, Emons AMC. 1999. The role of actin in root hair morphogenesis: Studies with lipochito-oligosaccharide as a growth stimulator and cytochalasin as an actin perturbing drug. Plant Journal 17: 141–154.

Miller DD, Leferink-ten Klooster HB, Emons AMC. 2000. Lipochito-oligosaccharide nodulation factors stimulate cytoplasmic polarity with longitudinal endoplasmic reticulum and vesicles at the tip in vetch root hairs. Molecular Plant –Microbe Interactions 13: 1385–1390.

Mylona P, Pawlowski K, Bisseling T. 1995. Symbiotic nitrogen fixation. Plant Cell 7: 869–885.

Peterson LR, Farquhar ML. 1996. Root hairs: specialized tubular cells extending root surfaces. Botanical Reviews 62: 1–35.

Ridge RW. 1988. Freeze-substitution improves the ultrastructural preservation of legume root hairs. Botanical Magazine Tokyo 101: 427–441.

Ridge RW. 1992. A model of legume root hair growth and Rhizobium infection. Symbiosis 14: 359–373.

Ridge RW. 1996. Root Hairs: Cell Biology and Development. In: Waisel Y, Eshel A, Kafkafi U, eds. *Plant Roots: The Hidden Half*. New York, USA: Marcel Dekker Inc, 2nd edition, 127-147.

Schiefelbein JW, Shipley A, Rowse P. 1992. Calcium influx at the tip of growing root-hair cells of *Arabidopsis thaliana*. Planta 187: 455-459.

Shaw SL, Dumais J, Long SR. 2000. Cell surface expansion in polarly growing root hairs of *Medicago truncatula*. Plant Physiology 124: 959–969.

Shaw SL, Kamyar R, Erhardt DW. 2003. Sustained microtubule treadmilling in Arabidopsis cortical arrays. Science 300: 1715–1718.

Sherrier DJ, Van den Bosch KA. 1994. Secretion of cell wall polysaccharides in Vicia root hairs. Plant Journal 5: 185–195.

Sieberer B, Emons AMC. 2000. Cytoarchitecture and pattern of cytoplasmic streaming in root hairs of *Medicago truncatula* during development and deformation by nodulation factors. Protoplasma 214: 118-127.

Sieberer BJ, Timmers ACJ, Lhuissier FGP, Emons AMC. 2002. Endoplasmic microtubules configure the subapical cytoplasm and are required for fast growth of *Medicago truncatula* root hairs. Plant Physiology 130: 977–988.

Snaith HA, Sawin KE. 2003. Fission yeast mod5p regulates polarized growth through anchoring of tea1p at cell tips. Nature 423: 647-651.

Sugimoto K, Williamson RE, Wasteneys GO. 2000. New techniques enable comparative analysis of microtubule orientation, wall texture, and growth rate in intact roots of Arabidopsis. Plant Physiology 124: 1493–1506.

Takahashi H, Kawahara A, Inoue Y. 2003. Randomization of cortical microtubules in root epidermal cells induces root hair initiation in Lettuce (*Lactuca sativa* L.) seedlings. Plant Cell Physiology 44:350-359.

Thion L, Mazars C, Nacry P, Bouchez D, Moreau M, Ranjeva R, Thuleau P. 1998. Plasma membrane depolarization-activated calcium channels, stimulated by microtubule depolymerizing drugs in wild-type *Arabidopsis thaliana* protoplasts, display constitutively large activities and longer half life in ton2 mutant cells

affected in the organization of cortical microtubules. Plant Journal 13: 603–610.

Traas JA, Braat P, Emons AMC, Meeks H, Derksen J. 1985. Microtubules in root hairs. *Journal of Cell Science* **76**: 303-320.

Van Bruaene N, Joss G, Thas O, van Oostveldt P. 2003. Four-dimensional imaging and computer-assisted track analysis of nuclear migration in root hairs of *Arabidopsis thaliana*. Journal of Microscopy 211: 167–178.

Van Bruaene, Joss G, van Oostveldt. 2004. Reorganization and in vivo dynamics of microtubules during Arabidopsis root hair development. Plant Physiology 136: 3905–3919.

Vos JW, Sieberer B, Timmers ACJ, Emons AMC. 2003. Microtubule dynamics during preprophase band formation and the role of endoplasmic microtubules during root hair elongation. Cell Biology International 27: 295.

Vos JW, Dogterom M, Emons AMC. 2004. Microtubules become more dynamic but not shorter during preprophase band formation: a possible "search-and-capture"mechanism for microtubule translocation. Cell Motility and the Cytoskeleton 57: 246-258.

Wasteneys G, Galway ME. 2003. Remodeling the cytoskeleton for growth and form: an overview with some new views. Annual Review in Plant Biology 54: 691–722.

Weerashinge RR, Collings DA, Johannes E, Allen NS. 2003. The distributional changes and role of microtubules in Nod factor-challenged *Medicago sativa* root hairs. Planta 218: 276–287.

Wymer CL Bibikova TN, Gilroy S. 1997. Cytoplasmic free calcium distributions during the development of root hairs of *Arabidopsis thaliana*. Plant Journal 12:427-439.

Samenvatting

In dit proefschrift wordt celbiologisch onderzoek gepresenteerd waarvan de resultaten bijdragen tot een beter begrip van de rol van het cytoskelet gedurende de ontwikkeling van wortelharen en de respons ervan op bacteriële nodulatie factoren (Nod factoren). Nod factoren zijn lipochito-oligosaccharide signaalmoleculen die uitgescheiden worden door *Rhizobium* bacteriën. Zij zijn essentieel voor het opzetten van een succesvolle symbiose tussen vlinderbloemige planten en rhizobia. Deze symbiose leidt tot de vorming van een nieuw orgaan, een wortelknolletje, waarin atmosferische stikstof vastgelegd wordt in een voor de plant bruikbare stikstofbron. De bacteriën komen de wortel van de plant binnen via de wortelharen. Deze penetratie wordt voorafgegaan door een krulling van de wortelhaartop rondom de bacteriën d.m.v. een topgroeiproces. Als experimenteel systeem gebruikten we wortelharen van de modelplant *Medicago truncatula*. Aspecten van wortelhaarontwikkeling, het microtubulaire cytoskelet in topgroeiende wortelharen en de respons van dit celskelet op Nod factoren worden achtereenvolgens behandeld in de verschillende hoofdstukken.

Hoofdstuk 1 beschrijft de stand van zaken bij de start van het project, met de nadruk op het actine cytoskelet, waarvan bekend was dat het cruciaal is voor het topgroeiproces van wortelharen en een aangrijppunt voor de door Nod factor geïnduceerde celsignalering.

Hoofstuk 2 is een celbiologische karakterisering van wortelharen van *M. truncatula* tijdens hun ontwikkeling en tijdens de deformatie teweeggebracht door Nod factor. Bij het ontstaan van een wortelhaar, vanuit een uitstulping van een wortelepidermiscel, hoopt cytoplasma zich op aan de top van de cel zodat de polaire celstructuur verkregen wordt die karakteristiek is voor een topgroeiende plantencel. Organellen worden geconcentreerd in het subapicale gebied, terwijl het basale deel van de haar een steeds groter wordende vacuole bevat. Dit subapicale gebied bevat organellen zoals het endoplasmatisch reticulum, mitochondria, plastiden, Golgi lichaampjes en de kern. Deze laatste volgt de groeiende haartop op een afstand van 30 à 40 micrometer. De uiterste top, waar de groei in feite plaats vindt, bevat deze organellen niet. Elektronenmicroscopische analyses hebben laten zien dat in de uiterste top bijna uitsluitend vesikels voorkomen, zowel exocytotische als endocytotische. Wanneer de wortelharen stoppen met groeien wordt dit subapicale gebied korter, waarna het verdwijnt. Volgroeide haren hebben een dunne laag van perifeer cytoplasma, gelijkelijk verdeeld rondom een centrale vacuole. De kern heeft dan geen vaste plaats meer ten opzichte van de wortelhaartop.

Het patroon van cytoplasmastroming, de beweging van alle zichtbare organellen behalve kern en vacuole, verandert tijdens de ontwikkeling van de wortelharen en ook wanneer de haren in contact komen met Nod factor. Wortelepidermiscellen, inclusief die met uitstulpingen waaruit de wortelharen zullen groeien, en volgroeide haren vertonen circulatiestroming. Organeltransport in deze cellen heeft een snelheid van 8-14 micrometer per seconde. In het gevacuoliseerde deel van groeiende wortelharen is de cytoplasmastroming van hetzelfde type en de organellen bewegen met dezelfde snelheid, terwijl in het cytoplasma-dichte subapicale gebied omgekeerde-fonteinstroming plaatsvindt. Individuele organellen bewegen in het subapicale gebied in de richting van de top, verblijven daar enkele seconden en keren om voordat ze de uiterste top bereikt hebben.

Nod factoren veranderen het patroon van cytoplasmastroming in haren die aan het stoppen zijn met groeien. Deze haren reageren op Nod factor met een zwelling van de haartop en een daaropvolgende uitgroei van een nieuwe haar vanuit die zwelling in een afwijkende richting van de oorspronkelijke groeirichting. Binnen enkele minuten na het toevoegen van Nod factor verandert de omgekeerde-fonteinstroming in circulatiestroming. In de nieuwe uitgroei ontstaat opnieuw omgekeerde-fonteinstroming. De verschillende types van cytoplasmastroming bewerkstelligen een ongelijke distributie van organellen in de cel en reflecteren het organisatiepatroon van het actine cytoskelet, dat in plantencellen verantwoordelijk is voor organeltransport.

In *hoofdstuk 3* wordt het veranderende microtubulaire cytoskelet in ontwikkelende wortelharen van *M. truncatula* beschreven. Microtubuli werden zichtbaar gemaakt via immunocytochemie na vriesfixatie en in levende cellen door het tot expressie brengen van een fusie-eiwit van 'green fluorescent protein' met een microtubuli-bindend domein van een microtubuli-bindend eiwit (GFP-MBD). Groeiende wortelharen van *M. truncatula* hebben een uitgebreid stelsel van endoplasmatische microtubuli in de subapex, wat niet eerder gevonden is bij wortelharen. Deze dichte set van endoplasmatische microtubuli verschijnt als de topgroei start en blijft aanwezig zolang de groei duurt. Corticale microtubuli, die voor zover bekend in wortelharen van alle plantensoorten aanwezig zijn, lopen in een net-axiale richting en komen voor in alle ontwikkelingsstadia van de *M. truncatula* wortelharen. De uiterste top van groeiende wortelharen is grotendeels vrij van endoplasmatische en corticale microtubuli. In groeiende haren is echter te zien dat dynamische microtubuli van beide categorieën regelmatig de top raken. Ze buigen nooit mee met de kromming van de top, zoals dat wel het geval is na de groei.

Na behandeling van groeiende haren met 1 μM van de microtubuli afbrekende stof oryzaline verdwijnen de endoplasmatische microtubuli, maar de corticale bijven aanwezig. Het subapicale gebied met dicht cytoplasma wordt even kort als wanneer de haren aan het stoppen zijn met groeien, de afstand van de kern tot de top van de haar neemt toe, de groeisnelheid neemt af en de kern volgt de top, maar op een grotere afstand dan voor de behandeling. De microtubuli-stabiliserende stof taxol heeft in een concentratie van 1 μM geen effect op de celstructuur van groeiende wortelharen. De cytoplasmatisch dichte subapex blijft intact, de nucleus behoudt zijn karakteristieke afstand tot de top, maar de groeisnelheid neemt af tot hetzelfde niveau als in haren die met 1 μM oryzaline zijn behandeld. Deze resultaten laten zien dat endoplasmatische microtubuli essentieel zijn voor het in stand houden van de specifieke celstructuur van groeiende wortelharen van *M. truncatula,* met inbegrip van een gefixeerde afstand tussen kern en celtop, maar dat ze dynamisch moeten zijn om de groeisnelheid op niveau te houden.

In *hoofdstuk 4* worden de effecten beschreven die Nod factor heeft op het microtubulaire cytoskelet van *M. truncatula*. Nod factor veroorzaakt een snelle subtiele, en voorbijgaande verkorting van de subapicale endoplasmatische microtubuli van groeiende haren. Het effect is sterker op de endoplasmatische dan op de corticale microtubuli. De endoplasmatische set van korte microtubuli, die aanwezig is in haren die aan het stoppen zijn met groeien, verdwijnt volledig binnen enkele minuten nadat de Nod factor is toegevoegd, maar ontstaat weer na 20 tot 30 minuten, waarna ook de wortelhaargroei weer start, maar dan wel in een andere richting. Deze afwijking van de groeirichting van de nieuwe uitgroei t.o.v. de met de oorspronkelijke groeirichting is groter wanneer samen met Nod factor ook oryzaline wordt toegevoegd aan de wortels, en zo goed als afwezig als Nod factor gebruikt wordt in combinatie met taxol. Behandeling met alleen oryzaline geeft wel wortelhaardeformatie in de vorm van zwelling en uitgroei, maar zonder dat nieuwe endoplasmatische microtubuli ontstaan en zonder het verkrijgen van nieuw groeipotentieel. Samen laten deze bevindingen zien dat het microtubulaire cytoskelet een factor is in het groeiproces van wortelharen, namelijk in het bepalen van de groeirichting, en dat het een direct of indirect doelwit is voor de vroege door Nod factor geïnduceerde celsignalering. De laatste twee eigenschappen zijn cruciaal voor het krullen van wortelharen rond bacteriën.

Terwijl het actine cytoskelet de celmodule is die nieuw materiaal levert voor het groeiproces van de wortelhaarkrulling rond bacteriën, verschaffen de microtubuli de

wortelharen een celmechanisme om de groeirichting te veranderen, een essentieel ingrediënt van krulling. Aangezien het vasthouden van bacteriën in de krul een van de eerste beslissende stappen is in de interactie tussen *Rhizobia* en hun vlinderbloemige gastheren, zijn microtubuli onontbeerlijk voor het opzetten van een symbiose tussen deze twee organismen. Het goed ontwikkelde systeem van subapicale endoplasmatische microtubuli, dat tot nu toe alleen gevonden is bij vlinderbloemigen, zou een van de eigenschappen kunnen zijn die deze soorten geschikt maakt voor symbiose met rhizobia.

In *hoofdstuk 5* wordt een hypothese ontwikkeld over de bijdrage van microtubuli aan wortelhaarontwikkeling en het opzetten en behouden van celpolariteit. Hierin wordt de kennis over het microtubulaire cytoskelet in wortelharen van de modelplanten *M. truncatula* en *Arabidopsis thaliana* vergeleken met wat bekend is over dit skelet in gist. Vanuit deze gecombineerde kennis stellen we een op microtubuli-gebaseerd mechanisme voor dat celpolariteit in wortelharen reguleert.

Summary

In this thesis, cell biological research is presented that contributes to a better understanding of the role of the microtubule cytoskeleton during development of legume root hairs and their response to rhizobacterial signal molecules, the nodulation factors (Nod factors). Nod factors are the key for the bacteria to enter the root hairs and thus are crucial for setting up a successful symbiosis between legume host plants and rhizobia. We used root hairs of the model legume *Medicago truncatula* as an experimental system. In the various chapters, aspects of root hair development, the microtubule cytoskeleton in root hair (tip) growth, and the response of root hairs to Nod factors are being covered.

Chapter 1 describes the state of research at the start of the project, with emphasis on the actin cytoskeleton, which is crucial for the tip-growth process of root hairs and a target of early Nod factor-induced cell signaling. The actin cytoskeleton responds to Nod factors within 3 minutes after application with an increase in the density of fine bundles of actin filaments in the sub-apex of the hairs. Elevated levels of cytoplasmic calcium and actin binding proteins may play an important role in altering the actin cytoskeleton. The implications of this process on cell polarity, exocytosis and cell wall formation, and eventually on root hair curing are being discussed.

Chapter 2 reports the cell biological characterization of *M. truncatula* root hairs during their development and deformation by Nod factors. When a root hair emerges from a bulge of the root epidermal cell, cytoplasm accumulates at the cell tip so that a highly polarized cytoarchitecture, characteristic of a tip-growing plant cell, is formed. Organelles become concentrated in the subapical region, whereas the basal part of the hair contains the enlarging vacuole. The subapical region contains organelles such as the endoplasmic reticulum, mitochondria, plastids, Golgi bodies, and the nucleus. The latter follows the expanding hair tip at a distance of 30 to 40 micrometer. The very apex, the actual site of tip-growth, is devoid of these organelles. Electron microscopical analyses have shown that here mainly exocytotic as well as endocytotic vesicles are located. At the end of root hair growth this subapical cytoplasmic dense region shortens, after which it completely disappears. Fully-grown hairs have a thin layer of peripheral cytoplasm, equally distributed around the central vacuole. The nucleus in these hairs does not have a fixed position relative to the hair tip anymore.

The pattern of cytoplasmic streaming, i.e., the movement of cell organelles, changes during hair development and after application of Nod factor. Normally, root epidermal

cells, bulges, and fully-grown root hairs exhibit circulation streaming. Organelle transport in these cells has a velocity of $8 - 14 \mu m\ s^{-1}$. In the vacuolated part of growing root hairs, cytoplasmic streaming is similar, whereas in the subapical cytoplasmically dense region a reverse fountain-like streaming pattern occurs. Individual organelles move in a stop-and-go manner towards the hair tip, linger there for a few seconds, and reverse direction before having reached the very tip.

In growth-arresting hairs, Nod factors change the pattern of cytoplasmic streaming. These hairs react to Nod factor morphologically with a swelling of the hair tip and a subsequent outgrowth from that swelling in a direction that deviates from the original growth axis. In the outgrowth, reverse-fountain streaming is set up again after it was initially lost after Nod factor application. The different types of cytoplasmic streaming in root hairs facilitate an unequal distribution of organelles within the cell and reflect the organization pattern of the actin cytoskeleton, which in plant cells is responsible for organelle transport. The results show that Nod factors alter cell polarity, cytoplasmic streaming and cell morphology all of which depend on the actin cytoskeleton.

In *chapter 3*, results are presented on the changing organization and function of the microtubule cytoskeleton in developing M. truncatula root hairs. Microtubules were labeled with immunocytochemistry after rapid freeze fixation and *in vivo* with a green fluorescent protein microtubule binding domain (GFP-MBD) fusion protein. I discovered that growing *M. truncatula* root hairs have an extensive endoplasmic microtubule array in their sub-apex, which had not been reported for root hairs. This set of endoplasmic microtubules appears when tip growth begins and is retained until growth stops. Cortical microtubules, which, as far as is known, are present in root hairs of all species, are net-axially aligned and present in all developmental stages of root hairs of *M. truncatula*. The very tip of elongating root hairs is largely free of endoplasmic and cortical microtubules. However, in living, growing hairs we observed dynamic microtubules of both categories regularly reaching the very tip. They never loop through the tip, as is the case in fully-grown hairs after hair elongation has ceased.

Upon treatment of growing hairs with 1 μM of the microtubule depolymerising drug oryzalin, endoplasmic microtubules disappear, but cortical microtubules remain present. The subapical cytoplasmic dense region becomes as short as during growth arrest, the distance from nucleus to hair tip increases, growth slows down, and the nucleus still follows the advancing tip, though at a much larger distance. Taxol, a microtubule-stabilizing drug, in the concentration of 1 μM has no effect on the cytoarchitecture of

growing hairs: the subapical cytoplasmic dense region remains intact and the nucleus keeps its characteristic distance from the tip. Only the growth rate drops to a similar level as in hairs treated with 1 μM oryzalin. These results show that endoplasmic microtubules are essential in maintaining the specific cytoarchitecture of growing root hairs of *M. truncatula*, including keeping a fixed distance between nucleus and hair tip, and that they have to be dynamic to keep the growth rate of these hairs at the normal high level.

In *chapter 4*, the effects that Nod factor exerts on the microtubule cytoskeleton of *M. truncatula* root hairs are described. Nod factor causes a rapid, subtle, and transient shortening of the subapical endoplasmic microtubule array of growing hairs. The effect is more severe on the endoplasmic than on the cortical microtubules. The short endoplasmic microtubule array of growth-arresting hairs completely disappears within minutes after Nod factor application, but reappears after 20 to 30 min, after which growth resumes from the hair swelling, albeit in a deviant orientation. This deviation of the new outgrowth from the original growth axis is larger when Nod factor and the microtubule depolymerizing drug oryzalin are applied together and almost absent when Nod factor is applied in combination with taxol. Oryzalin treatment alone produces the same root hair deformation consisting of swelling and outgrowth, but without a reappearance of endoplasmic microtubules and without acquisition of new growth potential. Together, these findings demonstrate that the microtubule cytoskeleton is a factor in the tip-growth process, in determining growth direction, and that it is a direct or indirect target of early Nod factor-induced cell signaling. The latter two features are crucial for root hair curling around rhizobia.

While the actin cytoskeleton is the cytoskeletal compound that transports and delivers the new material needed for the growth process and for hair curling around the bacteria, the microtubule cytoskeleton somehow enables the root hairs to alter the axis of elongation, another essential ingredient of curling. Since capturing the bacteria in a curl is one of the first go-no-go decision step in the interaction between *Rhizobia* and their legume hosts, microtubules are indispensable for setting up symbiosis between those organisms. The well-developed array of subapical endoplasmic microtubules, which so far has only been reported for leguminous plants, could be one of the properties that make these species fit for symbiosis.

In *chapter 5*, a hypothesis is presented on the involvement of microtubules in root hair development and setting up and maintaining cell polarity. The knowledge about the

microtubule cytoskeleton in the model plants *M. truncatula* and *Arabidopsis thaliana* is compared with what is known about this cytoskeleton compound in fission yeast, where bundles of endoplasmic microtubules place tip-marking proteins in the cell cortex of the expanding tip. These tip markers serve the actin cytoskeleton as spatial cues. Thereby microtubules determine the site where excocytosis, and therefore growth, takes place. From this combined knowledge, we propose a microtubule cytoskeleton-based mechanism that regulates cell polarity in root hairs.

Curriculum Vitae

I, Björn Sieberer, was born on the 11th of June 1972 in Krems/Donau, Austria. In the Bundesrealgymnasium Krems-Ringstrasse I got my high-school diploma in 1990. After army service I started in 1991 to study Biology at the Faculty for Natural Sciences, University of Vienna, and focused on Botany as my core study. As a guest student from 1997 to 1998 I followed courses in molecular biology at the University of Agricultural Sciences, Vienna, Austria. In 1997 I started with my master's project on a cell biological topic at the Laboratory of Cell Biology and Cinematography, Institute of Ecology, University of Vienna, under the supervision of assistant professor Dr. Irene Lichtscheidl. During a short project in February 1997 at the Institute for Molecular Cell Biology, University of Amsterdam, supervised by Dr J.L. Oud and Prof. Dr N. Nanninga, I used optical tweezers for the micromanipulation of cell organelles. There, I not only could develop my interests in cell biology further, but also got familiar with the Dutch approach towards science. After I got my masters degree in Biology in 1999, I started with my PhD project in the group of Prof. Dr. Anne Mie Emons at Wageningen University. The work presented here was funded by a grant of the European Union and mainly was carried out in the period February 1999 to January 2003. During this time I had the chance to work at CNRS/INRA in Toulouse, France, attend courses such as the EMBO course on Molecular and Cellular Basis of Plant Development at the Gulbenkian Institute, Oeiras, Portugal, and to present my work at national and international scientific meetings. Before finishing my thesis work, I got the opportunity to work on an experiment for a manned space mission. Our TUBUL experiment was part of the life-science package of the Dutch Soyuz Mission DELTA in April 2004, which was conducted by the Dutch astronaut André Kuipers on board the International Space Station. The experience I got from the collaboration with industries, the European and Russian Space Agencies, from personal contact with the astronaut team, from media attention and the enthusiasm and interest of colleagues, friends, and students, and finally the events at the launch site goes beyond the scientific interest in this topic. I am currently continuing this project at the laboratory of Plant Cell Biology of Wageningen University – funded by the Dutch National Institute for Space Research, SRON – and am using micro- and macrogravity ground facilities at the Free University of Amsterdam. The project aims to investigate the role of gravity on the microtubule cytoskeleton of plant cells. In 2006 we will again face the exciting challenge of a new ESA space flight-experiment.

List of publications

Peer-review journals

Sieberer BJ, Ketelaar T, Esseling JJ, and Emons AMC (2004). Microtubules steer polarity in root hairs. Review article submitted to New Phytologist.

Sieberer BJ, Timmers ACJ, and Emons AMC (2004). Nod factors alter the microtubule cytoskeleton in Medicago truncatula root hair to allow root hair reorientation, and thus curling around rhizobia. Submitted to Molecular Plant-Microbe Interaction.

Vos JW, Sieberer B, Timmers ACJ, and Emons AMC (2003). Microtubule dynamics during preprophase band formation and the role of endoplasmic microtubules during root hair elongation. Cell Biol. Int. 27:295.

Sieberer BJ, Timmers ACJ, Lhuissier FGP, and Emons AMC (2002). Endoplasmic microtubules configure the subapical cytoplasm and are required for fast growth of Medicago truncatula root hairs. Plant Physiology 130: 977-988.

Lhuissier FGP, De Ruijter NCA, Sieberer BJ, Esseling JJ and Emons AMC (2001). Time Course of Cell Biological Events Evoked in Legume Root Hairs by Rhizobium Nod Factors: State of the Art. Ann. Bot. 87: 289 - 302.

Sieberer B and Emons AMC (2000). Cytoarchitecture and pattern of cytoplasmic streaming in root hairs of Medicago truncatula during development and deformation by nodulation factors. Protoplasma 214: 118-127.

Non peer-review journals

Sieberer B (2003): Plant cells in space. The TUBUL Experiment of the Dutch Soyuz DELTA Mission. Nieuwsbrief van de KNBV, October 2003.

Presentations and Abstracts (selection)

SRON National Institute for Space Research, Utrecht, The Netherlands.
"Influence of gravity on the microtubule cytoskeleton in plant cells". March 2004, oral presentation.

7th International Botanical Microscopy Meeting, Lisbon, Portugal.
"Endoplasmic microtubules during tip-growth and response to rhizobacterial signal molecules in root hairs of *Medicago truncatula*". April 2003, oral presentation.

University of Gent, Belgium. Host: Prof. Dr. P. van Oostvelt.
"Microtubules during development of *Medicago truncatula* root hairs." October 2002, oral presentation.

CNRS/INRA, Toulouse, France. Host: Prof. Dr. G. Truchet.
"Cytoarchitecture and pattern of cytoplasmic streaming in developing root hairs of *Medicago truncatula* and during deformation by Nod factors." January 2000, oral presentation.

17th European Cytoskeleton Forum, Nyon, Switzerland.
"Endoplasmic microtubules in tip growing root hairs of *Medicago truncatula* and in response to rhizobacterial signal molecules." Sepember 2002, poster.

16th European Cytoskeleton Forum, Maastricht, The Netherlands. "Microtubules in *Medicago truncatula* root hairs." August 2001, poster.

Medicago truncatula workshop, Madison, Wisconsin, USA.
"Microtubules in *Medicago truncatula* root hairs." July 2001, poster.

Acknowledgments

Four of the last six years that I spent here in the Laboratory of Plant Cell Biology of Wageningen University have been dedicated to work on my thesis project. It took me a bit longer than expected, but finally I succeeded in finishing my thesis. Although the keen candidate for a PhD stands alone for most of the time when terminating his thesis, still there are plenty of people without whom the candidate perhaps would have remained a (keen) candidate for the next years to come.

Firstly, I would like to thank Anne Mie Emons for giving me the opportunity to do my PhD in her lab. Anne Mie, I have been learning a lot under your supervision, but most of all I appreciate that you motivated me to stay course with my own ideas despite some set backs, and that you taught me how to think scientifically. Putting my scientific thoughts into words was quite a task for me – thank you for never giving up on improving my writing skills!

My special thanks go to Franck with whom I have been working together and sharing office for some years in a true symbiosis. Franck, I could not wish for a better paranimf!

Many thanks to the people of the tip-growth group – Anja, Bela, Cathy, John, Norbert, and Tijs. In the early days of my project they introduced me in a stimulating atmosphere into the tip-growth world and later on showed their interest in my work during many discussions.

Jan (Vos), from your approach towards science I could learn a lot; thank you also for your critical and helpful comments on so many of my manuscripts.

Further, I want to thank all the other members of the Laboratory of Plant Cell Biology for making it a pleasant place to work at.

Many thanks go to Ton Timmers for hosting me in Toulouse and for the close cooperation we had.

There has been a whole legion of people who made my stay in the Netherlands enjoyable and I would like to thank some of them on this occasion: Berna & Victor, Canan & Umberto, Des, Gerard, Hauke & Yee, Karel, Peter (Griffith), Sandra & Ossi, and

Veronique & family.

Special thanks to my friends in Austria, for cheering me up and supporting me: Ali & Andreas & Eva-Luna, Andrea, Anja & Christian & Lena, Dagmar, Jutta, Laura, Michael, and many others.

Reinhard, since our early days as students we shared so many experiences; another one yet has to come – thanks for being my paranimf.

Finally, I want to thank my parents for their interest in my work, their support and encouragement, and their warm welcome during the few occasions of a trip to Austria.

Björn
April 2005

Abstract

Microtubules, which occur as hollow protein tubes with a diameter of 25 nanometers, are an important compound of the cytoskeleton and occur in plant cells as a highly organized and dynamic array, which actual arrangement will depend on its tasks during the cell cycle. Microtubules play a key-role in the spatial distribution of the cytoplasm, cell growth, and cell division, and they respond to external or internal stimuli. In this thesis the microtubule cytoskeleton in developing root hairs of the model legume *Medicago truncatula* is described. Cortical microtubules are present in all developmental stages, but the sub-apical cytoplasmic dense region of tip-growing root hairs contains a specific microtubule configuration that was not described for interphase cells in detail before. When tip growth begins, the hairs acquire an extensive endoplasmic microtubule array in their sub-apex, which they retain until growth stops. These endoplasmic microtubules may be specific for legume root hairs. They are essential in maintaining the highly polarized distribution of cytoplasm in growing root hairs, and in keeping the growth of these hairs at a high rate. Further, the endoplasmic microtubule cytoskeleton appears to be a target of early Nod factor signalling. Nod factors are rhizobacterial signal molecules, which cause several cellular responses in legume root hairs. The endoplasmic microtubule array in elongating hairs responds to Nod factors with a subtle and short termed shortening, whereas cortical microtubules are not obviously affected. The presented results demonstrate that the microtubule cytoskeleton contributes to sustaining tip-growth and to determining the growth direction of hairs after Nod factor application. The latter two features are crucial for root hair curling around rhizobia, which is one of the first steps in establishing symbiosis between legumes and rhizobia. A hypothesis how microtubules may determine the site of tip-growth and thereby the directionality of root hair growth is discussed.